ANALYSIS OF A BI-DESICCANT SYSTEM OF DEHUMIDIFICATION

by

Jeffrey Nadeau

A Thesis Submitted to the Faculty of the

DEPARTMENT OF CHEMICAL ENGINEERING

In Partial Fulfillment of the Requirements
for the Degree of

MASTER OF SCIENCE

In the Graduate College of

THE UNIVERSITY OF ARIZONA

1993

STATEMENT BY AUTHOR

This thesis has been submitted in partial fulfillment of requirements for an advanced degree at the University of Arizona and is deposited in the University Library to be made available to borrowers under rules of the Library.

Brief quotations from this thesis are allowable without special permission, provided that accurate acknowledgement of source is made. Requests for permission for extended quotation from or reproduction of this manuscript in whole or in part may be granted by the head of the major department or the Dean of the Graduate College when in his judgement the proposed use of the material is in the interests of scholarship. In all other instances, however, permission must be obtained from the author.

SIGNED: 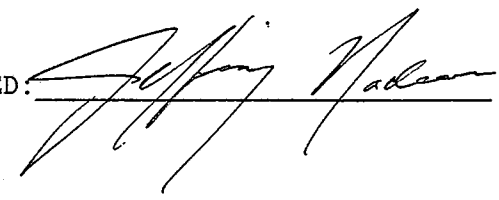

APPROVAL BY THESIS DIRECTOR

This thesis has been approved on the date shown below:

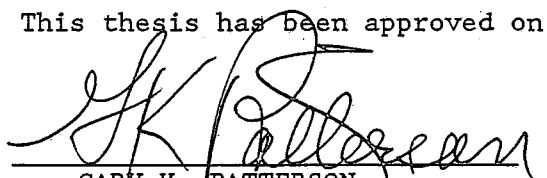

GARY K. PATTERSON
Professor of Chemical Engineering

Feb 23, 1990
DATE

ACKNOWLEDGEMENTS

The Author wishes to acknowledge the support of the Arizona Solar Energy Commission, ASEC contract No. 800 - 87, June, 1987. Also, this project would not have been possible without the support of Mr. Don Osborn, Director of the Solar Energy Research Facility, University of Arizona, and Dr. Simon Hanson, Assistant Professor of Chemical Engineering.

The Author would also like to thank Dr. Gary Patterson for his assistance and support throughout this project.

Finally, the Author would like to especially thank his wife, Katie, for her encouragement and love during this difficult period.

TABLE OF CONTENTS

LIST OF FIGURES 6
LIST OF TABLES 8
ABSTRACT 9
CHAPTER 1: INTRODUCTION 10
1.1 AIR CONDITIONING 10
1.1.1 Scope 10
1.1.2 Psychrometrics 10
1.1.3 Open and Closed Systems 14
1.1.3.1 Schematic Diagrams 14
1.1.3.2 Examples 14
1.1.4 Performance 24
1.2 DESICCANT SYSTEMS 25
1.2.1 Performance Limitations 25
1.2.2 Parameters Affecting Performance 27
1.2.3 Dynamics of Adsorption 30
1.3 ECONOMICS 39
1.4 CURRENT RESEARCH 40
1.4.1 Solid Desiccants 40
1.4.2 Liquid Desiccants 41
1.5 OBJECTIVES 43

CHAPTER 2: BREAKTHROUGH CURVE MODELS 45
2.1 CHOICE OF MODELS 45
2.2 GOVERNING EQUATIONS 45
2.3 DERIVATION OF SOLUTIONS 48
2.3.1 Isothermal Equilibrium Analysis 48
2.3.2 Adiabatic Equilibrium Analysis 52
2.3.3 Isothermal Analysis with Finite Mass Transfer Resistance 60
2.3.4 Adiabatic Adsorption with Finite Heat and Mass Transfer Resistance: Numerical Solution 62
2.4 PHASE EQUILIBRIUM AND KINETIC MODELS 65
2.4.1 Mass and Heat Transfer in Packed Beds 65
2.4.2 Solid & Liquid Desiccant Properties and Phase Equilibrium 70
2.4.2.1 Silica Gel 70
2.4.2.2 Ethylene Glycol 76

CHAPTER 3: THEORY OF BI-DESICCANT SYSTEM BEHAVIOR 79
3.1 IDEAL PERFORMANCE 79
3.2 SOLID-LIQUID EQUILIBRIUM 82
3.3 THEORETICAL MODEL OF BI-DESICCANT SYSTEM 85

CHAPTER 4: EXPERIMENTAL EQUIPMENT AND PROCEDURES 89

CHAPTER 5: EXPERIMENTAL AND THEORETICAL RESULTS 92
5.1 ISOTHERMAL EQUILIBRIUM 93
5.1.1 Silica Gel 93
5.1.2 Ethylene Glycol 97
5.2 ADIABATIC OPERATION 101
5.2.1 Silica Gel 101
5.2.2 Ethylene Glycol 110
5.3 THOMAS SOLUTION 120
5.4 NUMERICAL ANALYSIS 123
5.4.1 Silica Gel 123
5.4.2 Ethylene Glycol 128
5.5 EXPERIMENTAL RESULTS 130

CHAPTER 6: CONCLUSIONS AND RECOMMENDATIONS 143

APPENDIX 1: DATA 146

APPENDIX 2: FORTRAN PROGRAM ADSORB. 154

APPENDIX 3: FORTRAN PROGRAM FOR HODOGRAPHIC PLOTS 160

APPENDIX 4: HEAT LOSS ANALYSIS 167

APPENDIX 5: CALCULATIONS FOR THEORETICAL RESULTS 171

NOMENCLATURE 181

REFERENCES 185

LIST OF FIGURES

FIGURE 1.1 - Psychrometric Chart. 11
FIGURE 1.2 - Typical Summer Conditions. 13
FIGURE 1.3 - Comparison if Open and Closed Systems. 15
FIGURE 1.4 - Psychrometric Representation of Open and Closed Systems 16
FIGURE 1.5 - Examples of Closed Systems 20
FIGURE 1.6 - Examples of Open Systems 21
FIGURE 1.7 - Inlet Conditions for Simple Evaporative Cooler . . 23
FIGURE 1.8 - Solid Desiccant System; Ventilation Mode 26
FIGURE 1.9 - Typical Breakthrough Curve in a Packed Bed 31
FIGURE 1.10- Dehumidification and Regeneration Breakthrough on Psychrometric Diagram 33
FIGURE 1.11- Equilibrium Isotherms 35
FIGURE 1.12- Effect of Heat of Adsorption on Breakthrough . . . 37
FIGURE 1.13- Effect of Mass Transfer Resistance on Breakthrough 38

FIGURE 2.1 - Governing Heat and Mass Balance Equations 46
FIGURE 2.2 - Representation of Isothermal Adsorption and Desorption; Equilibrium Solution 51
FIGURE 2.3 - Effect of BET Isotherm on Breakthrough 53
FIGURE 2.4 - Representative Adiabatic Characteristics of a Desiccant Material 57
FIGURE 2.5 - Representation of Adiabatic Dehumidification and Regeneration; Equilibrium Solution 59
FIGURE 2.6 - Mass Transfer Processes in Porous Particles . . . 66
FIGURE 2.7 - Silica Gel Isotherms - Calculated 77
FIGURE 2.8 - Ethylene Glycol Isotherms - Calculated 78

FIGURE 3.1 - Comparison of Maximum Achievable Performances for Solid and Liquid Desiccants 80
FIGURE 3.2 - Theoretical Bi-Desiccant System Configuration . . 86
FIGURE 3.3 - Psychrometric Representation of Bi-Desiccant System 87

FIGURE 4.1 - Experimental Setup 90

FIGURE 5.1 - Isothermal Adsorption Breakthrough for Silica Gel; Equilibrium Solution 94
FIGURE 5.2 - Isothermal Desorption Greakthrough for Silica Gel; Equilibrium Solution 95
FIGURE 5.3 - Isothermal Dehumidification Breakthrough for Ethylene Glycol; Equilibrium Solution 98
FIGURE 5.4 - Isothermal Regeneration Breakthrough for Ethylene Glycol; Equilibrium Solution 99

FIGURE 5.5 - Adiabatic Characteristic Plot for Silica Gel Adsorption 102
FIGURE 5.6 - Adiabatic Adsorption Breakthrough for Silica Gel; Equilibrium Solution 105
FIGURE 5.7 - Adiabatic Characteristic Plot for Silica Gel Desorption 107
FIGURE 5.8 - Adiabatic Desorption Breakthrough for Silica Gel; Equilibrium Solution 111
FIGURE 5.9 - Adiabatic Characteristic Plot for Ethylene Glycol Dehumidification 112
FIGURE 5.10- Adiabatic Dehumidification Breakthrough for Ethylene Glycol; Equilibrium Solution 115
FIGURE 5.11- Adiabatic Characteristic Plot for Ethylene Glycol Regeneration 116
FIGURE 5.12- Adiabatic Regeneration Breakthrough for Ethylene Glycol; Equilibrium Solution 119
FIGURE 5.13- Isothermal Adsorption Breakthrough for Silica Gel; Thomas Solution 121
FIGURE 5.14- Adiabatic Adsorption Breakthrough for Silica Gel; Numerical Solution 124
FIGURE 5.15- Adiabatic Adsorption Breakthrough for Silica Gel; Numerical Solution 125
FIGURE 5.16- Adiabatic Desorption Breakthrough for Silica Gel; Numerical Solution 126
FIGURE 5.17- Numerically Calculated Temperature Breakthrough for Silica Gel - Dehumidification 127
FIGURE 5.18- Dehumidification Breakthrough for Ethylene Glycol; Numerical Solution 129
FIGURE 5.19- Experimental Dehumidification Breakthrough Curves for Silica Gel 131
FIGURE 5.20- Experimental Dehumidification Breakthrough Curves for Ethylene Glycol 132
FIGURE 5.21- Experimental Dehumidification Breakthrough Curves for Bi-Desiccant 133
FIGURE 5.22- Comparison of Silica Gel Breakthrough to Calculated Results 134
FIGURE 5.23- Comparison of Ethylene Glycol Breakthrough to Calculated Results 136
FIGURE 5.24- Comparison of Bi-Desiccant and Liquid Desiccant Breakthrough Curves 138
FIGURE 5.25- Experimental Breakthroughs Shown on the Psychrometric Diagram 140

LIST OF TABLES

TABLE 2.1 - Physical Properties 71

TABLE 2.2 - Silica Gel Isotherm Data 72

TABLE 2.3 - Glycol/H_2O Isotherms 74

TABLE 5.1 - Adsorption Characteristics - Silica Gel 103

TABLE 5.2 - Desorption Characteristics - Silica Gel 108

TABLE 5.3 - Absorption Characteristics - Glycol 113

TABLE 5.4 - Desorption Characteristics - Glycol 117

ABSTRACT

This research studies the behavior of a liquid-solid system of dehumidification which is applicable to passive energy applications such as solar energy. A liquid desiccant typically has better regeneration characteristics than a solid desiccant, and is therefore more easily regenerated using solar energy. Solid desiccants have much better drying characteristics than liquid desiccants, and serve well in the dehumidification step. An attempt has been made in this study to find a compatible pair of desiccants, one liquid and one solid, whereby the desirable characteristics of both are used.

The system evaluated involves a packed bed of solid desiccant which is wetted with the liquid desiccant. This be-desiccant bed is the dehumidifying section of the process. The liquid is then re-generated on its own. The bi-desiccant bed is regenerated by flushing it witn fresh liquid.

A thermodynamic analysis has shown that it is possible to achieve the desired result provided the appropriate solid and liquid desiccants are found. The critical factor in this determination is the distribution of moisture between the air stream, the solid, and the liquid. The capacity of a liquid desiccant which provides low humidity in the air stream can be improved with a solid partner provided the solid readily absorbs moisture from the liquid and can be regenerated with fresh liquid.

CHAPTER 1: INTRODUCTION

1.1 AIR CONDITIONING

1.1.1 Scope

The process of air conditioning encompasses any process designed to bring an air mass to within a zone of comfort for human beings. The method of conditioning used depends upon the beginning condition of the air and the desired condition. The temperature, humidity and cleanliness of the air may need to be controlled and this determines the equipment needed. The American Society for Heating, Refrigeration and Air Conditioning Engineers (ASHRAE, 1981) publishes a guide, the Handbook of Fundamentals, which shows the relationship between temperature and humidity to the degree of comfort experienced by an average person and the "comfort zone" so determined sets the criteria for the design of air conditioning equipment.

1.1.2 Psychrometrics (Perry, 1983; Felder & Rousseau, 1980)

The psychrometric chart for an air-water system is shown in figure 1.1. The x-axis represents the dry bulb (or actual) temperature of the air and the y-axis represents the absolute humidity of the air in mass of water per mass of dry air (i.e. air with no water vapor in it). The curved line at the left of the diagramm is the saturation line. Upon reaching this line, either by decreasing temperature at constant humidity or increasing humidity at constant temperature,

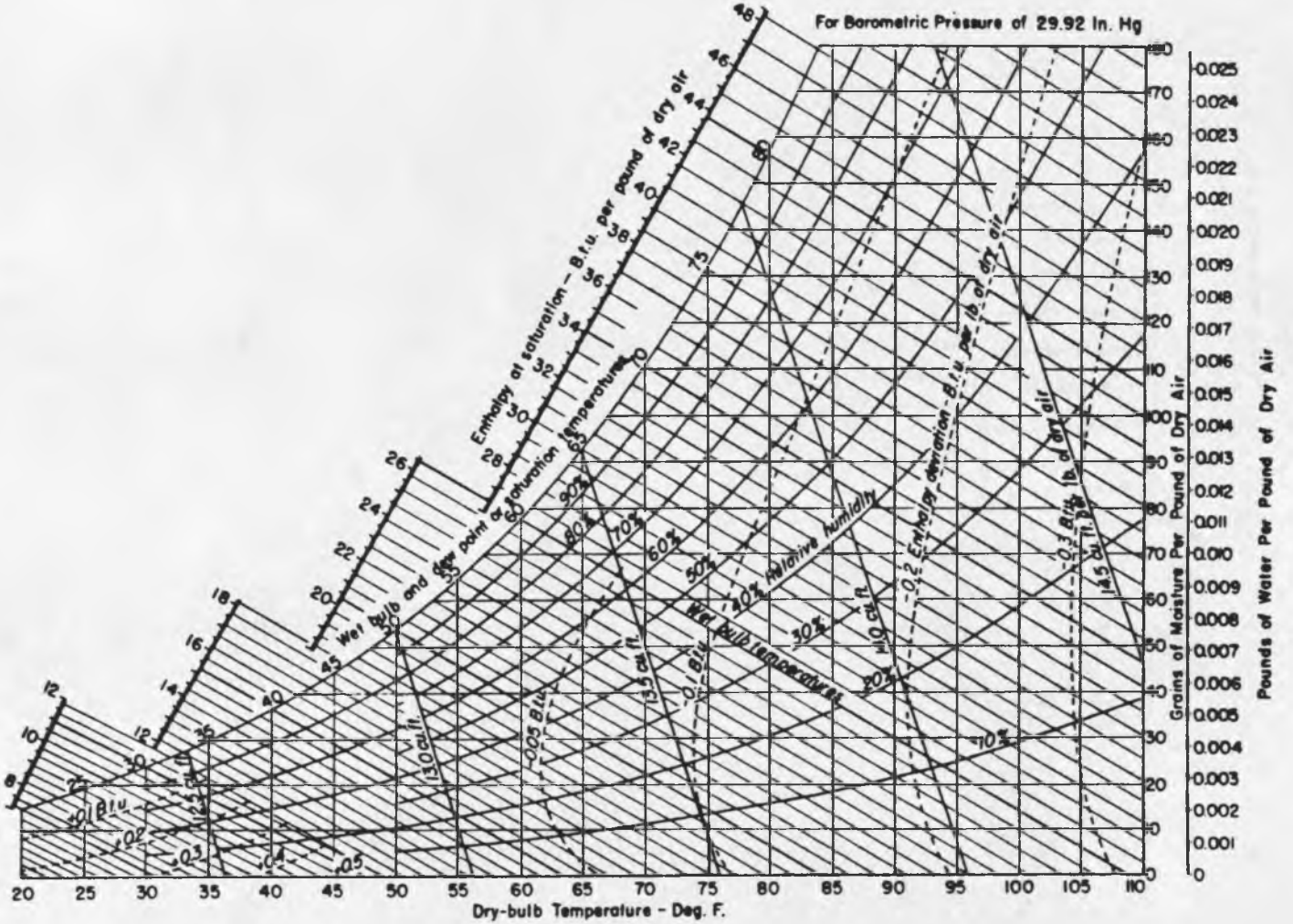

Figure 1.1 - Psychrometric Chart

condensation occurs since the air cannot hold any more water vapor. The diagonal lines represent conditions of equal enthalpy so that movement along one of these lines represents an adiabatic process. The temperature at the intersection of one of these lines and the saturation curve is the wet bulb temperature, or the temperature of an air-water system in an equilibrium (saturated) state. This is the temperature which is measured by a sling psychrometer.

There are numerous ways to measure humidity using the psychrometric chart. The first uses the measured wet and dry bulb temperatures. Since the wet bulb indicates the temperature at which adiabatic saturation of the air stream occurs, following the constant enthalpy line from the saturation line to the dry bulb temperature shows the initial humidity of the air. Another method of measuring humidity is to cool the air stream until condensation occurs. The temperature at which this happens is called the Dew Point temperature, and is read horizontally from the saturation curve back to the ambient air temperature. Finally, if the relative humidity of the air is known, the humidity can be determined directly by reading dry bulb temperature and relative humidity simultaneously.

Figure 1.2 shows some typical summer conditions (tabulated by ASHRAE,1981) for cities around the United States as depicted on the psychrometric chart. It is seen that except for a few cities in the southwest, most American cities have a high degree of humidity relative to the ASHRAE comfort zone, which is shown as the rectangular area.

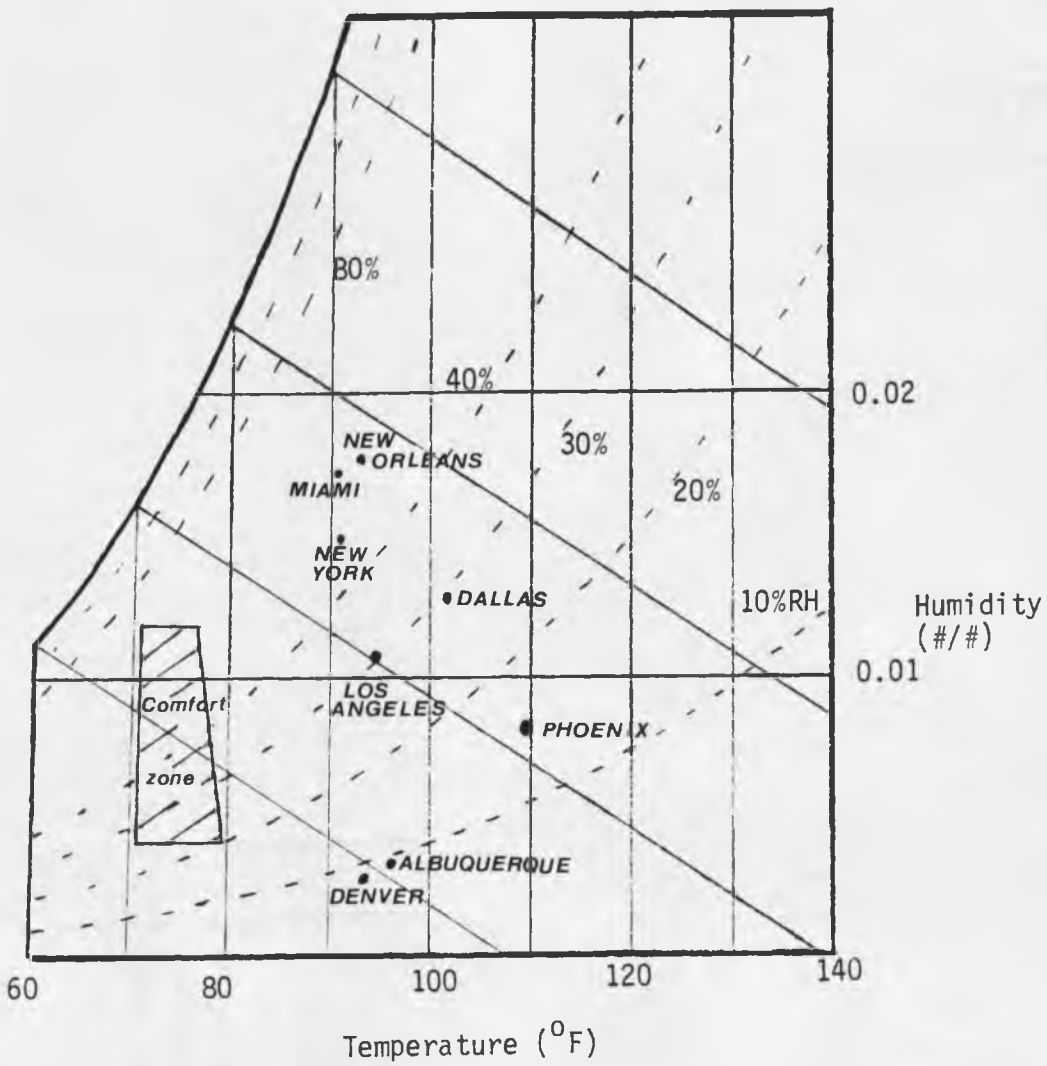

Figure 1.2 - Typical Summer Conditions

Therefore, latent loads, which are determined by the amount of humidity to be removed, can be much higher than sensible loads, which involve simple heat exchange. As a result, cost effective dehumidification techniques become all-important in choosing an air conditioning system.

1.1.3 Open and closed systems (Smith & Van Vess, 1981)

1.1.3.1 Shematic diagrams

Figure 1.3 shows a schematic comparison of an open and a closed system. The main difference is in the definition of the working fluid. In the closed cycle, the working fluid and the process air stream are separate and exchange only thermal energy across the system boundary. The working fluid is cycled in the manner shown and the system requires work to maintain this cycle. In the open cycle, the process air stream becomes the working fluid and there is an exchange of both thermal energy and mass across the system boundary. The process is to be maintained at steady state and energy is needed to maintain the dehumidification and cooling processes.

1.1.3.2 Examples

Figure 1.4 is a psychrometric diagram showing the comparison of an open and a closed cycle. These processes can be understood more easily this way since the diagram includes much more information. The psychrometric chart also allows an easier evaluation of system performance, since enthalpy data are also present on the diagram.

Since the closed system can only exchange thermal energy with the process air stream, the air conditions will follow the horizontal line

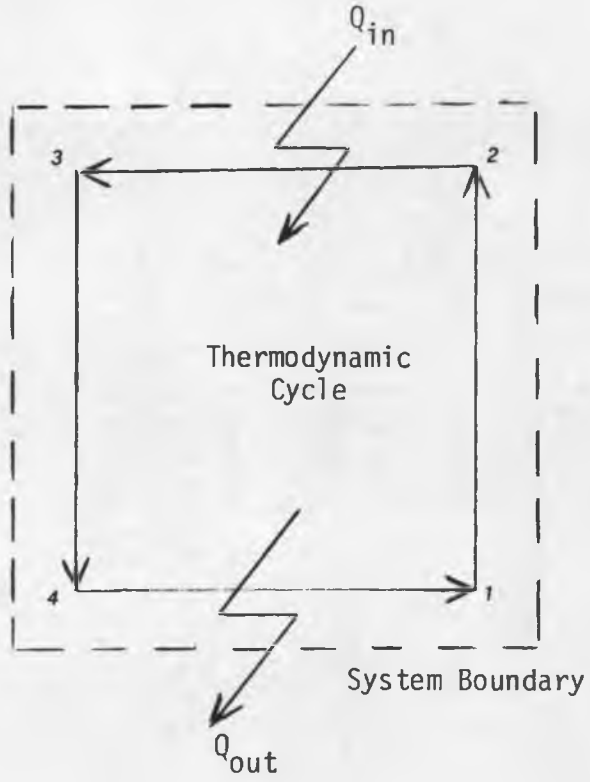

(1) Closed System

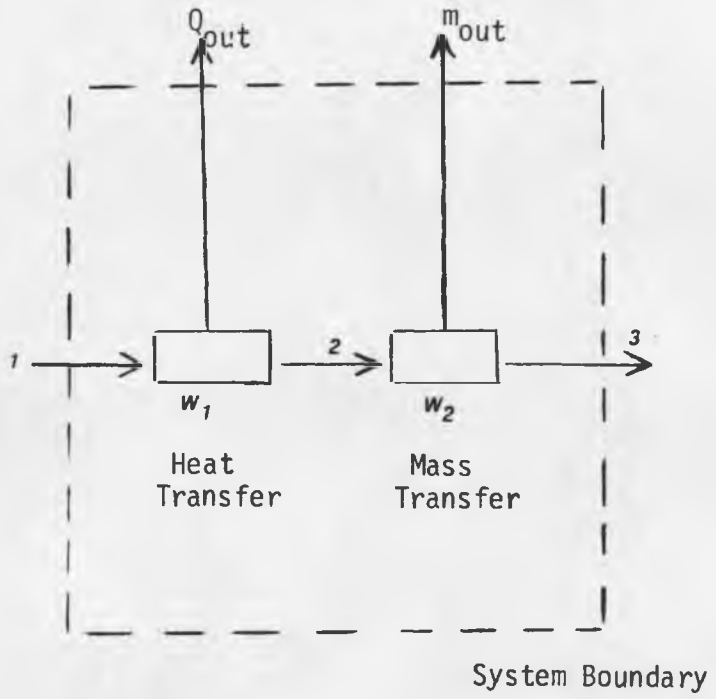

(2) Open System

Figure 1.3 - Comparison of Open and Closed Systems

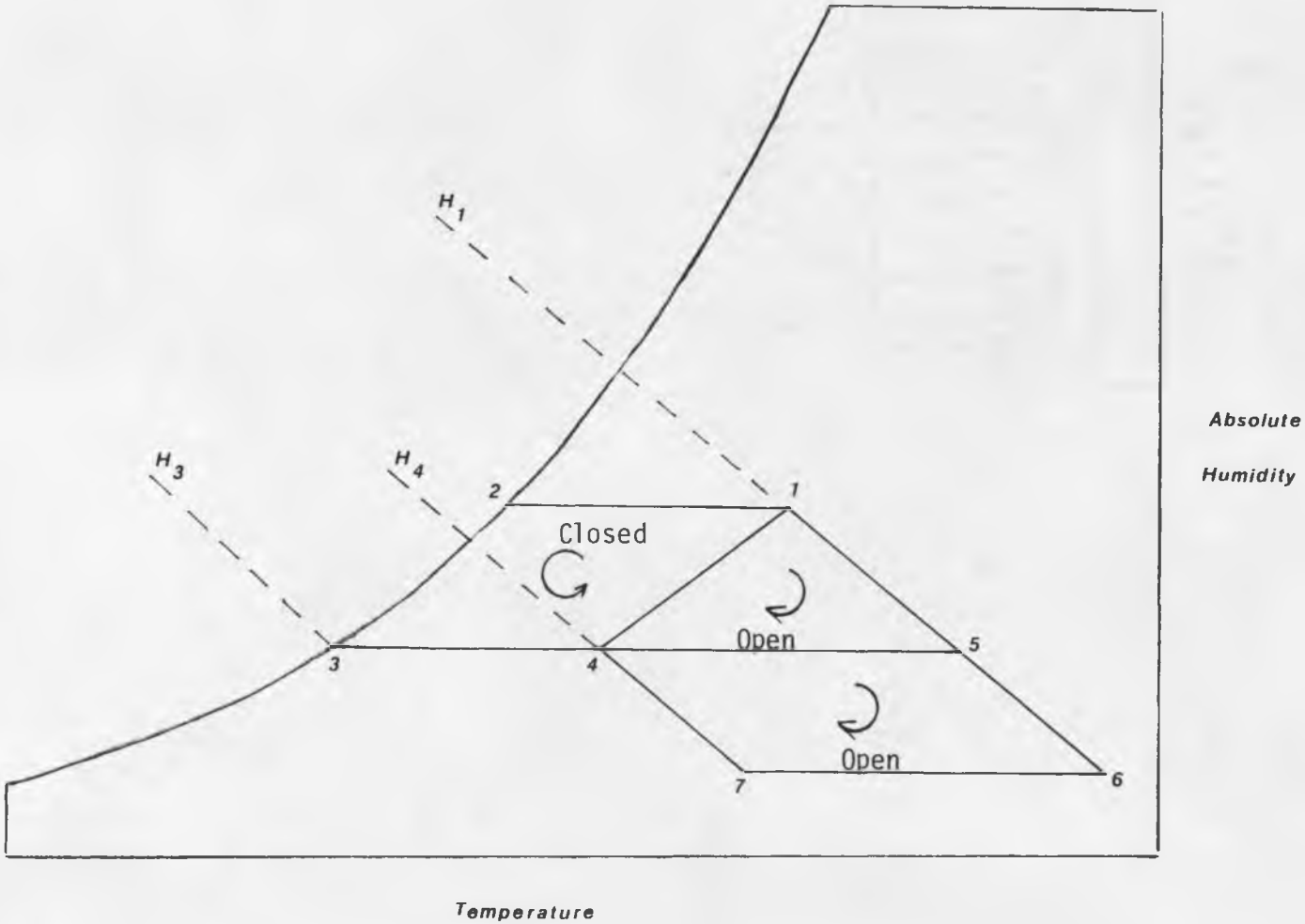

Figure 1.4 - Psychrometric Representation of Open and Closed Systems

from the initial condition (condition 1) to the Dew Point temperature at constant humidity (condition 2). From there, furthur thermal energy extraction comes by way of condensation, and the air stream follows the saturation curve to condition 3. H_1-H_3 represents the cooling load required to bring the room conditions into the comfort zone. Heating from condition 3 to condition 4 is accomplished by simple heat exchange and by production of thermal energy by the occupants. This is the only way that a closed system can achieve cooling. Therefore, latent loads can become predominant in regions of high humidity, thus making the process more expensive.

In the case of an open system, mass transfer is coincident with heat transfer so that the process air stream can follow any number of paths. For instance, if the process is set up appropriately, the path can consist of a simple jump from condition 1 to condition 4 as shown. This is common in liquid desiccant systems. The air stream could also be adiabatically dehumidified and then sensibly cooled as shown by process 1-5-4. This could be the result of a hybrid solid desiccant/vapor compression system. Finally, the air stream could be adibatically dehumidified, sensibly cooled, and then adiabatically humidified as shown in process 1-6-7-4. This would most likely be the case in a solid desiccant/evaporative cooling process. The possibilities are endless, restricted only by the thermodynamic limits of the design. As can be seen, the cooling load imposed on the system (H_1-H_4) is less than that for the closed system when latent loads are present.

Examples of closed systems include vapor compression, absorption, and jet pump systems (Kettleborough,1984). These systems all have one thing in common. The cooling in these systems is achieved through evaporation of the working fluid, whose physical characteristics are most desirable for this application. The difference between these systems is primarily in the method of bringing the vapor to the conditions suitable for condensation, and therefore maintaining the degree of cycling capacity of the working fluid.

In vapor compression, this is achieved by the use of a compressor, which increases the total pressure and temperature of the vapor. The temperature is raised much higher than ambient, thus allowing heat transfer away from the fluid . The high pressure prodvides condensation of the working fluid and the heat of condensation is given off as exhaust heat (Q_{out} in figure 1.3). Upon expansion, the working fluid enters the evaporater at a lower temperature and pressure. Evaporation is achieved as a result of a temperature difference between the fluid and the ambient air and the heat of evaporation is provided by the cooled space (Q_{out} in figure 1.3).

In the case of absorption refrigeration, the same result is achieved through contact with a strong solution containing the working fluid. Absorption occurs at low temperature and concentrated absorber solution. This gives rise to refrigerant vapor generation when the refrigerant laden absorber solution is now heated. The rest of the system is exactly the same as a vapor compression system. The absorber sub-system is effectively replacing the compressor.

In the case of the jet pump system, the compressor is replaced by

a convergent-divergent nozzle. The compression of the working fluid is accomplished within the jet pump by expanding the primary fluid, which receives heat from an external source. The jet pump system is still in the experimental stages. The three systems are shown in figure 1.5.

Examples of open systems include liquid and solid desiccant systems, rockbed storage systems, and simple evaporative coolers. Evaporative coolers and rockbed storage systems are typically used together with dehumidification systems since they are rarely effective on their own. Figure 1.6 shows examples of liquid and solid desiccant, and rockbed storage system applications.

The desiccant systems rely on efficient dehumidification combined with either evaporative cooling or sensible cooling via vapor compression. Solid systems typically are operated as adiabatic processes and follow the process 1-5-4, or 1-6-7-4 in figure 1.4. Liquid systems can approach isothermal, or one step operations, which more closely resemble process 1-4. The major drawbacks to a liquid system are typically its large size requirements, as well as the need for an existing cooling source such as cooling tower water. The benefits are seen in the favorable regeneration characteristics of the liquid. For solid systems, compact size can be achieved relative to the load requirements and this leads to promising residential uses. However, the performance of solid desiccants has for the most part reached a peak and market competitiveness still favors electrically operated units.

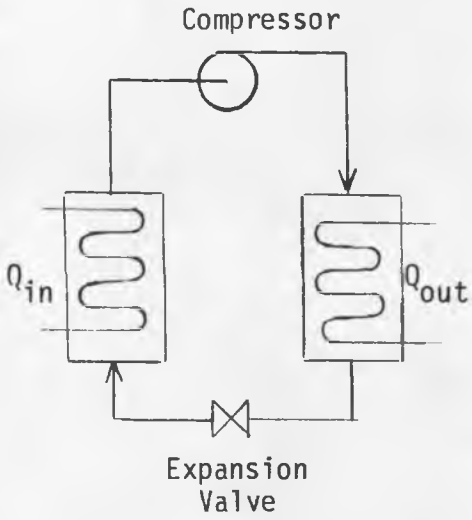

(1) Vapor Compression

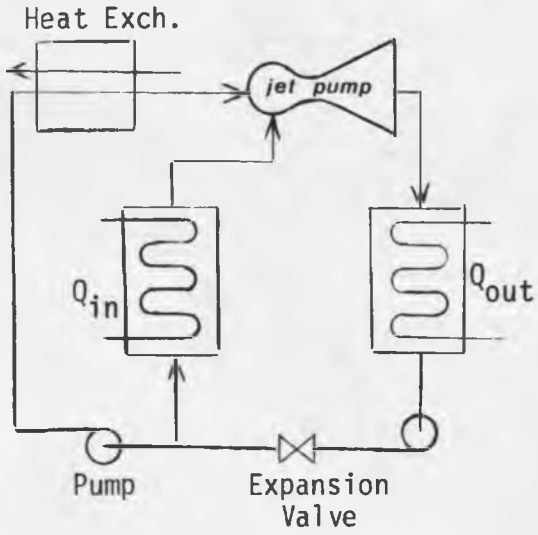

(2) Jet Pump

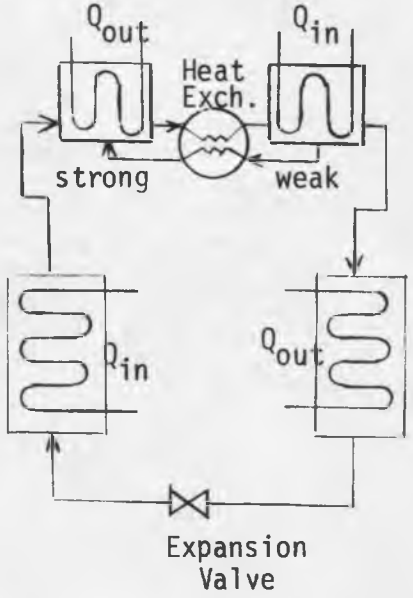

(3) Absorption System

Figure 1.5 - Examples of Closed Systems.

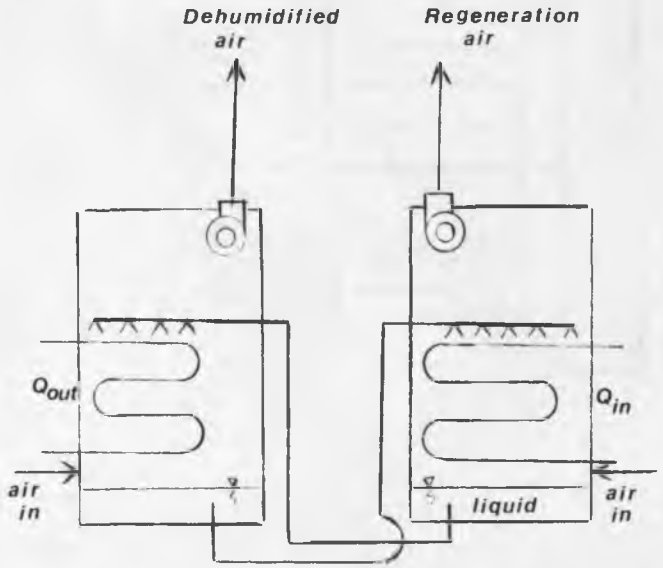

Liquid Desiccant

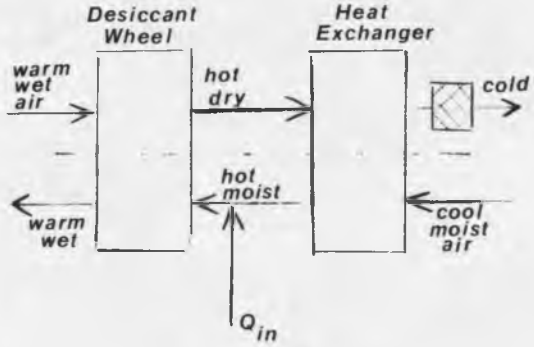

Solid Desiccant

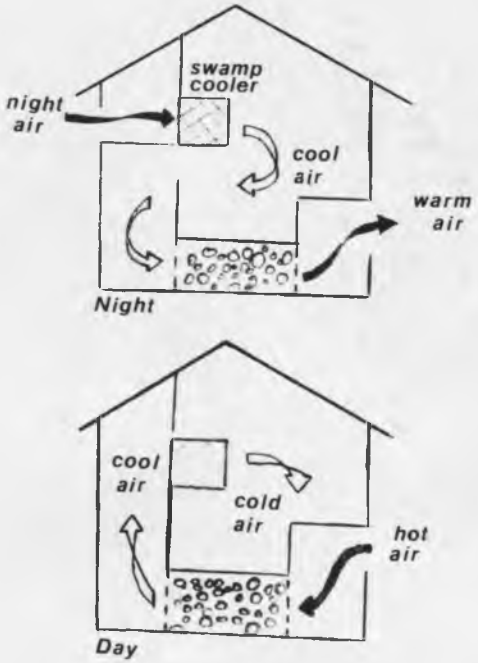

Rockbed System

Figure 1.6 - Examples of Open Systems.

The rockbed storage system is based on the use of a large bed of rocks cooled by drawing cool night air across them and where possible exposing them to night radiation. During the day, warm inside air is cooled by circulating it through the rockbed. This type of cooling is typically combined with other methods to reduce cooling loads. The most obvious disadvantage to a system of this type is its volume requirements. Existing houses cannot be easily modified to include a large bed of material and the increase in building costs can make the system uneconomical.

A simple evaporative cooler can be used when the conditions are such that they lie within the area shown in figure 1.7. This allows for a simple adiabatic humidification of the process air stream, landing directly in the comfort zone. The only conditions of this type exist in the desert southwest of the United States or occasionally elsewhere. This figure therefore indicates the conditions which a dehumidifier must bring the process air stream in order to use evaporative cooling as a sub-system.

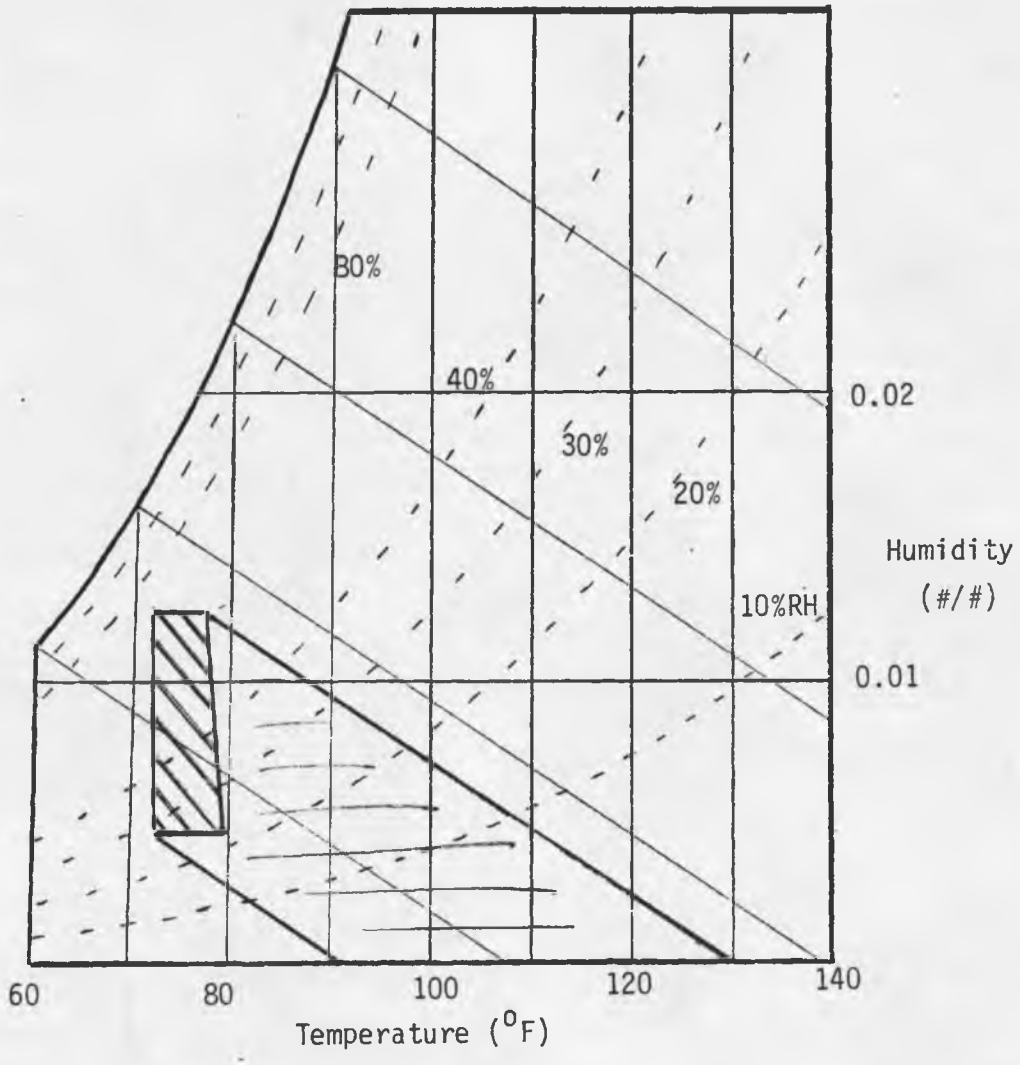

Figure 1.7 - Inlet Conditions for Simple Evaporative Cooler.

1.1.4 Performance

There are a number of key parameters which describe the performance of an air conditioning system. The first is the Coefficient of Performance which can be defined as the ratio of cooling capacity of the system and the work input to achieve that cooling capacity. In the case of a closed system, the cooling capacity is equal to the heat absorbed by the system, or Q_{in} as shown in figure 1.3. Q_{out} represents the thermal energy given off by the cycle to maintain steady state. The Coefficient of Performance is therefore Q_{in}/W. In the case of the open system, the cooling capacity is equal to the change in enthalpy of the process air stream, or H_2-H_1. The work to maintain that capacity is shown as the sum of W_1 and W_2. The Coefficient of Performance is therefore $(H_2-H_1)/(W_1+W_2)$. The most important difference in open system and closed system coefficients of performance is that the open system coefficient has no theoretical limit, whereas the closed cycle is limited by the Carnot cycle limit for closed systems.

The second most important parameter in system performance assessment is the specific cooling capacity. This parameter gives an indication as to what amount of cooling is achieved by a certain volume of air processed by the system. The amount of cooling is usually referred to in terms of "tons" of cooling. The specific cooling capacity is therefore given with the units of (tons of cooling)/CFM. The higher the specific cooling capacity, the less volume of process air is needed to achieve the desired cooling load. This parameter and the Coefficient of Performance are the two most important factors in

the evaluation of air conditioning system performance.

There is some discrepancy as to the definition of the Coefficient of Performance, hereafter referred to as the COP. For example, the thermal COP is different from the electrical COP since electricity ultimately comes from a thermal source with an efficiency of some 25%. Most gas fired and solar fired systems use thermal COP's, whereas vapor compression uses electrical COP. Also, the COP can be defined from an isolated load such as the latent load of dehumidification, neglecting the sensible load. This would therefore be designated as a COP of dehumidification as opposed to the overall COP. Work to maintain the cooling portion can also be excluded for some purposes, unless a hybrid desiccant/vapor compression system is used, for example. Clearly, a comparison of air conditioning systems must be done on an equivalent basis to evaluate their thermodynamic merit.

1.2 DESICCANT SYSTEMS

1.2.1 Performance limitations

In a desiccant dehumidifier, the cycling capacity is affected by the desiccants' performance in both dehumidification and regeneration. If one process is limiting, then the whole operation is limited to that capacity. The specific cooling capacity is dependent on the humidity reduction in the dehumidifying section only, and is therefore strongly dependent on the regeneration conditions.

For example, figure 1.8 illustrates a rotary wheel solid desiccant system using evaporative cooling, along with the process shown on the

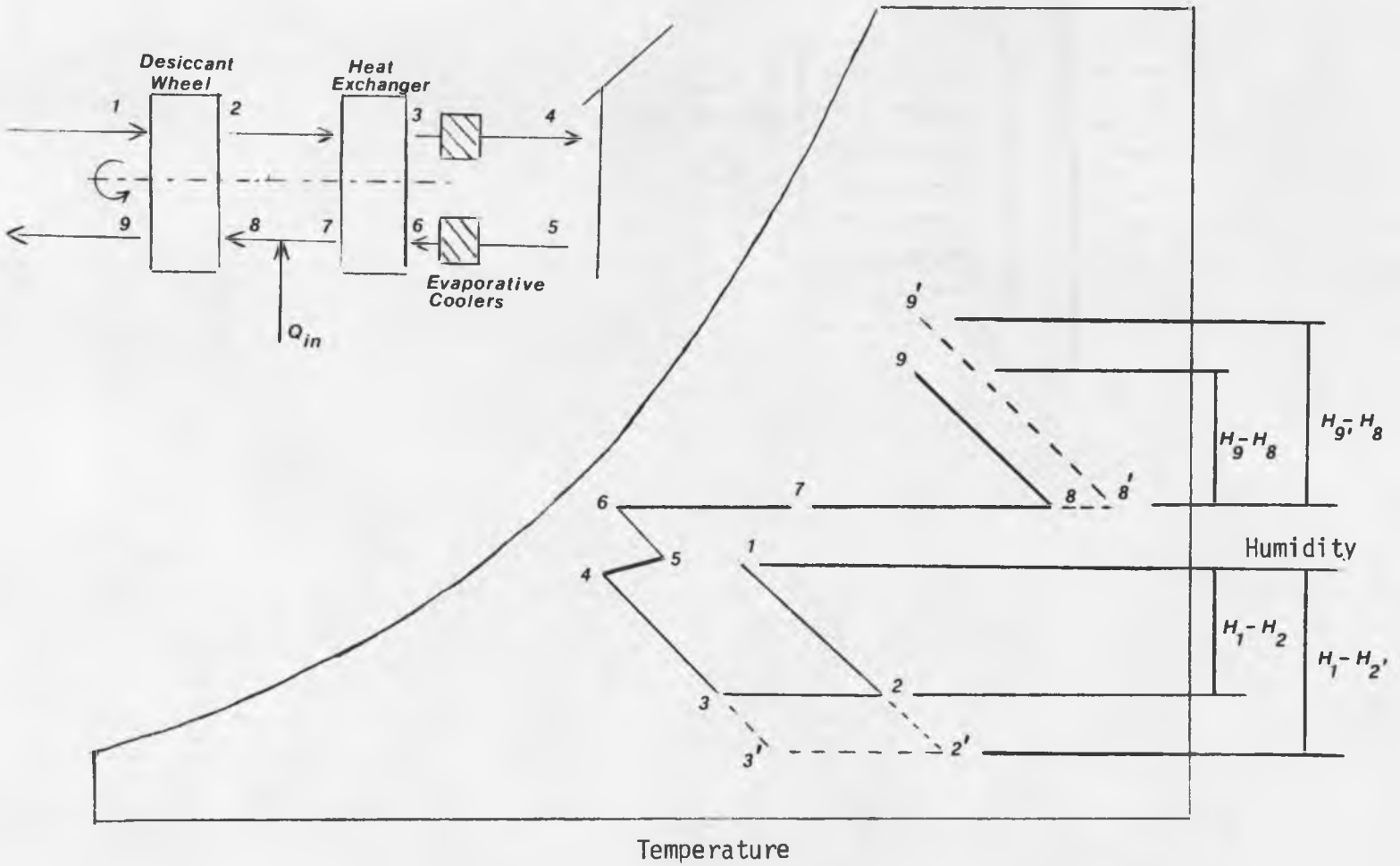

Figure 1.8 - Solid Desiccant System ; Ventilation Mode

psychrometric chart. The system is in the ventilation mode, which means that the cool air stream is drawn from the outside with no recycle. The cooling process is seen as an adiabatic dehumidification followed by sensible heat exchange and then evaporative cooling. The amount of water removed from the air during the dehumidification is seen as H_1-H_2. This determines the specific cooling capacity. The regeneration proceeds with heat input to the return air stream followed by adiabatic humidification (desorption). The amount of water put back into the air stream is seen as H_9-H_8. In order for the system to stabilize, these two amounts must be equal if the flowrates of the dehumidification and regeneration streams are equal.

The dashed lines show the effect of increased regeneration temperature on the cycling capacity of the solid desiccant unit. It can be seen that the increased temperature increases the desorption rate ($H_{9'}$-H_8). This in turn reduces the amount of moisture left in the desiccant, thereby increasing the dehumidification capacity (H_1-$H_{2'}$). As a result, the specific cooling capacity increases. The two processes eventually equilibrate in order to not effect a net build-up or depletion of moisture in the desiccant bed.

1.2.2 Parameters affecting performance

There are many parameters in a desiccant system which determine its performance. The nature of the process of dehumidification/regeneration, whether it is adiabatic, isothermal, isentropic, etc., has a great affect. Also, the physical characteristics of the desiccant itself play a key role in the

performance of the air conditioner. The process configuration is often determined by economics, but the choice can also effect the performance. A semi-batch operation could have better characteristics than a continuous operation, for example.

First of all, the thermodynamic nature of the processes of dehumidification and regeneration has a direct bearing on the system performance. For example, liquid desiccant systems are often maintained at isothermal conditions. This is an advantage in that most desiccants decrease in capacity as temperature is increased. Since adsorption or absorption is usually exothermic, temperatures do not generally decrease in adiabatic systems. On the other hand, most solid desiccant systems operate at near adiabatic conditions in a packed bed of desiccant particles. The adiabatic process lowers the overall capacity of the desiccant as well as its ability to regenerate, and this has an effect on the performance of the process. It has proven to be too un-economical to maintain a solid desiccant system in an isothermal mode due to the complexity of the system.

The physical characteristics of the desiccant have an enormous effect on the performance of the dehumidifier. The most notable characteristics of desiccants often referred to are the equilibrium isotherm, the absorption or adsorption capacity, the heat of adsorption or absorption, the moisture diffusivity, and the heat capacity of the desiccant. Some characteristics have a greater effect on performance of the dehumidifier than others, depending on the circumstances. Jurinak (1984) gives an excellent analysis on rotary wheel, solid

desiccant performance parameters.

The first characteristic is often considered the most important. The name "isotherm" is used since the property is observed at constant temperature. It is defined as the relationship between humidity content of the air and the equilibrium amount of water vapor absorbed or adsorbed onto or into the desiccant. An isotherm, which is concave in the direction of atmospheric humidity is favorable for adsorption, while a convex isotherm is unfavorable. The opposite effect is seen for desorption processes, however. A concave isotherm is unfavorable for desorption, while a convex isotherm is favorable. This will be explained in more detail in the next chapter.

The heat of absorption or adsorption also has an effect on the performance of the dehumidifier. The more heat given off as a result of absorption or adsorption of the water vapor , the higher the temperature increase and/or the more difficult it is to maintain an isothermal condition. Most adsorption or absorption processes closely approach the heat of condensation/evaporation of water, which makes the adsorption/absorption process closely follow an adiabatic saturation line on the psychrometric chart.

Finally, the moisture diffusivity and thermal capacity of the desiccant also have an effect on the overall performance of the dehumidifier. The moisture diffusivity is a measure of the mass transfer resistance in the bed, which influences the average outlet humidity, and the thermal capacity influences the temperature rise in the bed. A rotary wheel, cross flow dehumidifier as depicted in figure 1.8 loses capacity with increased thermal capacity, for instance.

The process configuration is chosen from knowledge of the process characteristics and economics in order to maximize effectiveness. Most industrial desiccants are used in a semi-batch mode, due to the large capacities of the desiccant beds. One bed is usually drying while the other is in regeneration. On the residential scale, however, the dehumidifier is usually operated in a continuous mode. Solid systems usually employ a rotary wheel, cross flow dehumidifier and liquid systems usually use spray chambers or packed spray columns.

1.2.3 Dynamics of adsorption

A packed bed of solid desiccant adsorbs water vapor from an incident flow stream until equilibrium is reached between the adsorbent and the air stream. This proceeds until the bed is completely saturated with adsorbate. The dehumidification proceeds such that the inlet portion of the bed is saturated first and a concentration profile forms in the bed which moves through the bed until complete saturation. In the case of adiabatic adsorption, a temperature wave also forms, thereby influencing the accompanying concentration front. The concentration and temperature waves produce what is called a "breakthrough" curve of outlet humidity and temperature versus time. Figure 1.9 is a typical adsorption breakthrough curve of humidity for a packed bed of desiccant material. Shown above the curve are bed profiles at various times. The profile is seen to move through the bed at a constant rate and the breakthrough curve takes the opposite shape with the steepness being dependent on the velocity and the shape of the

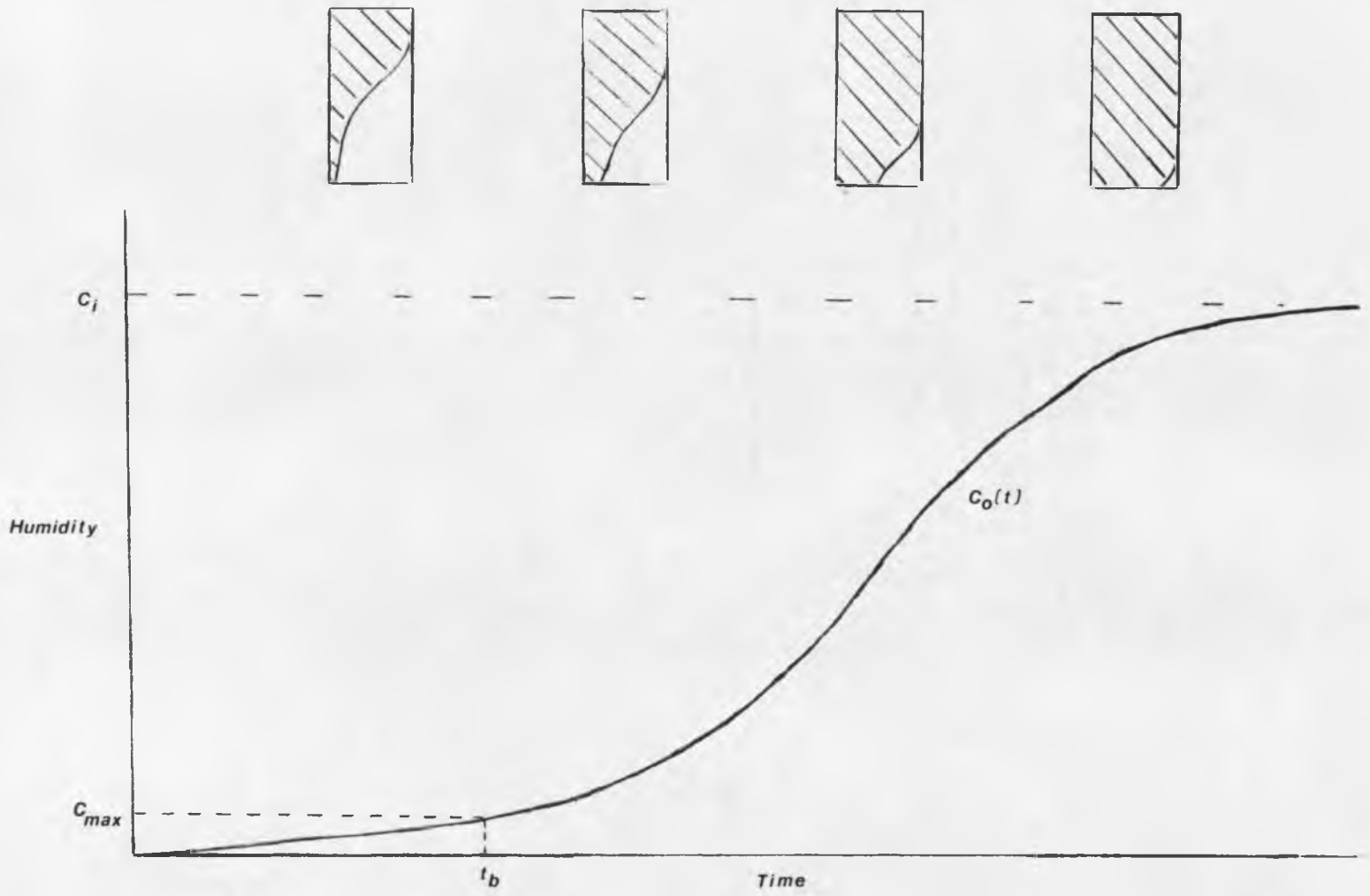

Figure 1.9 - Typical Breakthrough Curve in a Packed Bed. (Illustrations above curve represent loading profiles of the bed at the given time on the breakthrough curve)

concentration profile. The process air stream enters the bed at a constant humidity of C_i, and the outlet humidity is represented as a function of time $C_o(t)$. The breakthrough time t_b is that time (determined by choice) when the bed can no longer remove moisture from the air stream at a sufficient rate. At this point, the desiccant bed must be regenerated so that the cycle can be repeated.

Figure 1.10 is a representation of the adsorption and desorption processes in the bed. This is the same representation as processes 1-2 and 8-9 in figure 1.8 except that the dehumidification and regeneration processes are represented in a discrete fashion. Each dot on the psychrometric chart represents a point on the corresponding concentration and temperature breakthrough curves of adsorption or desorption. The dehumidification and regeneration in figure 1.8 actually represent the average outlet conditions over the whole breakthrough time up to t_b. It can be seen that the steeper the breakthrough curve, the lower the average outlet humidity becomes and the better the performance of the system.

The breakthrough curve is therefore a very important factor in determining the performance of the dehumidifier as well as the operating conditions. Actually, the shape of the breakthrough curve is determined largely by the desiccant properties mentioned previously and also by the the process thermodynamics. The following parameters influence the breakthrough curve (or equivalently the bed profiles):

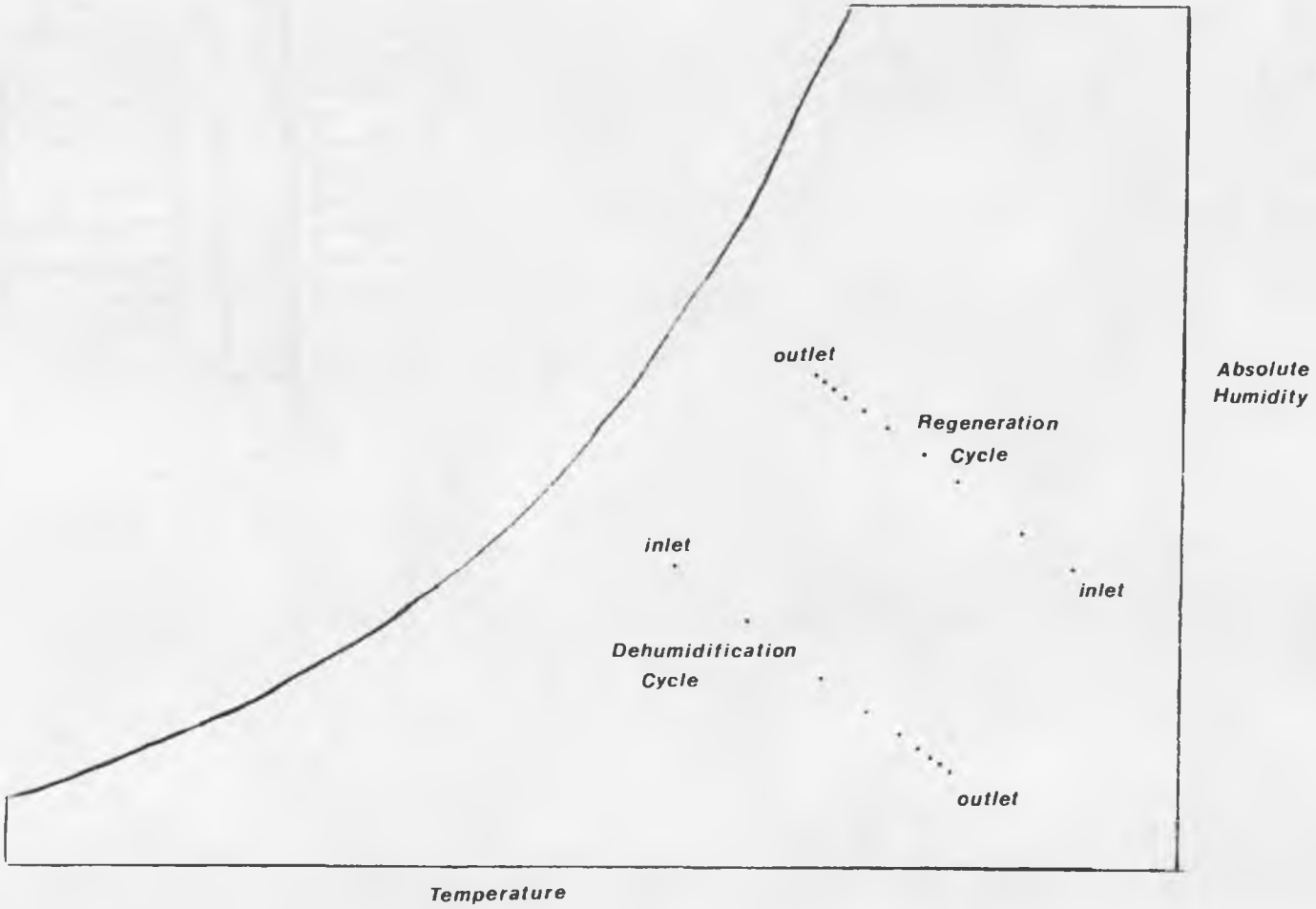

Figure 1.10 - Dehumidification (Adsorption) and Regeneration (Desorption) Breakthroughs on Psychrometric Diagram (Each point represents air conditions in a constant time increment)

A. Equilibrium Isotherm

The equilibrium isotherm influences the breakthrough of the adsorbate by influencing the velocity of the concentration or temperature wavefront. The velocity is inversely proportional to the slope of the isotherm at the concentration and temperature of any point in the bed, and is always less than or equal to the incident velocity of the air stream. Therefore, an isotherm as shown in figure 1.11 which has a convex shape in the direction of fluid concentration is considered "favorable" for adsorption. This is because areas of lower concentration, that is areas furthur down in the bed, move slower than areas of higher concentration, i.e. areas at the beginning of the bed. This causes a self-sharpening of the bed profile and consequently the breakthrough curve, which is desireable for optimium performance. Unfortunately, the opposite situation occurs for desorption assuming that the isotherm remains the same. The front of the bed now contains areas of lower concentration, and the bed profiles become more disperse, or spread as they move down the column. The longer the column, the flatter the breakthrough curve becomes.

A linear isotherm does not produce identical adsorption and desorption curves as might be expected, except in the case of isothermal operation. This is rarely the case, however, and a compromised isotherm shape most like that of silica gel has been determined to be the best available (Collier, 1986).

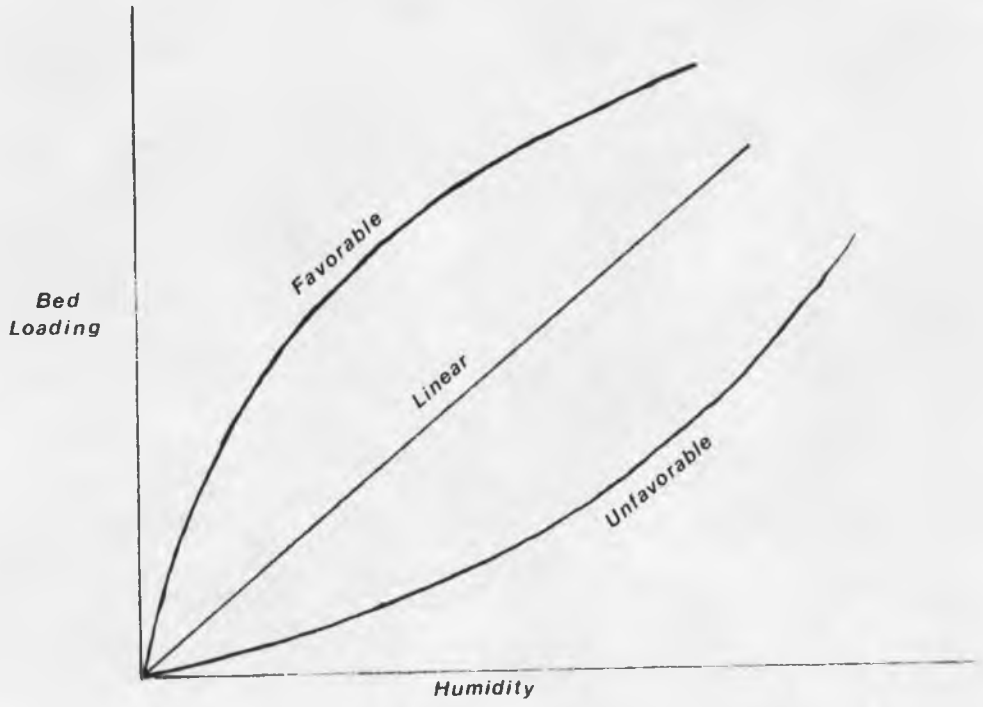

Figure 1.11- Equilibrium Isotherms

B. Heat of adsorption/absorption

The heat of absorption/adsorption influences the breakthrough curve with the amount of heat released when water vapor is condensed from the vapor phase. Usually, these values do not stray very much from the heat of condensation of water, but the temperature breakthrough can be greatly affected. The overall affect is to divert the dehumidification curve as seen in figure 1.12 from the constant enthalpy line. A heat of adsorption/absorption which is greater than the heat of condensation causes the curve to increase in slope whereas a value less than the heat of condensation causes the curve to decrease in slope. A value less than the heat of condensation is physically unrealistic, however. Therefore, any desiccant with a heat of absorption/adsorption appreciably greater than the heat of condensation of the adsorbate is not desirable.

C. Moisture diffusivity (Mass Transfer Resistance) of desiccant.

As the isotherm determines the velocity of the bed profiles, the moisture diffusivity adds resistance to this flow. Therefore, in favorable adsorption, the mass transfer curbs the sharpening effect of the isotherm and the breakthrough curve takes on a curved shape which is independent of bed length. With no dispersion, the breakthrough curve would have been a vertical step from inlet to outlet concentration as shown in figure 1.13. The effect on an unfavorable adsorption is one of furthur flattening of the curve. Desiccant configurations are desired with good mass transfer characteristics, therefore.

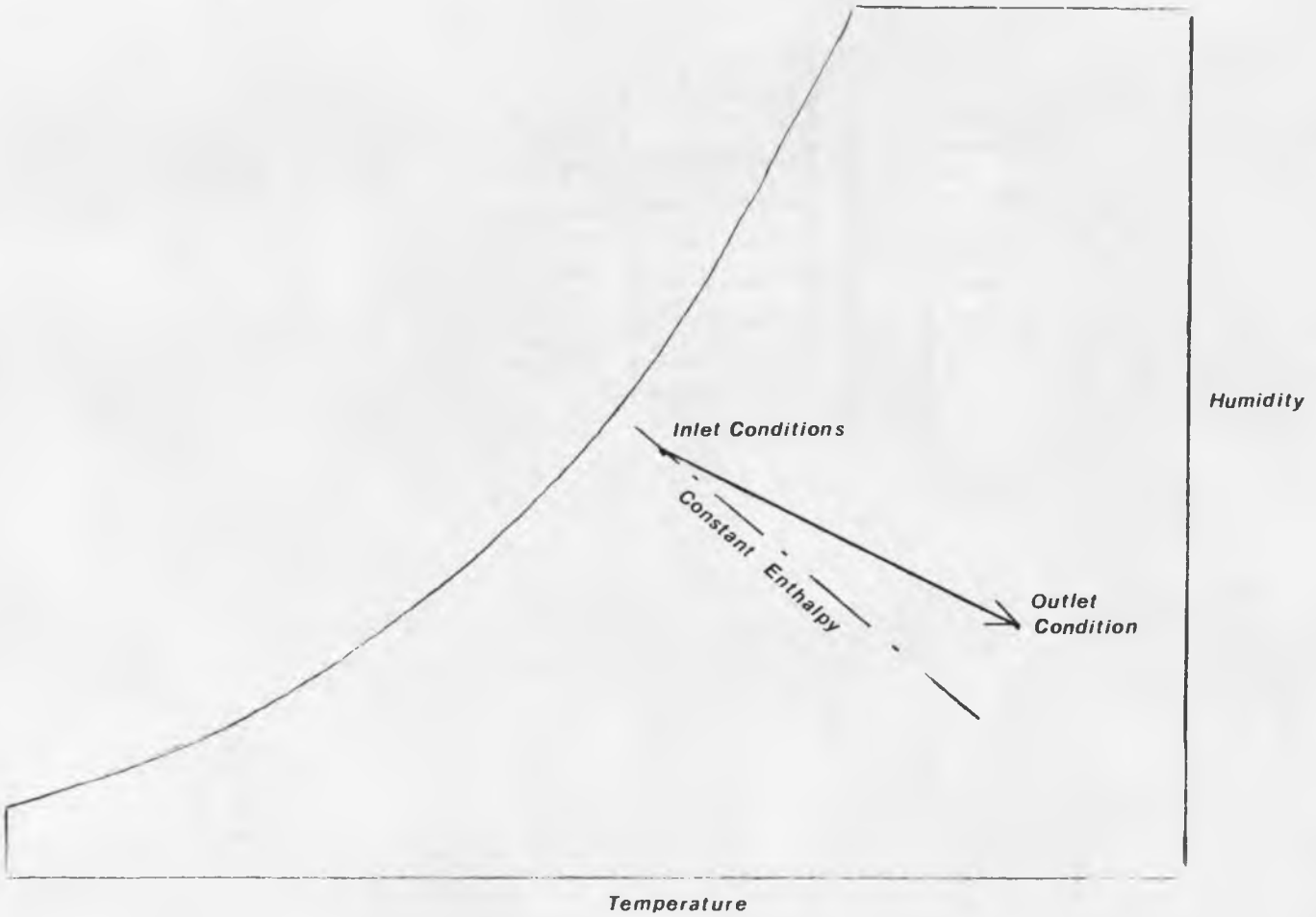

Figure 1.12- Effect of Heat of Adsorption on Breakthrough

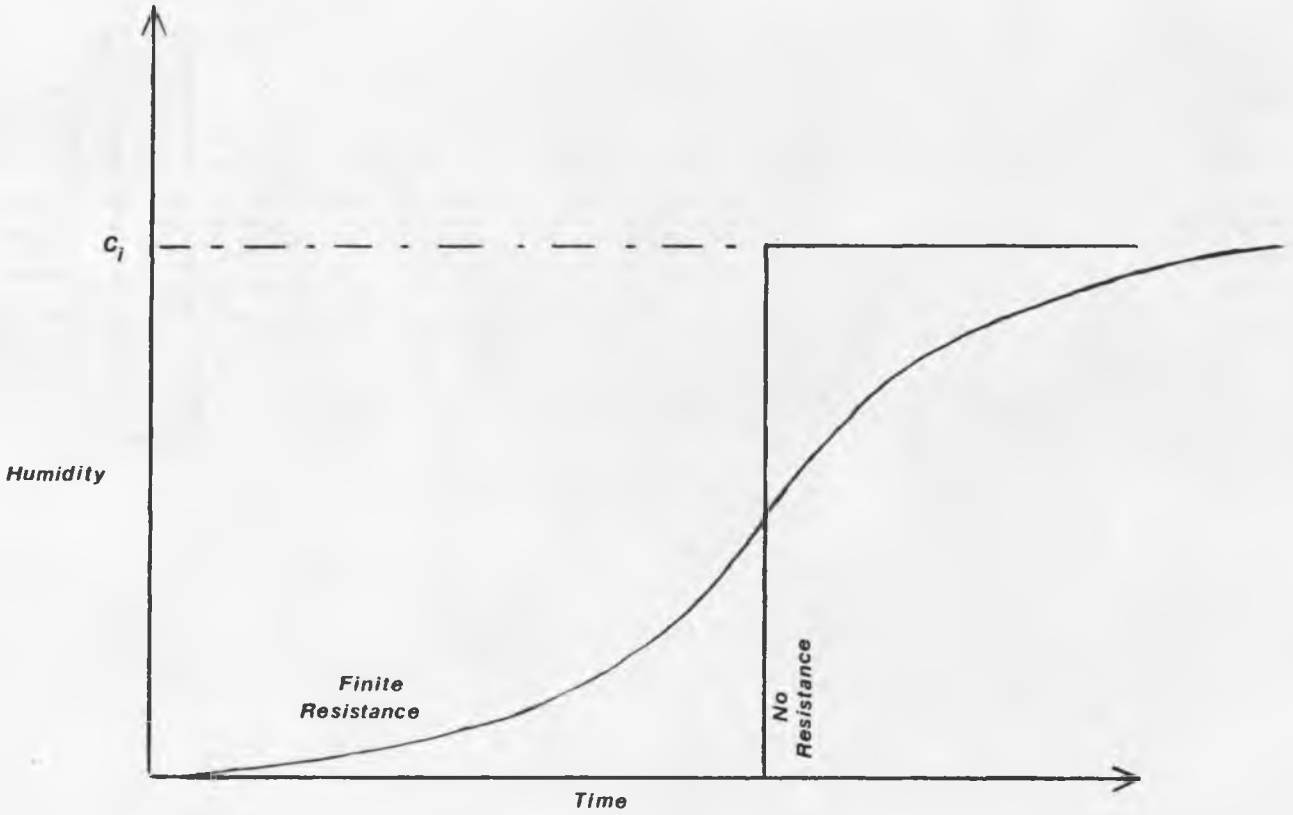

Figure 1.13- Effect of Mass Transfer Resistance on Breakthrough

D. Capacity of desiccant.

In cases where the amount of cycling is not important, the desiccant capacity (in mass adsorbate/mass desiccant) does not play a key role. The cycling rate is simply increased for a desiccant with a smaller capacity. However, when coupled with the heat capacity of the desiccant matrix, this can become significant. A rotary wheel desiccant system usually has an optimum rotation rate as a result.

1.3 ECONOMICS

The cost involved in dehumidifying the air stream can constitute the major portion of an air conditioning process. In an open cycle desiccant dehumidifier, the air stream passes through the desiccant, exchanging humidity and heat in the process. The dehumidifier must then be regenerated by removal of moisture and return to conditions prior to dehumidification. The comparison in cost between a vapor compression system and a desiccant system can then be seen to be between the cost to run the compressor and the cost to regenerate the desiccant.

Investigations (SERI, 1984) into the feasability of desiccant systems have revealed that at the present time a vapor compression system with an electrical COP of approximately 2.5 would be equivalent in operating costs to a desiccant system with a thermal COP of approximately 1.2. State of the art desiccant air conditioning systems have COP's of approximately 0.9 and with the expected cost increase in electrical energy in the future, even these low COP's can become competitive.

1.4 CURRENT RESEARCH

Desiccant dehumidification systems used for air conditioning purposes have been thoroughly researched and are becoming more and more competitive with vapor compression systems. Exhaustive research on single desiccant systems has yielded excellent system models which can be used for design purposes. Hybrid systems such as vapor compression/desiccant integrated systems have also been researched. However, all of these systems involve only a single component acting alone in a dehumidification unit or subsystem. Osborn and Hanson (1987) have developed the bi-desiccant system concept on which this work is based.

1.4.1 Solid Desiccants

For solid desiccants, such as silica gel, most systems involve a packed bed of desiccant material. Used in either a rotary wheel fashion, where the same bed undergoes adsorption and desorption cyclically, or with two beds used cyclically where one is doing the drying while the other is being regenerated. Researchers at UCLA (Biswas,1984) have investigated the use of low pressure drop desiccant beds to achieve higher performances. The Solar Energy Research Institute (SERI,1982) has extended this research which has resulted in an innovative parallel passage dehumidifier wheel design yielding possible system coefficients of performance of 1.1-1.2 BTU cooling output/BTU thermal input. The Illinois Institute of Technology (Gidaspow, 1979) has also tested a similar experimental system using two fixed bed, cross-cooled dehumidifiers of teflon sheets impregnated

with silica gel.

Theoretical investigations into advanced open cycle desiccant dehumidifiers has resulted in predictions for second law limits on thermal COP's. Lavan (1982) has calculated the thermal COP for a thermodynamically reversible process at standard test conditions as 4.66. Also, Maclaine-Cross (1985) has proposed an ideal system which utilizes no thermal energy (i.e infinite COP). These investigations are theoretical, however, and indicate that there is no limit to an open cycle system in its possible performance whereas a closed system is limited.

1.4.2 Liquid Desiccants

Liquid systems have found wide application as well. Typical systems such as tri-ethylene glycol or lithium chloride are set up with a spray dehumidification chamber for the liquid desiccant and an inclined plate solar collector or packed bed for the desiccant regeneration. An example of successfully developed commercial systems is the Kathabar Systems air conditioning units. These are finding increased use in large facilities such as hospitals, municipal buildings, etc., where facilities exist to supply cooling water to the process. However, no residential liquid desiccant unit has been developed.

Peng and Howell (1984) have investigated the regeneration of liquid desiccants and compared different methods. They concluded that regenerators which are open to the atmosphere become less effective as the temperature and humidity of the ambient air stream increase.

Therefore, system which uses process air as the regeneration air stream is recommended. Collier (1979) describes an open cycle absorption refrigeration system with a typical thermal COP of about 0.2 - 0.45. Thermal COP's for liquid systems are generally lower than solid system COP's.

Kettleborough (1983) has given a general view of the state of the technology of desiccant systems and the performance comparisons to more common systems of vapor compression. Generally, desiccant systems yield thermal COP's less than 1, while hybrid systems utilizing solar energy along with fossil energy yield better results.

Current research is being done on modelling of adsorption/absorption systems in varying degrees of complexity. Fundamental research at SERI (1985) is focusing on the understanding of sorption processes in order to assess the use of polymeric substances designed as desiccants. Research on solid desiccant rotary dehumidifiers is concentrating on obtaining optimum isotherm shape and low heat capacities. Computer simulations (Jurinak, 1984) on single desiccant systems have shown that modification of desiccant properties can produce limited increases in performance. Many models of cyclic dehumidification wheels have been proposed (Holmberg, 1979, Maclaine-Cross, 1972) which involve coupled heat and mass transfer effects, but these have yielded limited usage since they generally do not account for non-uniform inlet conditions or undeveloped temperature and concentration profiles in the bed.

1.5 OBJECTIVES

This research intends to introduce a new approach to desiccant dehumidification by using a bi-desiccant (liquid-solid) system in a manner which utilizes the strengths of each particular desiccant. One desiccant serves to dehumidify the air stream while the other desiccant regenerates the first. It has been seen that solid desiccants show superior adsorption characteristics and poor regeneration characteristics and that liquid desiccants show the opposite behavior. The use of a single desiccant therefore typically ends up in a compromise situation. In the bi-desiccant approach, one desiccant is regenerated by the other, which is then regenerated using methods commonly used for single desiccant systems. Finding suitable desiccants to fit their specific function is the key to success for this method.

In order to evaluate the performance of an experimental bi-desiccant dehumidification system, a theoretical analysis will be performed to assess maximum achievable performances as compared to single desiccant systems. Non-ideal models of a more realistic nature will then be compared (i.e. non-isothermal, non-equilibrium) in order to determine possible benefits of using a bi-desiccant system. As system performance depends heavily on material properties, both kinetic and thermodynamic, a certain degree of latitude will be given to the system parameters since there are enormous possibilities for liquid-solid combinations.

For purposes of quantitative reinforcement, experimental data will be collected for a few systems and compared with theoretical

performance determined for those systems. Hopefully in this way, the theoretical model can be validated to an extent that value judgements can be made upon possible bi-desiccant dehumidification systems.

CHAPTER 2: BREAKTHROUGH CURVE MODELS

2.1 CHOICE OF MODELS

There are many models of adsorption processes available in the literature. Their use depends upon the degree to which the real system approaches the model. If the mass transfer resistance is low, for instance, the system could be approximated by an equilibrium analysis. If the adsorbable species concentration is low enough to neglect heat effects, the system could be approximated by an isothermal analysis. If neither mass transfer resistance nor heat effects can be neglected, numerical methods of solution are normally required. Four analyses will be introduced in this section. The first deals with equilibrium behavior in isothermal systems. This is the most ideal situation since the maximum performance is obtained from a given desiccant. The second analysis deals with adiabatic equilibrium behavior and shows the reduction in performance with heat effects. The third analysis deals with isothermal behavior with mass transfer resistance. The fourth analysis will introduce a numerical method of solution of the coupled heat and mass balance equations associated with the desiccant bed.

2.2 GOVERNING EQUATIONS

The governing heat and mass balance equations are shown in figure 2.1 for a section of the desiccant bed of width Δz. The flow terms

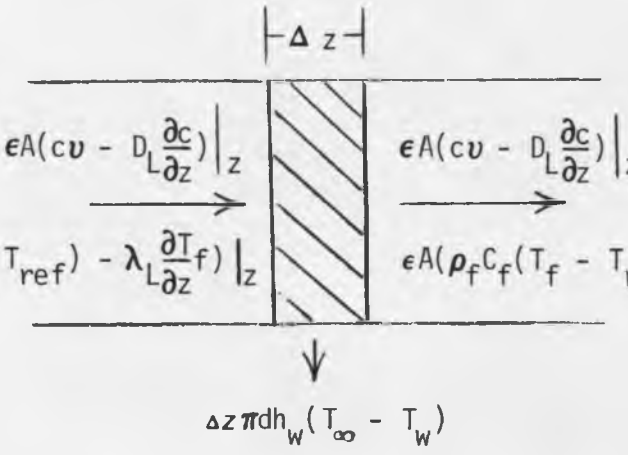

FLOW TERMS: Mass; Energy

STORAGE TERMS:

$$\epsilon A \Delta z \frac{\partial c}{\partial t}\Big|_z + \rho_b A \Delta z \frac{\partial q}{\partial t}\Big|_z \qquad \text{Mass}$$

$$\epsilon A \rho_f C_{pf} \Delta z \frac{\partial T_f}{\partial t}\Big|_z + (1-\epsilon) A \rho_s C_{ps} \Delta z \frac{\partial T_s}{\partial t}\Big|_z \qquad \text{Energy}$$

GENERATION TERMS:

$$(-\Delta H_{ads})\rho_b A \Delta z \frac{\partial q}{\partial t} \qquad \text{Energy}$$

Figure 2.1 - Governing Heat and Mass Balance Equations

include bulk flow and dispersion terms, as well as heat transfer from the bed to the surroundings through the wall. Thermal and mass storage terms include accumulation in the fluid as well as the solid fraction and generation includes only the heat of adsorption. Using the law of conservation of mass and energy, i.e.

$$\text{INPUT} - \text{OUTPUT} + \text{GENERATION} = \text{ACCUMULATION}$$

we have the following expression for the material balance (dividing by $\epsilon A \Delta z$ and taking the limit as Δz goes to zero),

$$v\frac{\partial c}{\partial z} - D_L\frac{\partial^2 c}{\partial z^2} + \frac{\rho_b}{\epsilon}\frac{\partial q}{\partial t} + \frac{\partial c}{\partial t} = 0 \qquad (2\text{-}1)$$

and for the energy balance,

$$\rho_f v C_{pf}\frac{\partial T_f}{\partial z} - \lambda_L\frac{\partial^2 T_f}{\partial z^2} + \rho_f C_{pf}\frac{\partial T_f}{\partial t} + \frac{(1-\epsilon)}{\epsilon}\rho_s C_{ps}\frac{\partial T_s}{\partial t} =$$

$$-\Delta H_{ads}\frac{\rho_b}{\epsilon}\frac{\partial q}{\partial t} - \frac{4h_w}{d\epsilon}(T_\infty - T_w) \qquad (2\text{-}2)$$

From these governing equations, the method of solution can be chosen by making the appropriate assumptions and reducing the equations to the desired form.

2.3 DERIVATION OF SOLUTIONS

2.3.1 Isothermal Equilibrium Analysis (Ruthven, 1982)

This method is commonly called the "Local Equilibrium Theory" and solution is by the method of characteristics. The analysis assumes that there is no mass transfer resistance (equilibrium at all points in the column), and that the process is isothermal. For this system, assuming plug flow and no axial dispersion, the mass balance for the adsorbable species becomes:

$$v\frac{\partial c}{\partial z} + \frac{\rho_b}{\epsilon}\frac{\partial q}{\partial t} + \frac{\partial c}{\partial t} = 0 \qquad (2\text{-}3)$$

The equilibrium isotherm is a function of concentration only and is represented as follows:

$$q^* = f(c)$$

Assuming no mass transfer resistance

$$\frac{\partial q}{\partial t} = \frac{\partial q^*}{\partial t} = \frac{dq^*}{dc}\frac{\partial c}{\partial t}$$

Equation (2-3) therefore becomes

$$\frac{\partial c}{\partial t} + \omega(c)\frac{\partial c}{\partial z} = 0 \qquad (2\text{-}4)$$

Where

$$\omega(c) = \frac{v}{\left(1 + \frac{\rho_b}{\epsilon}\frac{dq^*}{dc}\right)}$$

is the concentration wave velocity. The solvent fluid travels at velocity v, which is greater than ω . This is because the adsorbable

species spends part of its time in the fixed state while the fluid is moving past it. The concentration wave velocity thus varies between zero and the fluid velocity.

Method of Characteristics (Sherwood)

If equation (2-4) is compared to the total differential,

$$dc = \frac{\partial c}{\partial t}dt + \frac{\partial c}{\partial z}dz$$

$$0 = \frac{\partial c}{\partial t} + \omega(c)\frac{\partial c}{\partial z}$$

then with the use of Kramer's rule;

$$\frac{\partial c}{\partial t} = \frac{\begin{vmatrix} 0 & v \\ dc & dz \end{vmatrix}}{\begin{vmatrix} 1+\frac{\rho_b}{\epsilon} f'(c) & v \\ dt & dz \end{vmatrix}}$$

It can be seen that certain ratios of dz to dt make the denominator equal to 0. When this occurs, the numerator must also be equal to 0 in order for $\frac{\partial c}{\partial t}$ to be finite. Then dc must be zero. These ratios are designated as characteristic directions in the z-t plane. Concentration c is constant along the "characteristic lines" corresponding to

$$\frac{dz}{dt} = \frac{v}{1 + (\rho_b/\epsilon)f'(c)} \qquad (2\text{-}5)$$

so that along any of these characteristic lines, the concentration remains the same for corresponding values of z and t.

Figure 2.2 is a graphical representation of a fixed bed adsorption and desorption process in which the isotherm has a type 1, or Langmuir shape. This indicates that the desiccant is favorable for adsorption but unfavorable for desorption. This can be understood by examining the characteristic lines for adsorption (a) and desorption (b). Since $\omega(c)$ for a favorable isotherm is greater at higher concentrations than at lower concentrations, the characteristic lines for the bed inlet are shown to be steeper than those for the fluid initially in the column. The two families of lines intersect each other and at the point of intersection the concentration has two values, and the solution becomes discontinuous. This produces a "shock" wave as shown and the velocity of this wave must be calculated from a material balance instead of from equation 2-5. This is done by considering the amount of solute flowing in the fluid stream over a time period t. This is adsorbed into the bed and the outlet concentration of the fluid stream is that which is in equilibrium with the initial bed loading. The amount removed from the air stream is therefore equal to $A(c_o-c^*)v\epsilon t$. The amount of solute accumulated in the column is equal to $A(\epsilon(c_o-c^*)z + \rho_b(q^*-q_o)z)$. Equating the two quantities gives

$$\frac{z}{t} = \frac{v}{1 + \frac{\rho_b}{\epsilon}\left(\frac{q^*-q_o}{c_o-c^*}\right)} \qquad (2\text{-}6)$$

which is the velocity (constant) of the shock front. In this equation, q^* represents the loading of the column in equilibrium with

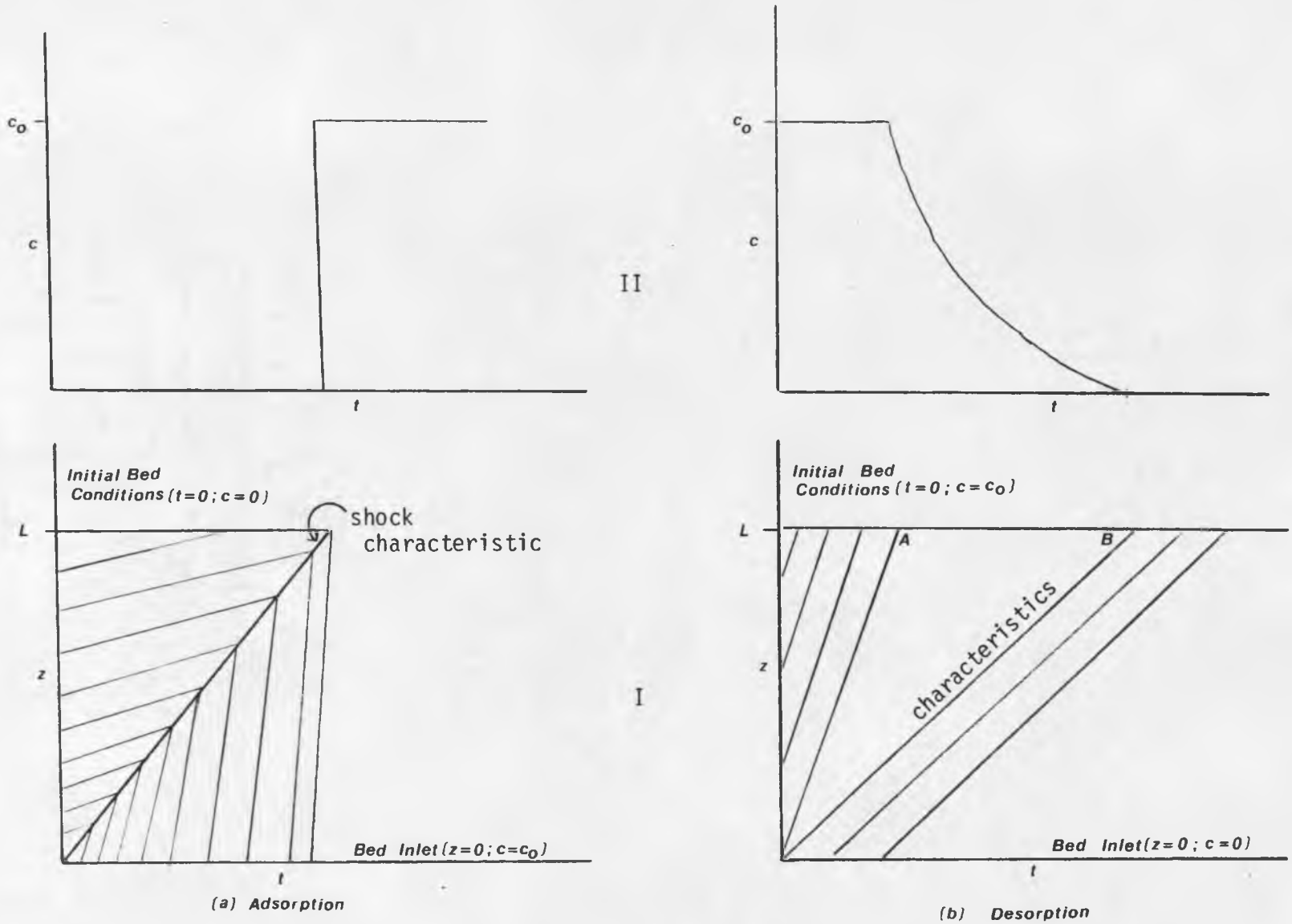

Figure 2.2 - Representation of Isothermal Adsorption and Desorption ; Equilibrium Solution
(I = z-t Characteristics, II = Breakthrough curves)

the inlet stream concentration and c^* represents the outlet stream concentration in equilibrium with the initial loading of the column.

For the desorption case, the family of characteristic curves for the bed inlet are flatter than those for the initial column conditions. Then the region between points A and B constitutes the proportionate pattern region of the breakthrough curve. For times between times t_A and t_B, characteristics have slopes lying between the extremes and the concentration at corresponding points is determined from the slope of these lines using the equation

$$\frac{z}{t} = \frac{v}{1 + (\rho_b/\epsilon)f'(c)} \qquad (2\text{-}7)$$

In the case of an isotherm with an inflection, such as a BET isotherm, the wavefront consists of a shock front followed by a dispersive wave as shown by figure 2.3. The transition occurs at the tangent of the isotherm which passes through the origin (in the case of an initially adsorbate-free bed), since the slope must equal $\Delta q/\Delta c$. The breakthrough curve therefore has an abrupt jump in outlet humidity and from then on becomes a dispersive front which flattens with increased bed length. The jump height remains the same at all times since the transition composition must remain the same per the isotherm.

2.3.2 Adiabatic Equilibrium Analysis (Rhee & Amundson, 1970)

If the total enthalpy of the system, like the mass, is conserved, enthalpy can be considered as an additional component. The system then becomes one of coupled temperature and concentration effects.

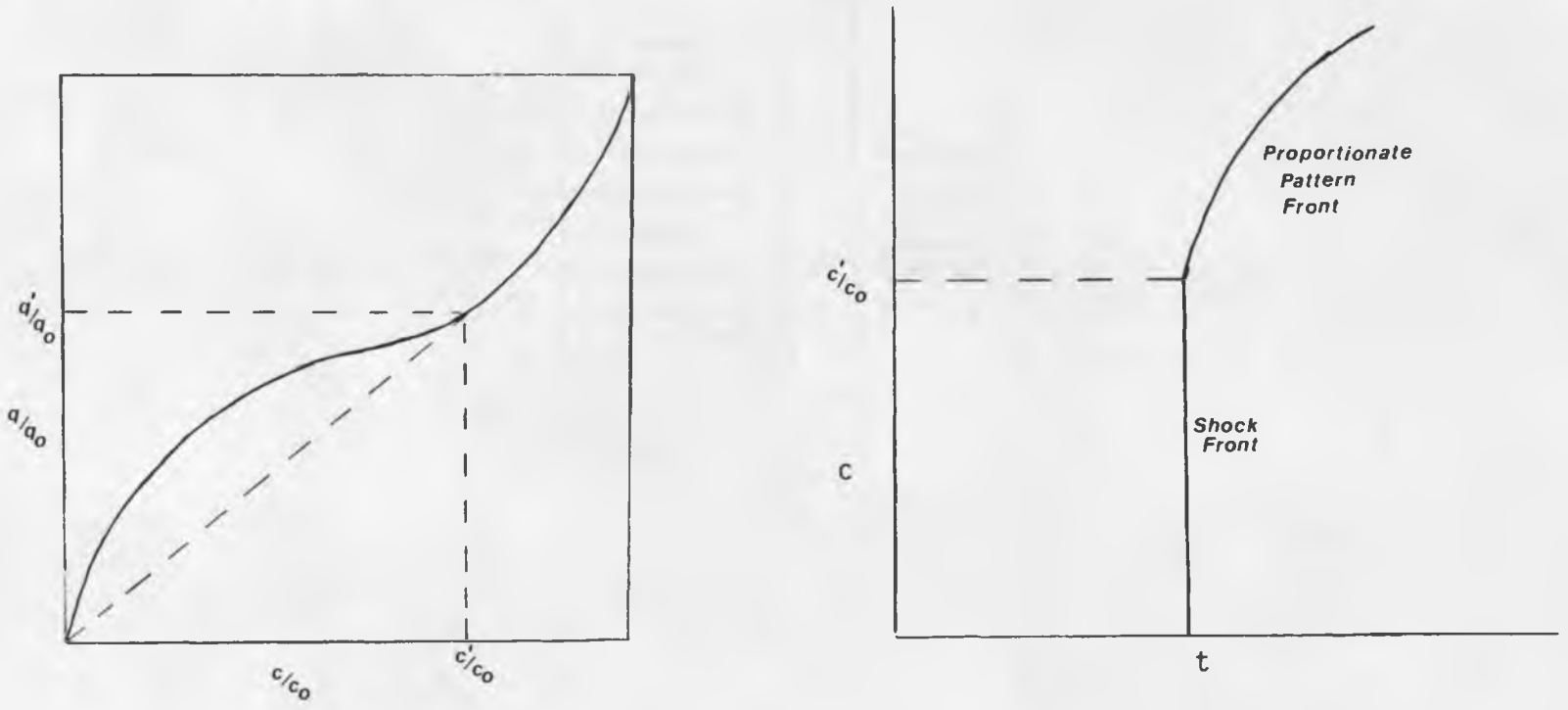

Figure 2.3 - Effect of BET Isotherm on Breakthrough.

Since the system is still in equilibrium, the method of characteristics can still be used to determine breakthrough curves as well as bed profiles. However, a relation must be found between concentration and temperature in order to determine the coupled concentration and temperature breakthrough curves. The equilibrium theory of adiabatic adsorption has been thoroughly expanded by Amundson (1970) and Glueckauf, and generalized by Ruthven (1982). The treatment of Glueckauf is followed here for brevity.

In order to evaluate the effect of temperature on the concentration breakthrough, coherence is assumed between the temperature and concentration fronts. This means that a given concentration which moves along the bed always carries with it an accompanying temperature. Therefore, the temperature and concentration breakthroughs will both spread (or sharpen) simultaneously. The mathematical justification for the assumption of coherent fronts has been proven and is beyond the scope of this text. The assumption requires that the characteristic wave velocities of the temperature and concentration fronts are the same.

For this system, assuming no heat flux from the walls of the column and no axial heat conduction, the differential mass and heat balances become:

$$v\frac{\partial c}{\partial z} + \frac{\partial c}{\partial t} + \frac{\rho_b}{\epsilon}\frac{\partial q}{\partial t} = 0 \qquad (2\text{-}8)$$

and

$$\rho_f C_f v\frac{\partial T_f}{\partial z} + \rho_f C_f\frac{\partial T_f}{\partial t} + C_s\frac{\rho_b}{\epsilon}\frac{\partial T_s}{\partial t} = -\Delta H_{ads}\frac{\rho_b}{\epsilon}\frac{\partial q}{\partial t} \qquad (2\text{-}9)$$

Mass and thermal equilibrium dictate that:

$$T_s = T_f = T$$

$$q = q^* = f(c,T)$$

$$\frac{\partial q}{\partial t} = \frac{dq^*}{dc}\frac{\partial c}{\partial t} = \frac{dq^*}{dT}\frac{\partial T}{\partial t}$$

Equations (2-8) and (2-9) then become

$$\frac{\partial c}{\partial z} + \frac{1}{\omega_c}\frac{\partial c}{\partial t} = 0$$

and

$$\frac{\partial T}{\partial z} + \frac{1}{\omega_T}\frac{\partial T}{\partial t} = 0$$

respectively.

The propagation velocities are given as follows:

$$\omega_c = \frac{v}{\left(1+\frac{\rho_b}{\epsilon}\frac{dq^*}{dc}\right)} \qquad (2\text{-}10)$$

and

$$\omega_T = \frac{v}{\left(1+\frac{\rho_b}{\epsilon\rho_f}\frac{C_s}{C_f} - \frac{-\Delta H_{ads}}{C_f}\frac{\rho_b}{\epsilon\rho_f}\frac{dq^*}{dT}\right)} \qquad (2\text{-}11)$$

Assuming these velocities are equal to each other, according to the coherence condition:

$$\frac{dq^*}{dc} = \frac{C_s}{\rho_f C_f} - \frac{-\Delta H_{ads}}{\rho_f C_f}\frac{dq^*}{dT} \qquad (2\text{-}12)$$

This equation can be expanded according to partial differentials to yield:

$$\frac{\partial q^*}{\partial c} + \frac{\partial q}{\partial T}\frac{dT}{dc} = \frac{C_s}{\rho_f C_f} - \frac{-\Delta H_{ads}}{\rho_f Cf}\left(\frac{\partial q^*}{\partial T} + \frac{\partial q^*}{\partial c}\frac{dc}{dT}\right) \qquad (2\text{-}13)$$

Rearranging this equation yields a quadratic equation for $\frac{dT}{dc}$:

$$\frac{\partial q^*}{\partial T}\left(\frac{dT}{dc}\right)^2 + \left(\frac{\partial q^*}{\partial c} - \frac{C_s}{\rho_f C_f} + \frac{-\Delta H_{ads}}{\rho_f C_f}\frac{\partial q^*}{\partial T}\right)\frac{dT}{dc} + \frac{-\Delta H_{ads}}{\rho_f C_f}\frac{\partial q^*}{\partial c} = 0 \qquad (2\text{-}14)$$

All derivatives can be evaluated from the equilibrium isotherms, provided the temperature dependence is known. Corresponding to the two roots of the above equation, there are two families of curves (Γ^+ and Γ^-) and two corresponding velocities (ω^+ and ω^-), at each point (T,c). The path between any two points (T_o,c_o) and (T_f,c_f) will follow along these characteristic c-T curves which, when coupled with the isothermal z-t characteristics described earlier, produce the desired breakthrough curves.

The c-T characteristics must be calculated numerically, i.e.

$$T' = T_o - \Delta T \qquad c' = c_o - \left.\frac{dc}{dT}\right|_{T_o,c_o}\Delta T$$

$$T'' = T' - \Delta T \qquad c'' = c' - \left.\frac{dc}{dt}\right|_{T',c'}\Delta T$$

where dc/dT is given by the roots of equation (2-14). An example of a characteristic plot (c vs. T) calculated in this way is given in figure 2.4. Each point (c,T) has two coherent wave velocities and there are two families of curves produced corresponding to the two

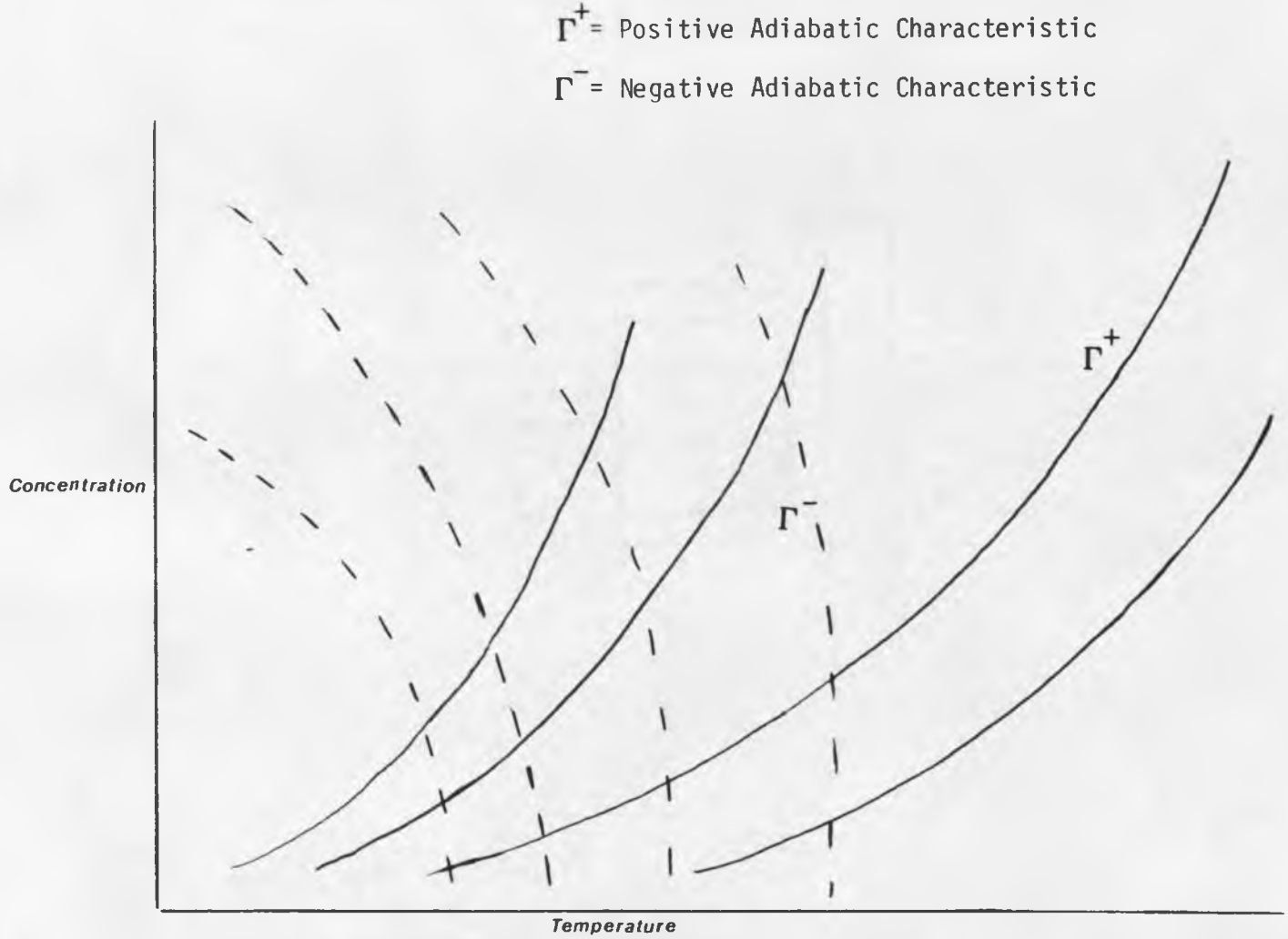

Figure 2.4 - Representative Adiabatic Characteristics of a Desiccant Material (Dehumidification/Regeneration proceeds along a pair of these lines determined by the initial and final states)

different roots of the equation. The positive root is always associated with the higher wave velocity.

Figure 2.5 shows an example of how the z-t and c-T plots are coordinated to calculate adiabatic breakthrough curves.

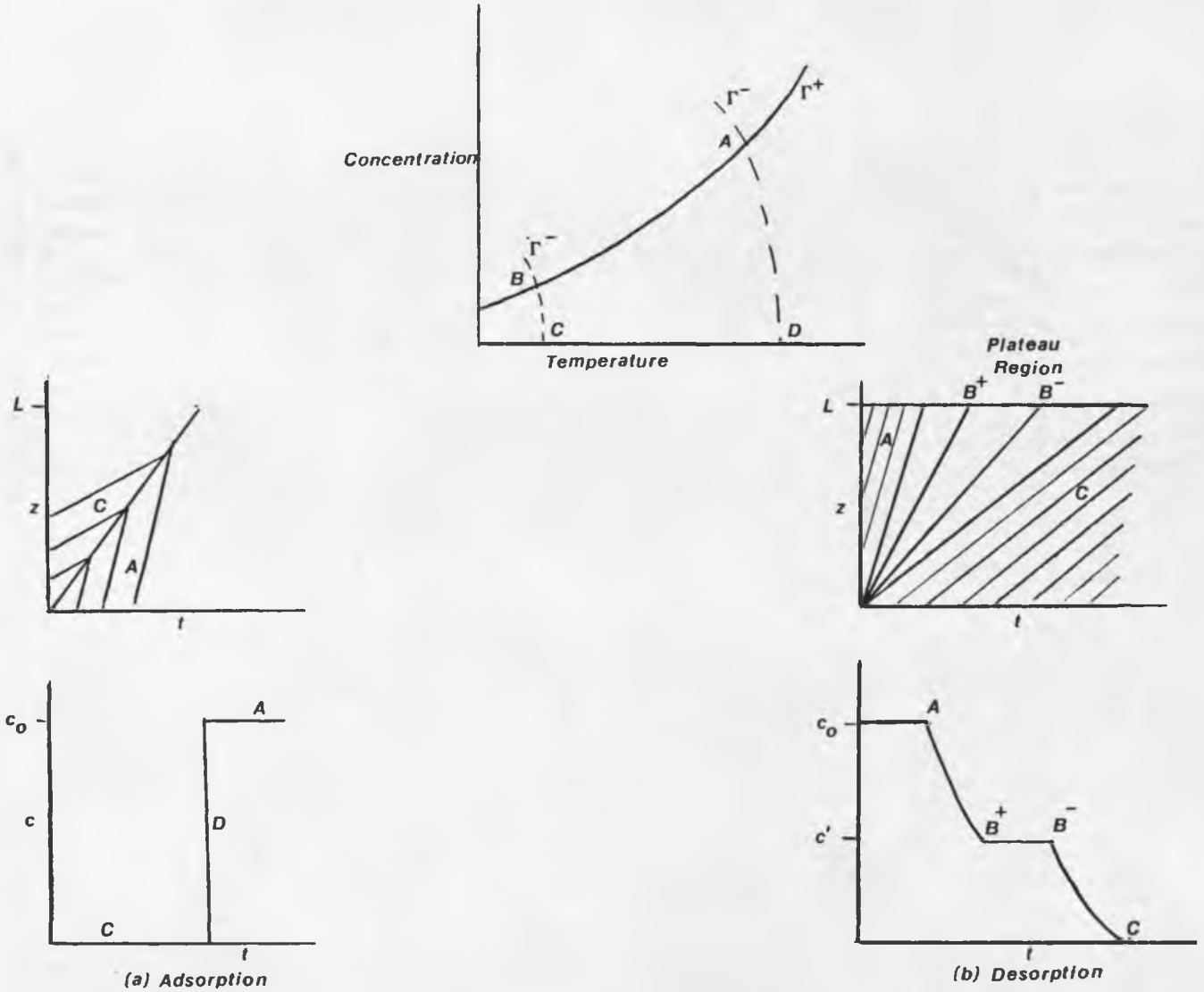

Figure 2.5 - Representation of Adiabatic Dehumidification and Regeneration ; Equibrium Solution (I = Breakthrough, II = z-t Characteristics, III = Adiabatic Characteristics)

2.3.3 Isothermal Analysis with Finite Mass Transfer Resistance

The effect of mass transfer resistance on the concentration breakthrough of a packed bed system can be very great. Analytic results can be achieved if the assumptions are made that the system is isothermal, axial plug flow, and that storage terms in the fluid are neglegible compared to the bulk flow. Assuming a linear isotherm:

$$\frac{\partial c}{\partial z} + \frac{\rho_b}{\epsilon}\frac{\partial q}{\partial t} = 0 \qquad (2\text{-}15)$$

There are two ways to attack this problem. One is to assume a priori a linear driving force mechanism to characterize the mass flux into the solid particles (Thomas, Hougen). The other method is to couple the mass balance equation with the equation for radial diffusion into a spherical particle and solve simultaneously (Rosen, 1954). The first method will be shown here since both methods yield very similar results.

Assuming a linear driving force:

$$\frac{\partial q}{\partial t} = \frac{K_f a}{\rho_b}(c-c^*) \qquad (2\text{-}16)$$

where c^* is the equilibrium value of fluid concentration

A linear isotherm dictates:

$$q^* = K_D c^* \qquad (2\text{-}17)$$

De-dimensionalizing the above coupled differential equations;

$$\zeta = \frac{ZK_f a}{\epsilon v}$$

$$\tau = \frac{K_f a}{K_D \rho_b}(t - z/v)$$

$$X = \frac{c}{c_o}$$

$$Q = \frac{q}{q^*} = \frac{q}{K_D c_o}$$

This leads to the coupled differential equations;

$$\frac{\partial Q}{\partial \tau} = X - Q$$

$$\frac{\partial X}{\partial \zeta} = -X + Q$$

with boundary conditions;

$c = c_o$	at	$z = 0$	
$q = 0$	at	$t - z/v = 0$	
$X = 1$	at	$\zeta = 0$	for all τ
$Q = 0$	at	$\tau = 0$	for all ζ

The solution using the Laplace transform method is:

$$X = 1 - \int_{\epsilon}^{\zeta} (-\tau+\zeta) J_o(i\sqrt{4\zeta\tau})\, d\zeta = J(\tau,\zeta) \qquad (2\text{-}18)$$

$$Q = \int_{\epsilon}^{\tau} (-\tau+\zeta) J_o(i\sqrt{4\zeta\tau})\, d\tau \qquad (2\text{-}19)$$

2.3.3 Adiabatic Adsorption with Finite Heat and Mass Transfer Resistance : Numerical Solution (from Cooney, 1974)

This analysis solves the heat and mass continuity equations numerically coupled with linear driving force expressions for the heat and mass transfer coefficients. The axial diffusion is again assumed to be negilgible, and the inlet feed conditions are assumed to be uniform along with the initial bed conditions.

The solute continuity equation remains:

$$v\frac{\partial c}{\partial z} + \frac{\partial c}{\partial t} + \frac{\rho_b}{\epsilon}\frac{\partial q}{\partial t} = 0 \qquad (2\text{-}20)$$

The energy balance equation for the system becomes:

$$v\frac{\partial T_f}{\partial z} + \frac{\partial T_f}{\partial t} + \frac{\rho_b}{\epsilon\rho_f}\frac{C_s}{C_f}\frac{\partial T_s}{\partial t} + (-\Delta H_{ads})\frac{\rho_b}{\epsilon\rho_f C_f}\frac{\partial q}{\partial t} = 0 \qquad (2\text{-}21)$$

This equation assumes no axial heat conduction, constant heat capacities and differing fluid and solid temperatures. The following linearized rate equations for mass and energy balances in the solid phase were also used:

$$\frac{\partial q}{\partial t} = \frac{K_p a}{\rho_b}(q^*-q) \qquad (2\text{-}22)$$

$$\frac{\partial T_s}{\partial t} = \frac{h^a}{\rho_b C_s}(T_f - T_s) - (-\Delta H_{ads})\frac{1}{C_s}\frac{\partial q}{\partial t} \qquad (2\text{-}23)$$

Boundary conditions are such that at time zero, temperature and concentration values in the bed are considered uniform. Also, the inlet feed conditions are considered constant throughout the processes of adsorption and desorption.

The numerical algorithm follows a finite difference method of solution. Each time derivative is replaced with a simple first order forward difference, e.g.

$$\frac{\partial c}{\partial t} = \frac{c(i,t+\Delta t) - c(i,t)}{\Delta t}$$

and each distance derivative is replaced with a simple backward difference, e.g.

$$\frac{\partial c}{\partial \zeta} = \frac{c(i,t) - c(i-1,t)}{\Delta z}$$

Equations (2-20) - (2-23) are then replaced by the following difference equations:

$$\text{(a)}\quad c(i,t+\Delta t) = c(i,t) + \frac{v\Delta t}{\Delta z}[c(i-1,t) - c(i,t)] + A[q(i,t) - q(i,t+\Delta t)]$$

$$\text{(b)}\quad T_f(i,t+\Delta t) = T_f(i,t) + B[T_s(i,t) - T_s(i,t+\Delta t)] + \frac{v\Delta t}{\Delta z}[T_f(i-1,t) - T_f(i,t)] + D[q(i,t) - q(i,t+\Delta t)]$$

$$\text{(c)}\quad q(i,t+\Delta t) = E\Delta t[q^*(i,t) - q(i,t)] + q(i,t)$$

$$\text{(d)}\quad T_s(i,t+\Delta t) = F\Delta t[T_f(i,t) - T_s(i,t)] + T_s(i,t) + G[q(i,t) - q(i,t+\Delta t)]$$

where the coefficients are defined from the differential equations as follows:

$$A = \frac{\rho_b}{\epsilon}$$

$$B = \frac{C_s}{A\rho_f C_f}$$

$$D = \frac{-\Delta H_{ads}}{A\rho_f C_f}$$

$$E = \frac{K_p a}{\rho_b}$$

$$F = \frac{ha}{\rho_b C_s}$$

$$G = \frac{-\Delta H_{ads}}{C_s}$$

The loading, q, is first calculated for the first spacial increment at the first time increment using equation (c). Using this new value, the new concentration and solid temperature are calculated with equations (a) and (d). The new value for the gas temperature is then calculated using equation (b). This process is then repeated for the next spacial increment until the entire bed has been done for the first time increment. This is repeated for as many time increments as are needed.

This is an explicit algorithm and is therefore stable only for a specified range of values of the ratio $\Delta t/\Delta z$. A stability analysis shows that the interval of convergence for this model is :

$$0 \leq \frac{\Delta t}{\Delta z} \leq \frac{1}{v}$$

2.4 PHASE EQUILIBRIUM AND KINETIC MODELS

The system chosen for analysis consists of Silica Gel for the solid and Ethylene Glycol for the liquid desiccant. The breakthrough models discussed earlier will be used to compare the performance of these two desiccants in a packed bed system and also to estimate the performance of the chosen bi-desiccant set-up. Physical and equilibrium data for the desiccants are well documented in the literature. However, the equilibrium between the liquid and the solid will affect the effectiveness of the bi-desiccant as a dehumidifier.

2.4.1 Mass and Heat Transfer in Packed Beds

Figure 2.6 shows the actual mass transfer processes that go on in a solid or liquid desiccant. It is seen that the solid desiccant process consists of diffusion from the gas phase to the solid surface followed by pore diffusion into the particle where most of the actual physical adsorption takes place. The rate of adsorption onto the solid is assumed to be infinitely faster than the rate of diffusion to the surface so that the effectiveness factor is nearly 0, and the adsorption process is not considered in the overall resistance. The liquid system, in which the liquid covers glass beads to provide surface area, shows no particle porosity and therefore the absorption takes place at the surface of the particle followed by diffusion into the liquid. Once again, the process of absorption at the liquid surface is assumed to be instantaneous.

A bi-desiccant set-up as shown in part 3 of figure 2.6 has characteristics of both systems. The absorbent/adsorbent must first

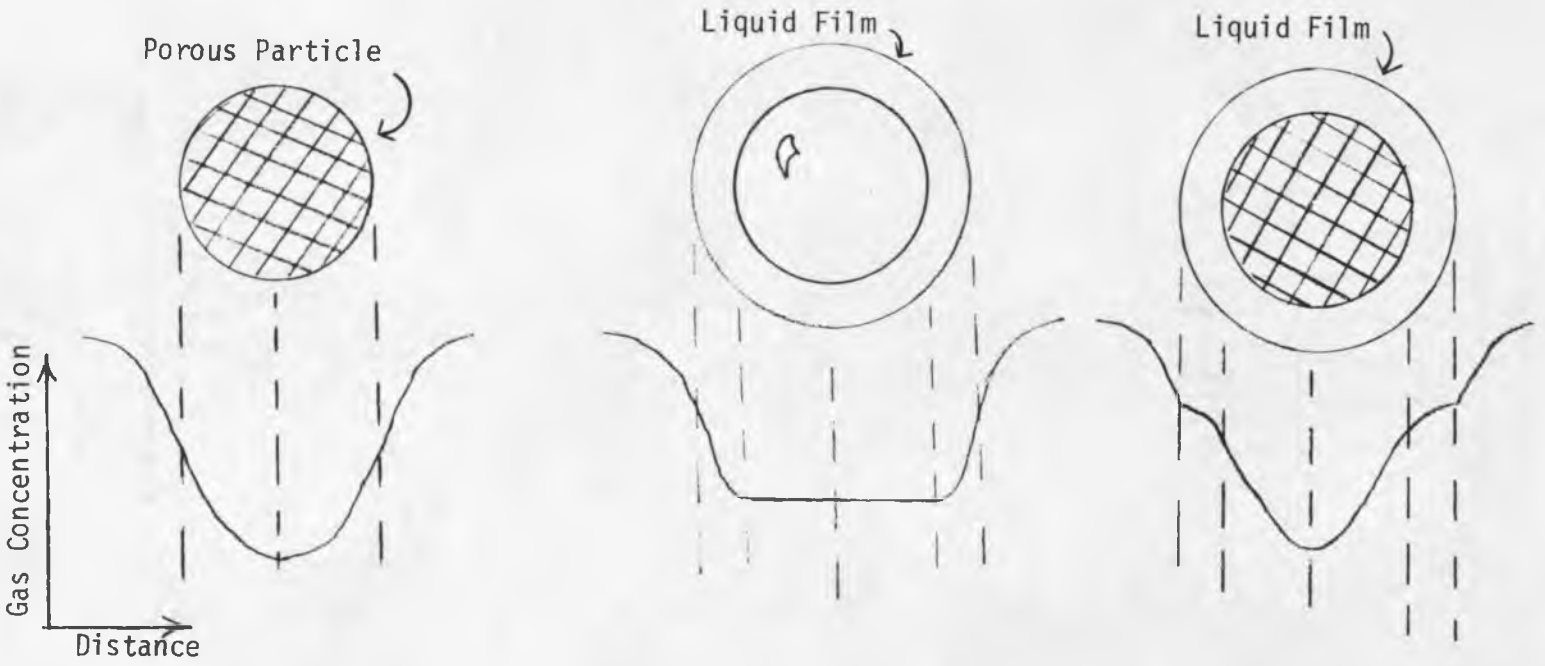

1. Solid Desiccant

2. Liquid Desiccant

3. Bi-Desiccant

Figure 2.6 - Mass Transfer Processes in Porous Particles

diffuse through the liquid layer and then into the pores before it reaches the surface of the solid. The rate of pore diffusion is therefore greatly reduced.

The rate of uptake of water vapor into a desiccant particle (in units of mass/time) can be represented by the equation for local transport through the fluid film:

$$N_w = \rho_f(\epsilon V)\, k_f a(c - c_i) \qquad (2\text{-}24)$$

or alternatively by the local uptake into the particle:

$$N_w = \rho_b V\, k_p a(q_i - q) \qquad (2\text{-}25)$$

where

c = fluid concentration of air stream

c_i = fluid concentration at particle interface

q = loading of particle in the interior

q_i = loading at particle/fluid interface

The mass transfer rate in both phases must be the same, therefore the two expressions (2-24) and (2-25) can be set equal.

The two gradients, one in the fluid film and one in the desiccant, are related to each other by the equilibrium isotherm as follows:

$$q^* = f(c,T)$$

Averaging the slope of the isotherm over the concentration range of interest, the following variable transformation can be made in the

fluid rate expression,

$$(c - c_i) = (q^* - q_i)/m$$

where q^* represents the loading in the solid which is in equilibrium with the incident fluid concentration. The slope of the isotherm is represented by m. With this transformation, an overall mass transfer coefficient can be calculated as follows:

$$N_w/V = K_p a\,(q^* - q)$$

where

$$K_p a = \left(\frac{1}{k_p a \rho_b} + \frac{m}{\epsilon \rho_f k_f a} \right)^{-1}$$

where $K_p a$ represents the overall mass transfer coefficient. Due to the huge difference in density between the desiccant and the air stream in most cases, the local coefficient for the gas phase is usually the more controlling influence.

The rate of uptake into the desiccant is then represented in terms of the differential increase of loading as

$$\frac{\partial q}{\partial t} = \frac{K_p a}{\rho_b} (q^* - q)$$

This equation is used for all estimations of mass transfer coefficient assuming linear approximations to equilibrium expressions.

Estimations for local mass and heat transfer coefficients have been correlated by many authors in the literature. The following expression, given by Wakao and Funazkri (1978), relates to the bulk diffusion from the gas phase to the solid particle surface in a packed

bed of desiccant material:

$$Sh = 2.0 + 1.1\ Sc^{0.33}Re^{0.6}$$

where

$$Sh = k_f d_p / D_{AB}$$

$$Sc = \mu_f / \rho_f D_{AB} \simeq 0.6 \quad \text{for air}$$

$$3.0 < Re < 10^4$$

This analogy is also directly transferrable to heat transfer as follows:

$$Nu = 2.0 + 1.1 Pr^{0.33}Re^{0.6}$$

where

$$Nu = h_f d_p / \lambda_f$$

The heat transfer resistance of the the desiccant particle is considered much less than that of the gas phase itself so that only the local gas phase coefficient is used as the overall coefficient.

For diffusion into the particle itself, the following equation (recommended by Helfferich) is used:

$$k_p = 10 D_{eff} / d_p (1-\epsilon)$$

This relation can be used to estimate the effective mass transfer coefficient into the porous particle and also the mass transfer through the stagnant liquid film surrounding the particle.

2.4.2 Solid & Liquid Desiccant Properties and Phase Equilibrium

Table 2.1 lists some physical properties of the two desiccants. Tables 2.2 and 2.3 list phase equilibrium behaviour at various temperatures for silica gel and ethylene glycol, respectively. The silica gel desiccant shows evidence of Type 1 behaviour (favorable for adsorption) whereas the ethylene glycol shows evidence of Type 3 behaviour (unfavorable for adsorption). This immediately indicates that the silica gel would be more applicable to an adsorption and the glycol would be more applicable to a desorption process.

Silica Gel

An equation has been fitted to the equilibrium data in table 2.2 which follows the form of the Langmuir isotherm equation as follows:

$$q = \frac{KQ_m c}{1 + Kc}$$

where

$$K(T) = 370.68 \text{ EXP} \left[\frac{-\Delta H_{ads}}{R} \left(\frac{1}{T} - \frac{1}{T_{ref}} \right) \right]$$

$$\Delta H_{ads} = -10{,}343 \text{ cal/mol}$$

$$R = 1.987 \text{ cal/mol-°K}$$

$$T_{ref} = 273.16 \text{ °K}$$

$$Q_m = 0.022 \text{ moles/g} \quad (= \text{maximum adsorption capacity})$$

These parameters were calculated using a least squares fit of the data and correlate well with expected values for the heat of adsorption (10 - 12 kcal/mol) and the maximum adsorption capacity Q_m. Figure 2.7 shows the calculated isotherms for 60,80,100 and 120° F.

Table 2.1 - Physical Properties

Silica Gel (6-16 mesh)

True Density = 137 lbs/ft^3

Bulk Density = 45 lbs/ft^3

Specific Heat = 0.22 BTU/lb-°F

Thermal Conductivity = 1.0 BTU/(ft^2-hr-°F-in)

Average Porosity = 50 - 65 %

Surface Area = 720 - 760 m^2/gram

Heat of Adsorption of H_2O = 1200 - 1400 BTU/lb H_2O

Ethylene Glycol

Formula = $C_2H_6O_2$

Molecular Weight = 62.1

Normal Boiling Point = 197.6 °C

Freezing Point = -12.7 °C

Density at 77 °F = 1.110 g/ml

Specific Heat = 0.58 BTU/lb-°F

Heat of Solution at Infinite Dilution = 72 BTU/lb H_2O

Heat of Absorption of H_2O = 1120 Btu/lb

Table 2.2 - Silica Gel Isotherm Data (from Literature)

Temperature (°F)= 60

Loading [g/g solid]	Humidity [°F DP]	Humidity [g/g dry air]
0.02	-36	0.0001
0.0375	-16	0.00033
0.0775	6	0.00108
0.105	18	0.00197
0.21	35	0.00428
0.35	53	0.00857

Temperature (°F) = 80

Loading [g/g solid]	Humidity [°F DP]	Humidity [g/g dry air]
0.012	-36	0.0001
0.024	-16	0.00033
0.0475	6	0.00108
0.065	18	0.00197
0.115	35	0.00428
0.215	53	0.00857
0.33	68	0.01475

Temperature (°F) = 100

Loading [g/g solid]	Humidity [°F DP]	Humidity [g/g dry air]
0.0175	-16	0.00033
0.03	6	0.00108
0.04	18	0.00197
0.07	35	0.00428
0.12	53	0.00857
0.2	68	0.01475
0.27	79	0.02159
0.36	92	0.0333

Table 2.2 cont'd

Temperature (°F) = 120

Loading [g/g solid]	Humidity [°F DP]	Humidity [g/g dry air]
0.01	-16	0.00033
0.0175	6	0.00108
0.025	18	0.00197
0.0425	35	0.00428
0.0675	53	0.00857
0.105	68	0.01475
0.16	79	0.02159
0.225	92	0.0333
0.285	101	0.0446
0.38	115	0.06965

Table 2.3 - Glycol/H_2O Isotherms (from Literature)

Humidity [moles/liter]	Liquid Concentration [moles/gram]
Temperature = 60 °F	
0.000149	0.0047
0.000223	0.0076
0.000304	0.0128
0.000377	0.021
0.000447	0.0347
0.00052	0.0555
0.000597	0.0925
0.000666	0.1807
Temperature = 80 °F	
0.000286	0.0045
0.000424	0.0076
0.000579	0.0126
0.00071	0.0195
0.000849	0.0299
0.000987	0.0492
0.001133	0.0832
0.001268	0.1579
Temperature = 90 °F	
0.000382	0.0045
0.000574	0.0076
0.000765	0.0122
0.000985	0.0185
0.001144	0.0244
0.001339	0.0454
0.001528	0.0751
Temperature = 100 °F	
0.000518	0.0046
0.000779	0.007
0.001032	0.0122
0.001283	0.018
0.001527	0.0273
0.001749	0.0427

Table 2.3 cont'd

Temperature = 110 °F

0.000674	0.0046
0.001013	0.0076
0.001348	0.0118
0.001749	0.0175
0.002058	0.0267
0.002416	0.0402
0.002713	0.0678

Ethylene Glycol

The data in table 2.3 has been estimated by use of an exponential function of humidity as follows:

$$q^* \text{ [mol/g]} = a(T) \exp(b(T)\ c)$$

where

$$a(T) = 0.001363 \exp(0.00874T)$$

$$b(T) = 644351T^{-1.6257}$$

T °C

c mol H_2O/mol air

The numerical parameters given above have no physical significance as in the solid case due to the fact that the model proposed is not derived from any physical representation (such as Langmuir-Hinshelwood). The model was chosen simply to come as close to representing the actual literature data as possible. Figure 2.8 shows the liquid isotherms for temperatures of 60,80,90,and 100 °F. With temperature and concentration dependence represented mathematically, the breakthrough models discussed previously can be applied.

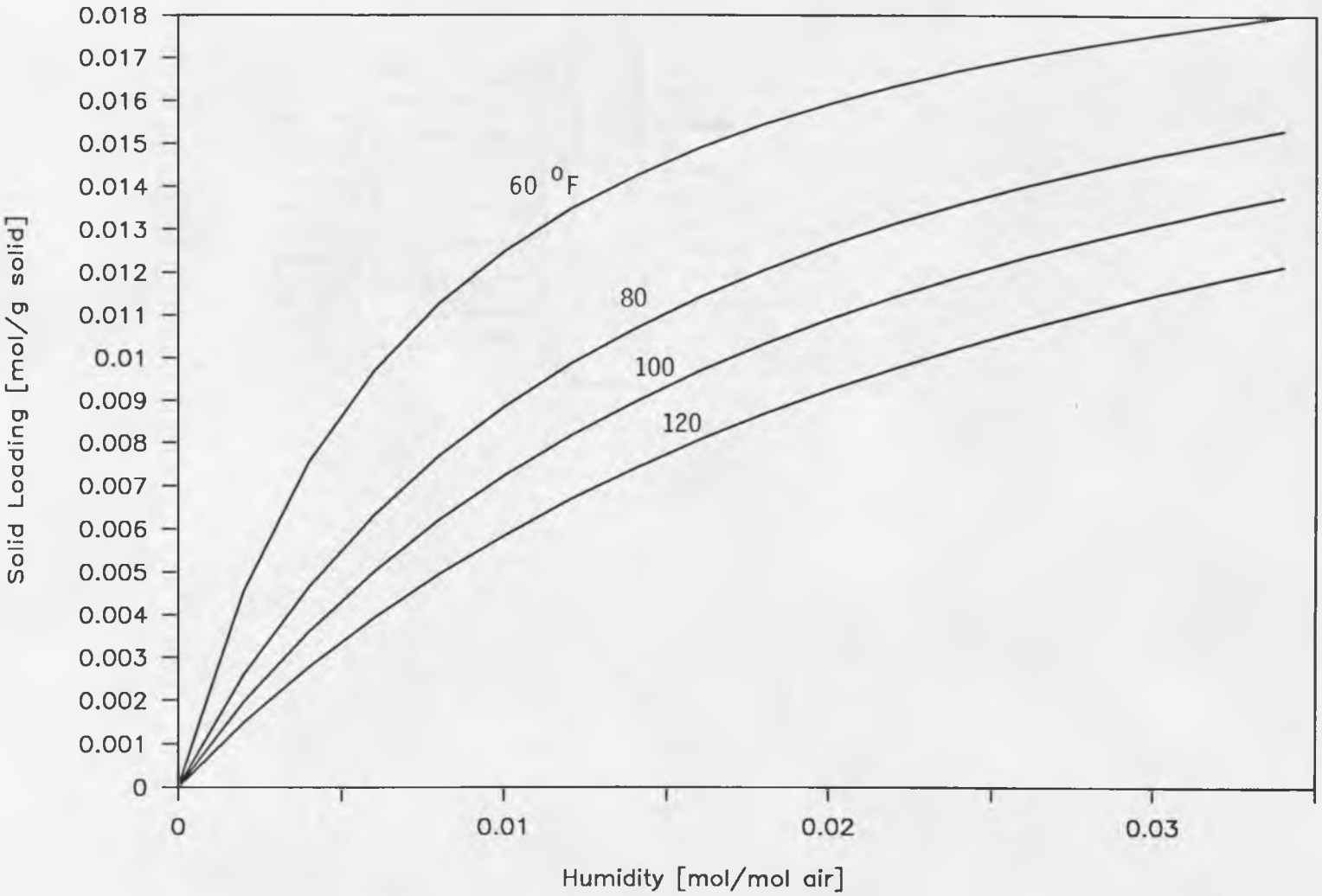

Figure 2.7 - Silica Gel Isotherms - Calculated

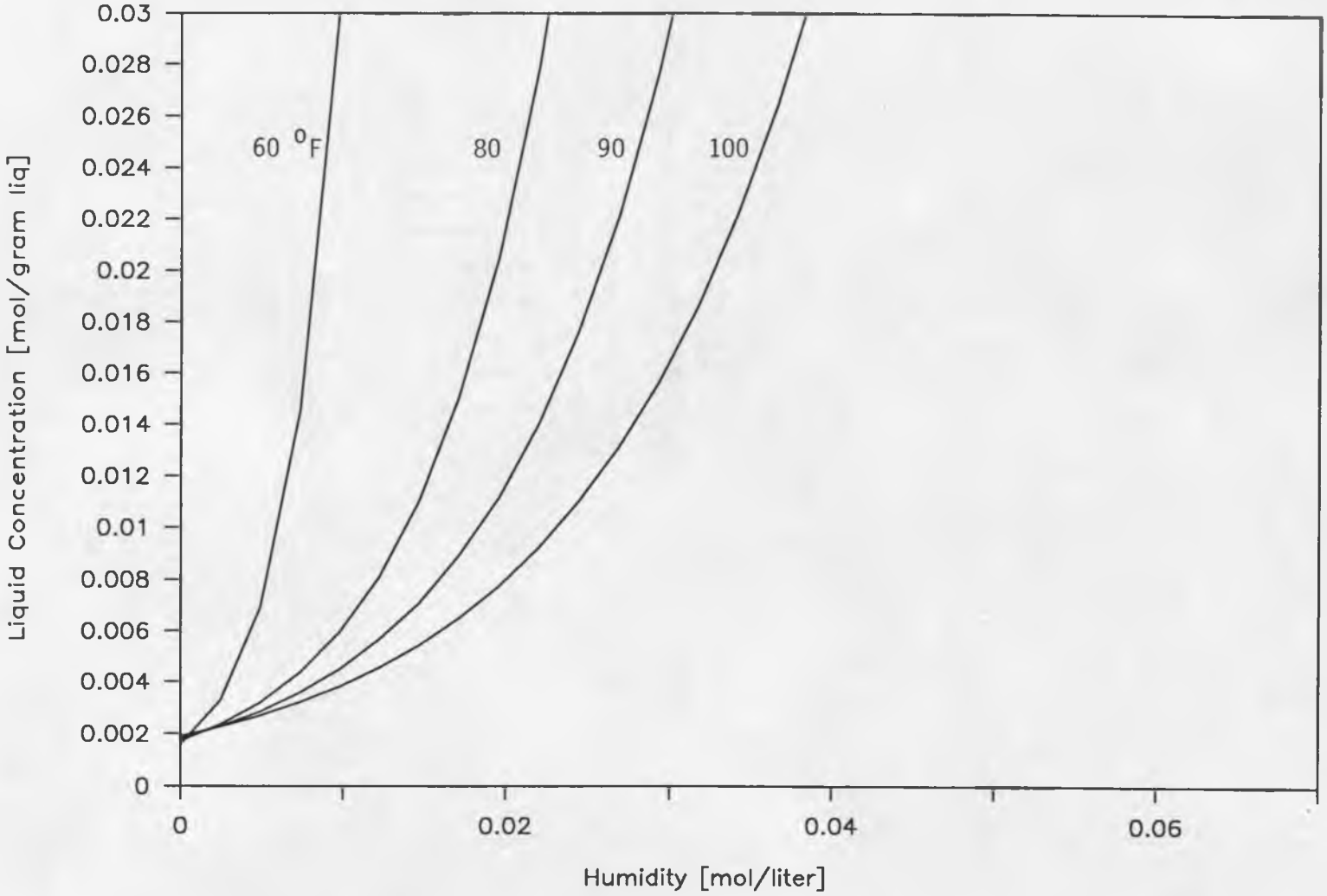

Figure 2.8 - Ethylene Glycol Isotherms - Calculated.

CHAPTER 3: THEORY OF BI-DESICCANT SYSTEM BEHAVIOR

3.1 Ideal performance.

The maximum achievable performance from a desiccant system can be calculated by assuming that the maximum amount of water vapor is cycled between the dehumidification and regeneration streams under given conditions. The isotherm gives information on the equilibrium humidity and desiccant loading and is used to determine the maximum performance. Figure 3.1 is a comparison of ideal performances calculated with the isotherm equations for silica gel and ethylene glycol. These systems have all been calculated under isothermal conditions since any heat effects would reduce the overall performance. It can be seen that the maximum achievable performance for system 1 (silica gel) is much higher than for system 2 (ethylene glycol). Also, the humidity reduction in the dehumidification stream is greater for silica gel (0.024 to 0.00169) than for ethylene glycol (0.024 to 0.0082). This means that both the COP and the specific cooling capacity (i.e. ton of cooling/CFM) are greater for system 1. This is all due to the thermodynamic advantage of the solid over the liquid.

Comparison of equilibrium isotherms (figures 2.7 and 2.8) show that desiccant loading is less dependent on humidity for silica gel than for glycol under most conditions. The result is that the humidity in equilibrium with the regeneration stream will be greater

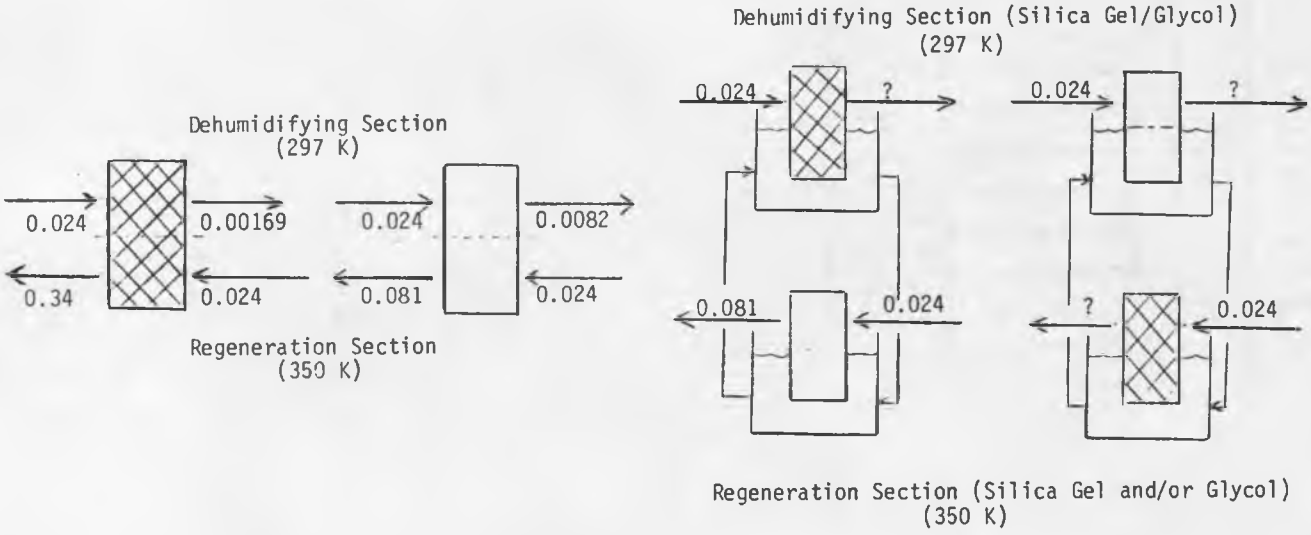

$COP_{max} = 8.5$	$COP_{max} = 1.65$	$COP_{max} = 1.65$	$1.65 < COP_{max} < 8.5$
1. Silica Gel	2. Ethylene Glycol	3. Silica Gel/Glycol	4. Silica Gel/Glycol

Figure 3.1 - Comparison of Maximum Achievable Performances for Solid and Liquid Desiccants (amounts indicate equilibrium humidity of stream in moles H_2O/mole air)

for the glycol system than for the solid. Consequently, in order to cycle the same amount of water, a higher regeneration temperature is needed. This explains the advantage of most solid systems over liquid systems, i.e. the isotherms are generally the wrong shape. The benefit of a liquid system is the ability to operate at nearly isothermal conditions. This is generally not possible with a solid system and there is a corresponding drop in the performance.

System 3 in figure 3.1 represents a bi-desiccant system in which the primary desiccant is the solid and the regenerating desiccant is the liquid. A question mark has been placed for the outlet humidity of the dehumidification stream since this depends on the interaction of the solid and liquid. This becomes the determining factor for the specific cooling capacity of the system. The COP is determined by the regeneration stream (assuming the change in humidity is greater than that for the dehumidification) and is therefore the same as that for system 2. System 4 is the opposite of system 3 so that the liquid becomes the primary desiccant. The opposite effect also occurs in that the COP depends on the interaction of the solid and liquid and the specific cooling capacity remains the same as for system 2.

Since the solid system is superior to the liquid system in both ideal capacity and ideal performance, what benefit could come out of a combination of the two? The answer comes from the comparison of inherent process limitations for each system. For instance, the solid system is usually run adiabatically in a packed bed or rotating wheel arrangement. The non-isothermal operation leads to a drop in the COP

as well as the specific cooling capacity. The liquid system is easier to maintain in an isothermal mode and can then become comparable to an adiabatic solid system. If the interaction of the solid and liquid is such that the dehumidification in system 3 remains as favorable as an adiabatic solid system, then the benefits of both desiccants could be realized. The solid being favorable for adsorption and the liquid favorable for desorption.

System 4 is less appropriate than system 3 for most materials. This is due to the fact that liquids generally show themselves to be better desorbents than adsorbents. The opposite is true for most solids. This does not mean that system 4 could not necessarily be appropriate for some cases. However, this study will concentrate on system 3.

3.2 Solid-Liquid Equilibrium

The COP of the bi-desiccant system is determined by the amount of moisture cycled by the process for a given heat input. For the bi-desiccant system (system 3), the maximum moisture cycled is equal to the maximum moisture cycled by the liquid system (system 2) as long as the regeneration controls the cycling capacity. The dehumidifier wheel therefore determines the specific cooling capacity, which determines the size and output of the air conditioner. The interaction between the solid and the liquid therefore determines the viability of this process as opposed to a strictly liquid or solid system.

For instance, if the liquid deactivates the solid for adsorption,

then the solid becomes simply a packing material for the liquid and the process becomes simply a liquid desiccant system with non-isothermal dehumidification. If the liquid doesn't interfere with the solid's capacity for adsorption and yet successfully regenerates the solid, then the system can theoretically maintain the high specific cooling capacity of the solid system. This then shows the range of possible behavior for a bi-desiccant system.

The phase rule for a bi-desiccant system with 3 phases and 4 components (solid, liquid, moisture, air) dictates that three intensive variables may be arbitrarily set in order to determine the system. Therefore with the temperature and pressure and one composition of the system set, the equilibrium concentrations in all phases must assume unique values. Therefore, the equilibrium loading of the bi-desiccant material can be related to the humidity of the air stream by combining solid-liquid and liquid-vapor isotherms.

$$\text{Let} \quad q_l = \frac{\text{moles water absorbed}}{\text{grams } C_2H_6O_2} = f_1(c)$$

$$q_s = \frac{\text{moles water adsorbed}}{\text{grams silica gel}} = g(q_l) = g(f_1(c))$$

$$q_{bi} = \frac{\text{moles water absorbed}}{\text{grams bi-desiccant}} = f_2(c)$$

The total amount of material present is:

$$g_{tot} = g_l + g_s$$

Therefore, the total moles of water adsorbed/absorbed into the bi-desiccant is equal to:

$$q_l g_l + q_s g_s = q_{bi} g_{tot} = n_{tot}$$

or

$$q_{bi} = q_l q_l + q_s \xi_s$$

where

$$q_l = \frac{g_l}{g_l + g_s} \quad \text{and} \quad q_s = \frac{g_s}{g_l + g_s}$$

and $$q_l + q_s = 1$$

This relates the bi-desiccant equilibrium loading on a per gram basis to the equilibrium relationships of the solid and liquid desiccants alone. The equilibrium between the air stream humidity and the solid moisture content depends on the equilibrium content in the liquid since the solid is assumed to be covered with liquid. The equation would be more complex if the solid adsorbent were only partially covered. The relationship can be seen to depend on the mass fractions of the liquid and solid. If the majority of the liquid has been drained off after washing the solid with the liquid desiccant, the mass fraction of the liquid may approach zero and the equilibrium can be dictated mostly by the liquid/solid equilibrium. However, if the liquid constitutes the major portion of the bi-desiccant material, then an isotherm similar to that of the liquid desiccant would result.

Also, in addition to the relative amounts of desiccant present, the effect which the two desiccants have on each other influences the overall equilibrium. If the liquid desiccant de-activates the solid capacity for adsorption by occupying all the sites normally available for water vapor adsorption, then the bi-desiccant isotherm equation reduces to that of the liquid. If equilibrium between the solid and

the liquid favors adsorption on the solid, then inadequate regeneration of the solid by the liquid may occur. The solid desiccant could also lower the absorption capacity of the liquid to some extent. The desirable result of the liquid/solid interaction is to have a highly favorable bi-desiccant isotherm (type 1) along with good regeneration of the solid by the liquid.

3.3 Theoretical model of bi-desiccant system

Figure 3.2 is a diagram of a theoretical bi-desiccant configuration. In comparison with figure 1.8, it can be seen that this unit is similar to the solid rotary wheel dehumidifier except for the configuration of the dehumidifying and regenerating sections. In the solid system, the same wheel is used for dehumidification and for regeneration. In the solid/liquid case, two separate units are needed; one for dehumidification, and one for regeneration. The liquid desiccant is used in the dehumidification as a co-component for vapor adsorption and in the regeneration as the sole medium for desorption. The liquid is cycled between the two processes at a rate sufficient to maintain the system performance. The rest of the system is exactly the same.

Figure 3.3 shows the process air conditions at various points in the system. This also parallels the process stream of the solid system. The difference lies in the dehumidification process (process 1-2) and the regeneration process (process 8-9). The dehumidification process is an adsorption of vapor onto a solid/liquid bi-desiccant matrix whereas the regeneration is a single phase desorption from the

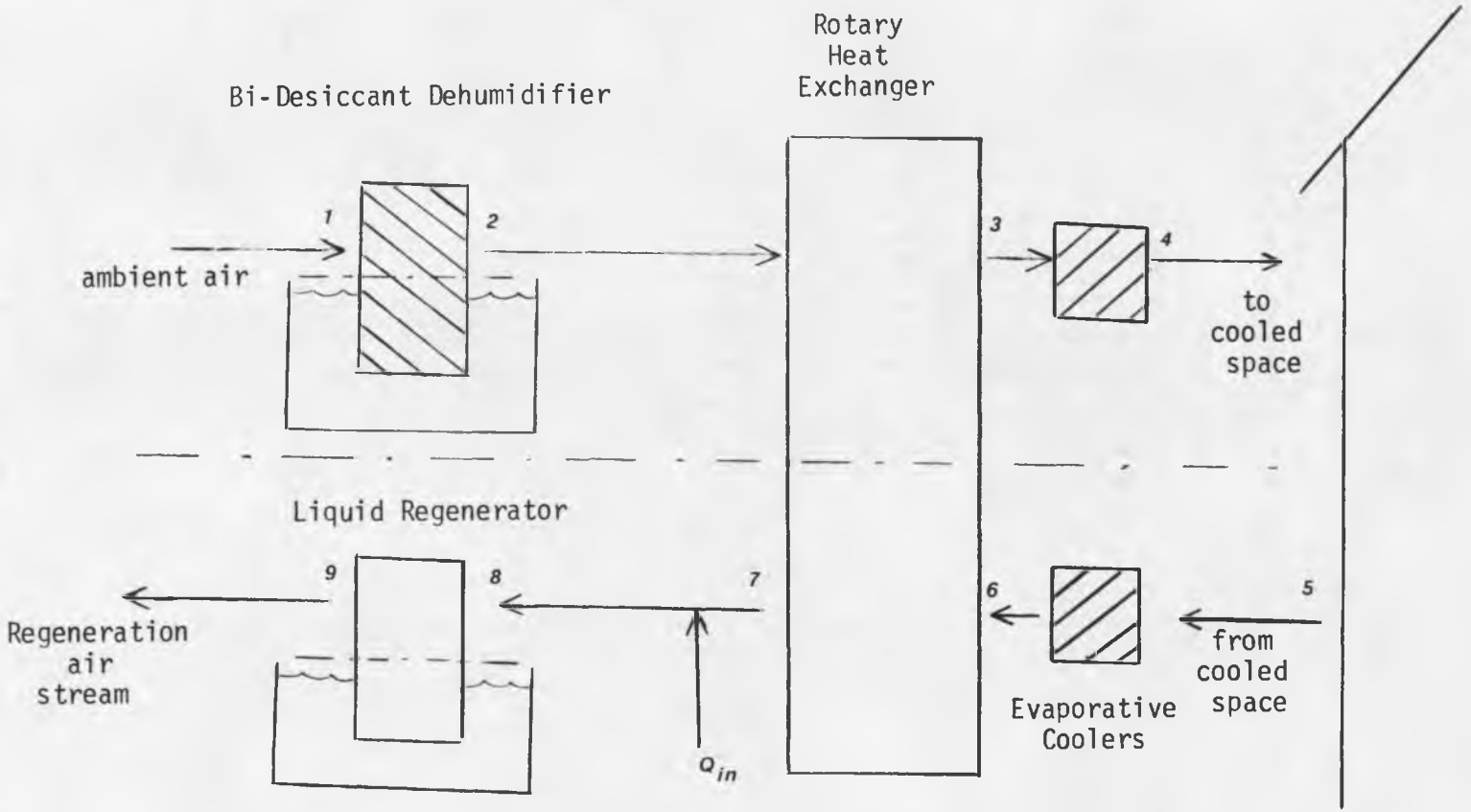

Figure 3.2 - Theoretical Bi-Desiccant System Configuration

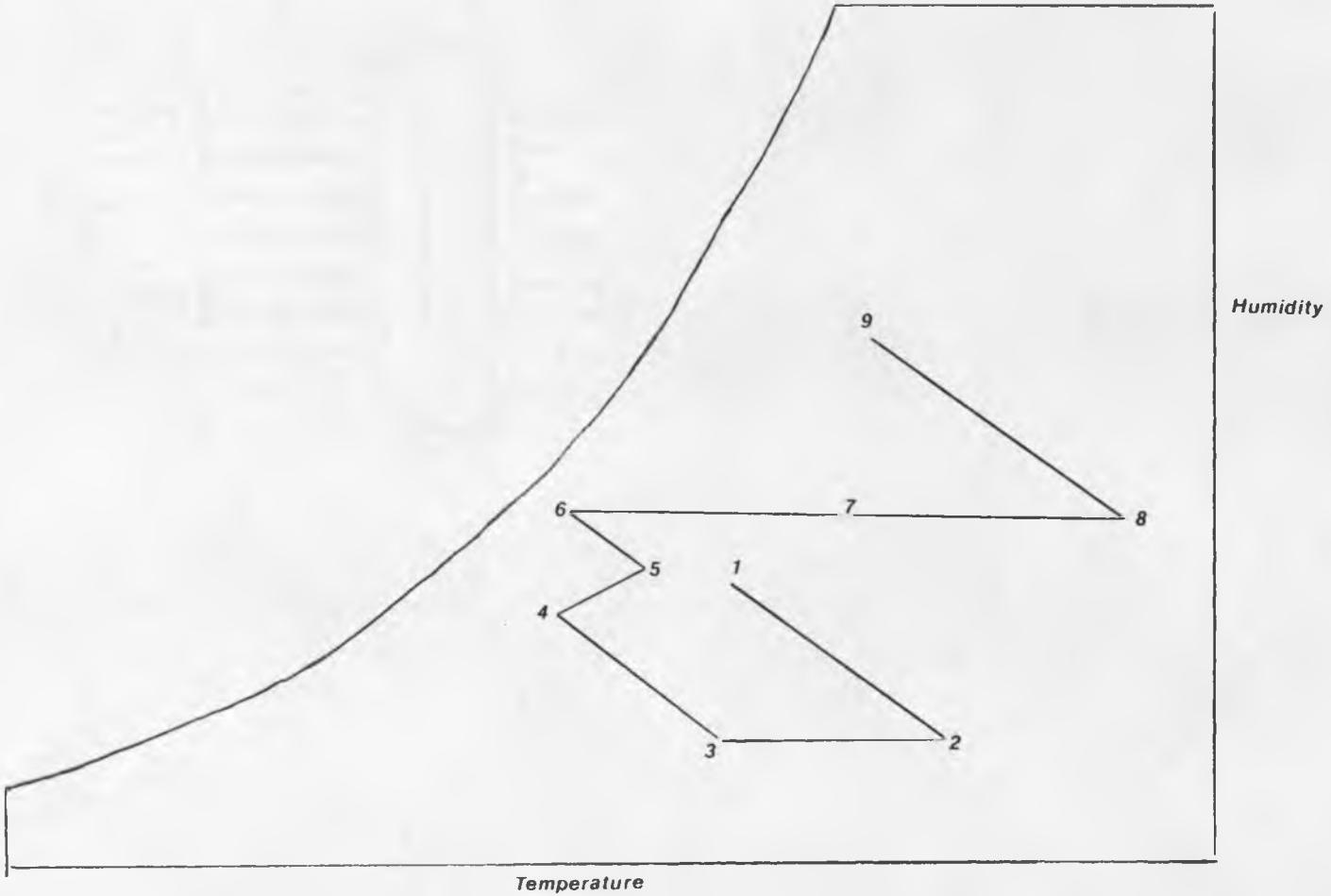

Figure 3.3 - Psychrometric Representation of Bi-Desiccant System
(Numbers represent stream locations in Figure 3.2)

liquid. The mass transfer surface is provided by packing material such as glass beads. The solid desiccant process in figure 1.8 is a single phase process in both dehumidification and regeneration.

This configuration was chosen in order to compare the system more closely with a solid desiccant system. An alternate system configuration could have included a flat plate solar collector where the liquid desiccant is regenerated by direct contact. However, it is more consistent to compare the desiccant performances by using breakthrough behavior with similar process variables. Once conclusions are made on suitable desiccant combinations, any form of regeneration can be used.

CHAPTER 4: EXPERIMENTAL EQUIPMENT AND PROCEDURE

The experimental setup is shown in figure 4.1. The purpose of this equipment is to collect transient response data of an adsorption column. The operating conditions therefore do not reach steady - state and the experiments must be carried out in a batch mode. The following will be a discussion of a typical experimental run.

The column being used is a molded acrylic plastic tube with 2.625 O.D. x 11.325. The anodized aluminum cap is fitted with an O - ring gasket and the column is fitted with two ports, one for the inlet stream and one for the outlet stream. There are two relative humidity sensors, one air flowmeter and two temperature sensors. The range of air flow is between 500 and 10,000 ml per minute. The relative humidity sensors, manufactured by Q - Systems, operate by conductivity on a film of organic substrate with the low conductivity at low relative humidity. They have a range of 0 - 100% with an accuracy of 2% over 95% of the range. The output from the sensors is in the form of 0 - 10 millivolts, which passes through a voltage divider to change it to 0 - 5 mV. The temperature sensors are two thermistors which send 0 - 5 mV signals as well.

The data acquisition system used is a Starbuck 8232 Signal Processing unit coupled with a Radioshack TRS 80 Model 100 Portable Computer. The Starbuck unit converts the analog input from the sensors to digital information for the computer. This digital

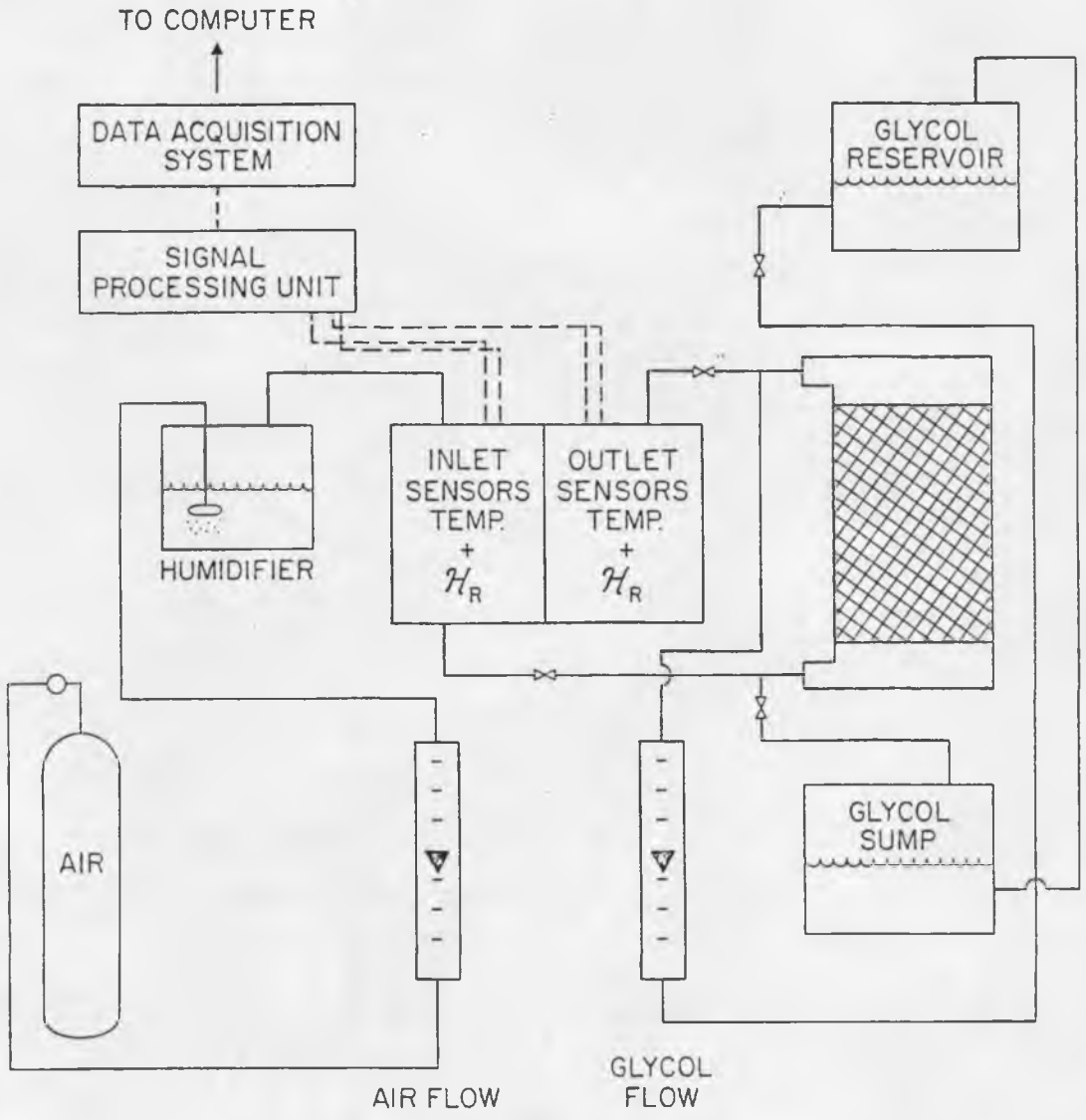

Figure 4.1 - Experimental Setup.

information is in the form of numerical code from 0 to 256, which correspond linearly to the signals from the sensors. This computer information can then be acquired and stored on a timewise basis and converted to units of relative humidity and plotted as a breakthrough curve.

A run is begun by washing the column, which consists of a solid desiccant material such as silica gel, with a suitable liquid desiccant (in this case ethylene glycol). Any excess liquid is removed. The inlet air is kept at nearly a constant relative humidity by using a bubble flask filled with water at ambient temperature. Relative humidity sensors are mounted at inlet and outlet ports as well as temperature sensors.

At the initial time t_o, ambient temperature and relative humidity are recorded and inlet RH, outlet RH, and temperatures are recorded each minute until the inlet conditions of the column are approached, indicating saturation of the column. The output is recorded as percent approach to saturation, which is determined as follows;

$$\% \text{ approach} = (H-H_o)/(H_f-H_o)$$

where

H = humidity at time t (or voltage)

H_o = lowest humidity reached by the system

H_f = final humidity (Saturated)

CHAPTER 5 : EXPERIMENTAL AND THEORETICAL RESULTS

Figure 3.1 illustrated the maximum theoretical performances for a silica gel and an ethylene glycol system and also for bi-desiccant systems of the two. This section deals with the deviations from this ideal behavior. The theoretical analysis will progress from ideal isothermal behavior to adiabatic equilibrium behavior and end with a numerical solution to an adiabatic system with finite heat and mass transfer resistance. This will be compared to experimental breakthrough data in order to validify the analysis.

The equations from chapter 2 describing the equilibrium relationships for silica gel and ethylene glycol with water will be used to describe a bi-desiccant system of these two components. The system parameters are as follows:

* volumetric flowrate of incoming air stream = 5000 ml/min
* height of packed bed column = 5 cm (≈ 2 inches)
* Temperature of inlet air = 297 °K (75 °F)
* Humidity of inlet air = 0.024 moles water/mole air (85 %RH)
* Temperature of regeneration stream = 350 °K (170 °F)
* Column cross sectional area = 25.6 cm^2 (≈ 4 in^2)

In the following analyses, the calculations will be shown in Appendix 5.

5.1 Isothermal Equilibrium (Ideal)

This analysis assumes that the temperature of the packed bed does not change during dehumidification or regeneration. Also, there is no resistance to mass or heat transfer from the fluid stream to the adsorbent/absorbent and there is no dispersion in the flow stream (i.e. plug flow). This yields the maximum achievable performance from a given material (assuming the adsorption/absorption process is exothermic and that the capacity of the material for water vapor reduces with increased temperature). The method of solution as described in chapter 2 is by use of the method of characteristics.

5.1.1 Silica Gel

From chapter 2, the maximum loading of the solid desiccant at 297°K and 0.024 moles water/mole air (85% relative humidity) is 0.0145 moles/gram solid. The minimum loading at 350°K and the same humidity is equal to 0.00263 moles/gram. The outlet air humidity of the dehumidifier, without breakthrough, will therefore be equal to the humidity in equilibrium with this loading at 297°K, or 0.00169 moles/mole. This yields a humidity reduction of the incoming air of (0.024-0.00169), or 0.02231 moles/mole.

Figures 5.1 and 5.2 show the adsorption and desorption curves, respectively, for a silica gel system with the ambient and regeneration conditions described above. The adsorption is seen as a shock front since the inlet air characteristics (region B) and the initial bed characteristics (region A) intersect. The shock time is determined by a mass balance over the column. Equation 2.11 is used to determine the

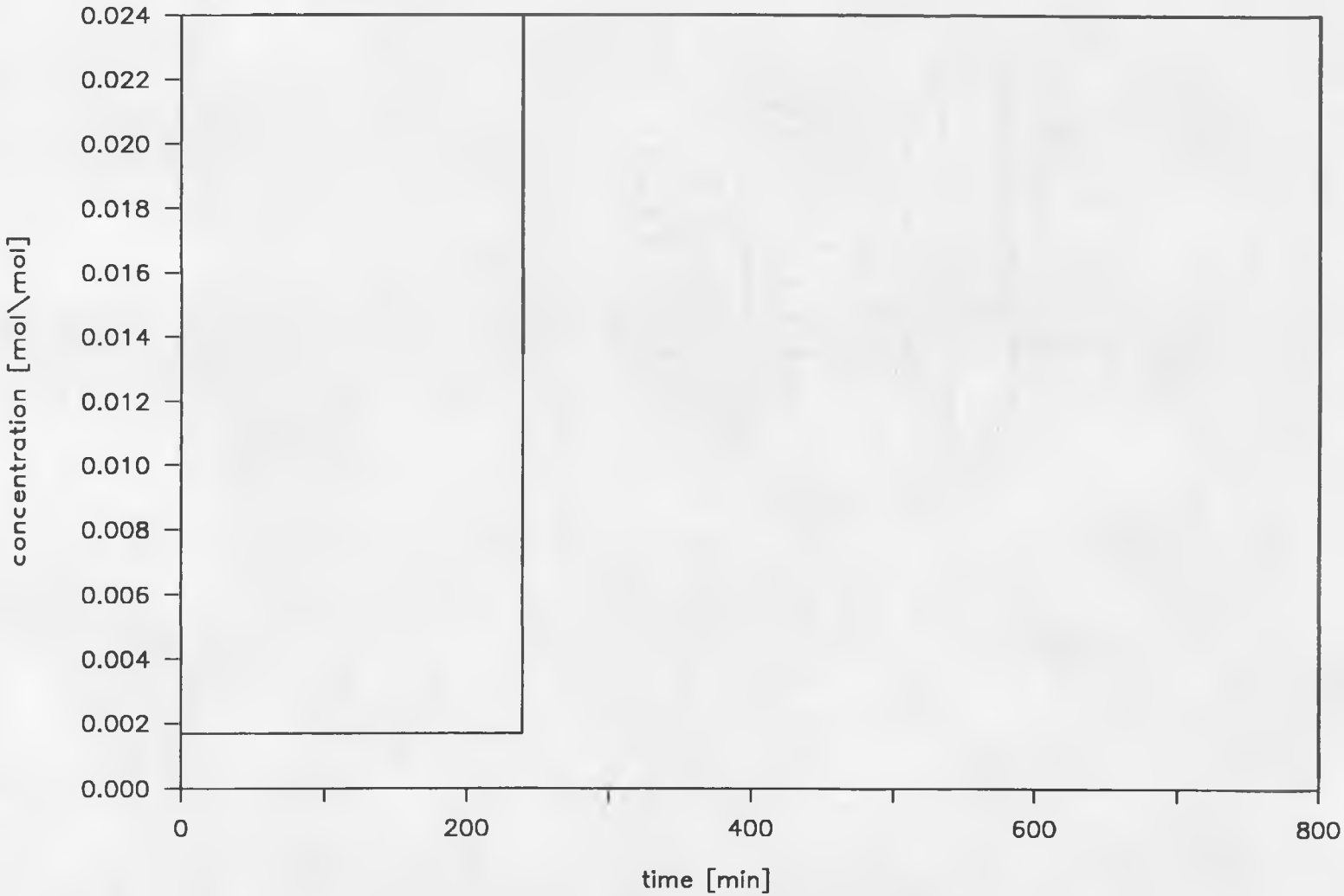

Figure 5.1 - Isothermal Adsorption Breakthrough for Silica Gel ; Equilibrium Solution (Initial equilibrium humidity of 0.0017 m/m)

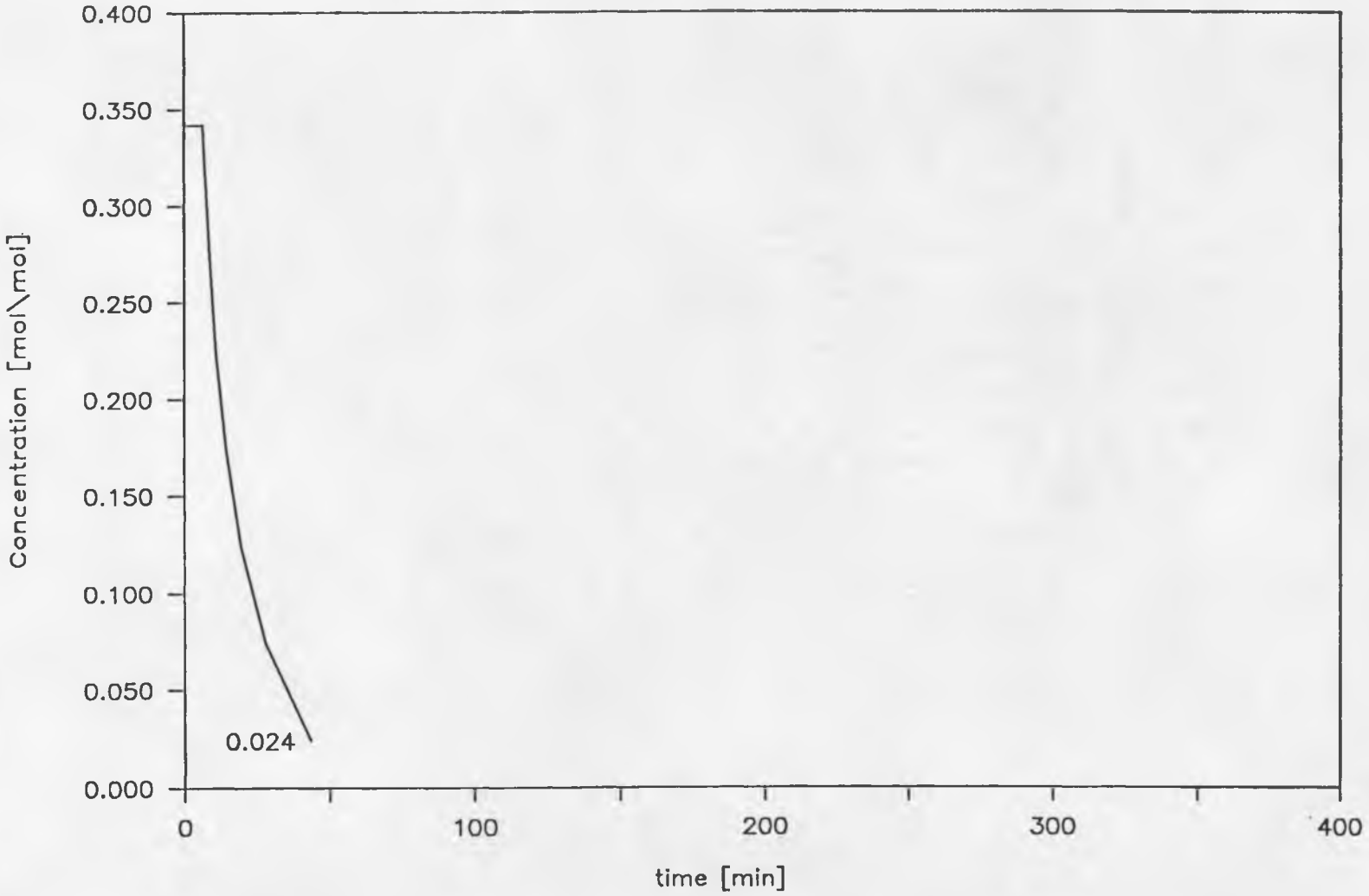

Figure 5.2 - Isothermal Desorption Breakthrough for Silica Gel ; Equilibrium Solution (Initially saturated bed, i.e. c_0 = 0.024 m/m)

shock velocity, which is equal to 0.021 cm/min. For a 5 cm column, the time for the shock front to reach the end of the column is 5/0.021, or 244 minutes.

The outlet humidity of the regeneration air stream before breakthrough occurs is calculated by first assuming that the column remains at its maximum loading of 0.0145 moles/gram. The equilibrium humidity for this loading at 350°K is equal to 0.34 moles/mole air according to equation 2.27. This will drop back down to the ambient humidity of 0.024 when the breakthrough occurs. The initial bed characteristics of the desorption case are shown as region A in figure 5.2. The inlet air characteristics as shown as region B. The relationship of these characteristics to each other shows that the initial bed concentration moves faster than the inlet air concentration and the breakthrough is therefore proportionate (dispersive). However, due to the high increase in the humidity and the fact that the areas under the adsorption and desorption curves are equal (mass balance), the breakthrough is very steep and can be seen to be practically a shock front also.

The coefficient of performance is determined as the latent energy removed from the air stream divided by the energy added to the air stream for regeneration.

$$COP = \frac{\Delta H_{out}}{\bar{W}_{in}} = \frac{(\text{water removed})\ \Delta H_{ads}}{\rho_{air} V_{air}\ C_p\ \Delta T\ t}$$

Assuming the regeneration determines the maximum value of the COP, plugging in the appropriate values determined from the isothermal

analysis for silica gel at 75°F, 85% RH, and a regeneration temperature of 170°F yields a maximum COP of approximately 8.5. This is assuming that the dehumidification stream flowrate is correspondingly increased to saturate the bed in the same time that the regeneration depletes it. This would put the dehumidification stream flowrate at 5.0(244/17.7), or 67.2 ltr/min.

The specific cooling capacity is determined as follows:

$$Q_{out}/V = (H_{in} - H_{out}) \times \Delta H_{evap}$$

where V is the volumetric flowrate of the airstream. This shows that the capacity is determined only by the humidity reduction and not on the amount of water cycled or the flowrate.

5.1.2 Ethylene Glycol

The same analysis can be done on ethylene glycol using the isotherm equation 2.28 developed in chapter 2. Here it can be seen that the equilibrium loading of the liquid desiccant is much higher than the solid, being about 0.6 moles water/gram liquid. This means that the capacity of the liquid to hold water is greater. The humidity in equilibrium with the liquid at its minimum loading is greater than the solid, however, being 0.0082 moles/mole air. This results in a lower humidity reduction than for the solid, (0.024-0.0082), or 0.0158 moles/mole.

Figures 5.3 and 5.4 show the isothermal analysis in the same manner as for the solid. In this case, the adsorption is seen to be proportionate pattern type whereas the desorption is a shock front. This is due to the shape of the isotherm, which dictates that areas of

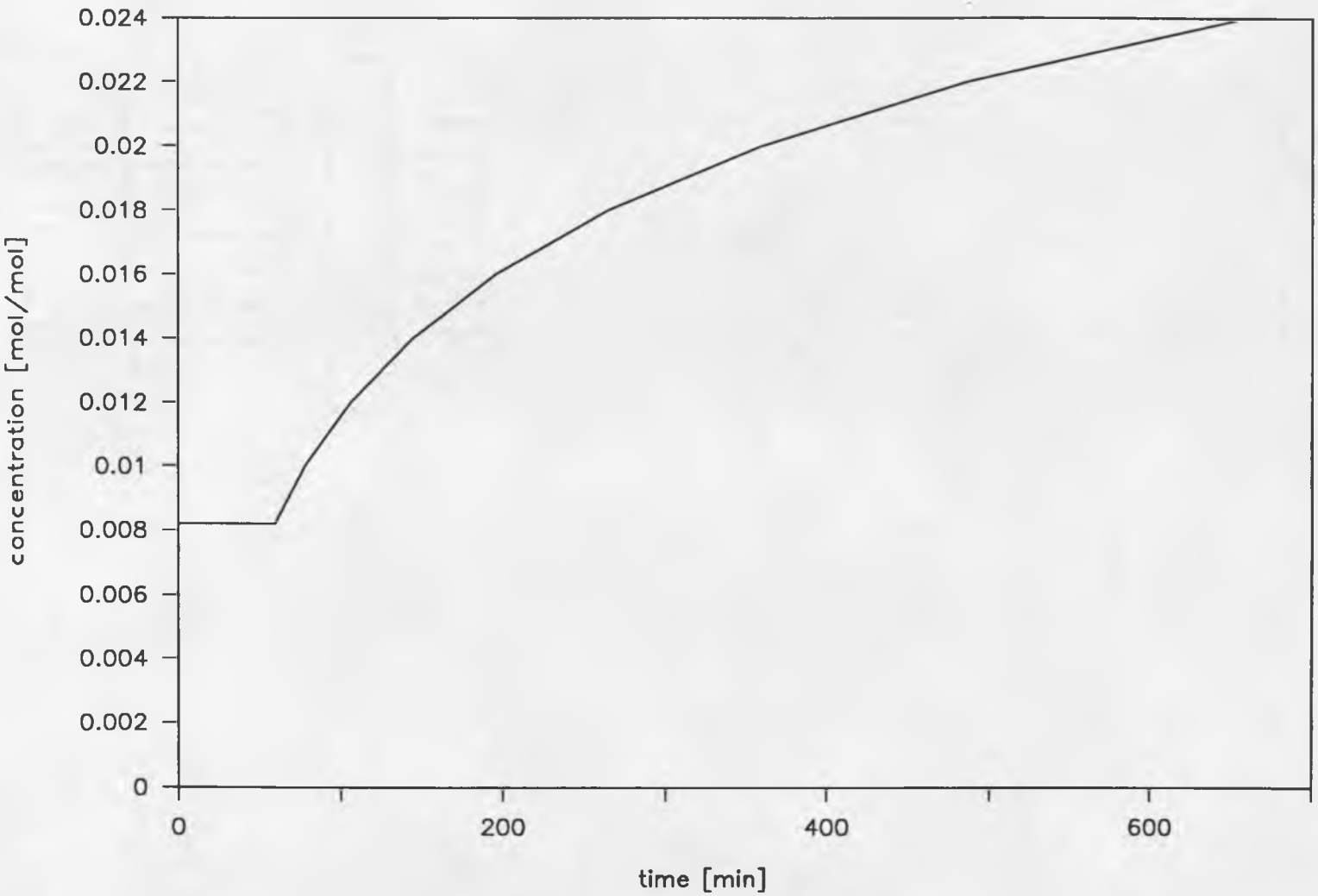

Figure 5.3 - Isothermal Dehumidification Breakthrough for Ethylene Glycol ; Equlibrium Solution (Initial equilibrium humidity of 0.0082 m/m)

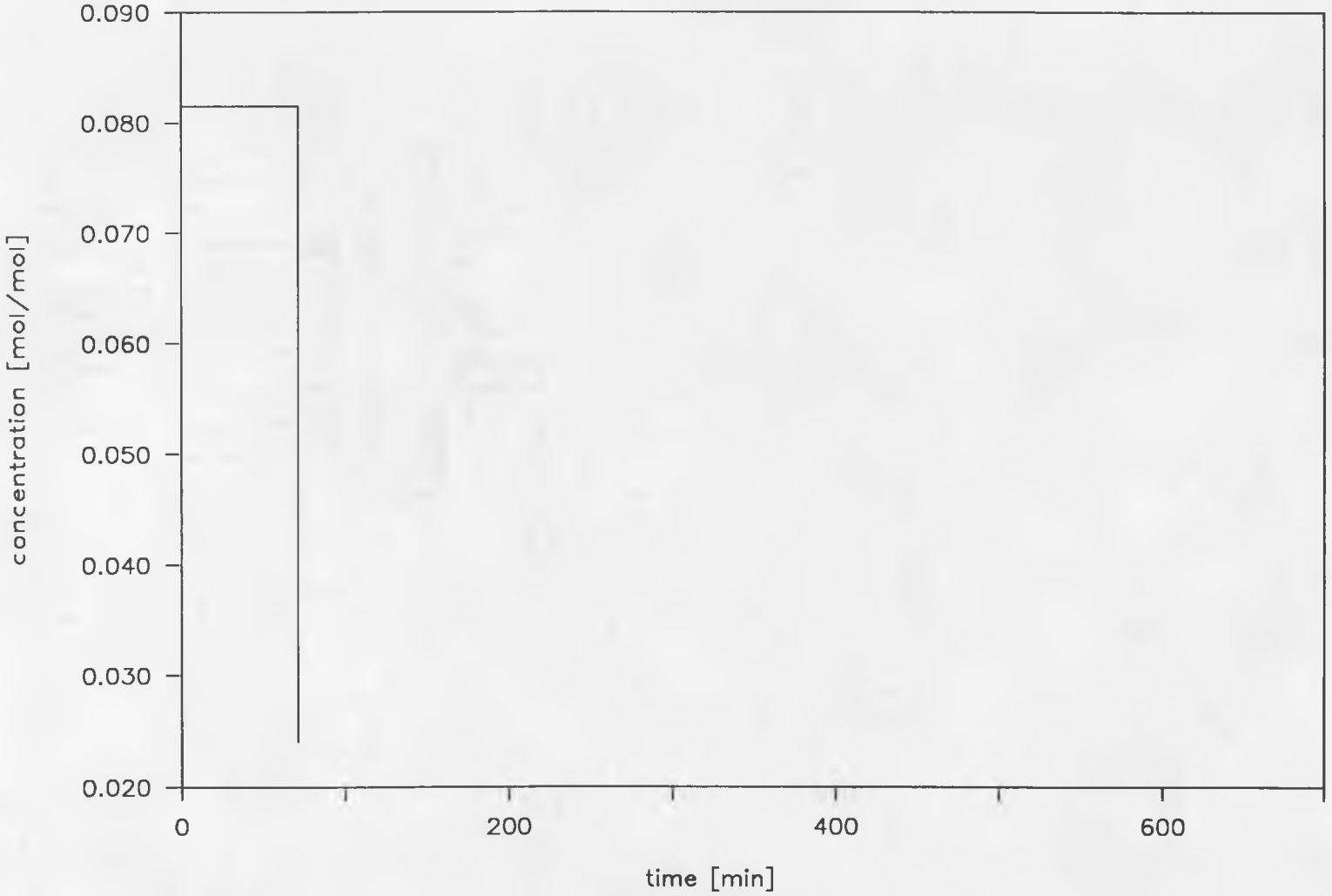

Figure 5.4 - Isothermal Regeneration Breakthrough for Ethylene Glycol ; Equilibrium Solution (Initially saturated liquid, i.e. c_0 = 0.024 m/m)

low concentration in the bed move faster than areas of higher concentration. Thus in the case of adsorption, the bed concentration is already lower than the saturation value, and in the case of desorption, the bed is already saturated and the incoming stream concentration wave overtakes the bed concentration wave to form a shock. Once again, the shock velocity is calculated by a mass balance over the column per equation 2.7, and the total areas under the adsorption and desorption curves are equal.

The COP for the liquid system is calculated in the same way as the solid system. Due to the equilibrium restrictions, the humidity reduction is much smaller for the liquid than for the solid system. The heat flux to the regeneration air stream remains the same as for the solid system since the flowrate and temperature rise are the same, but the rate of moisture removal is reduced. The maximum COP for this system is equal to 1.65.

The specific cooling capacity is seen to be proportionately lower than the solid capacity. Since the capacity is only determined by the amount of humidity drop in the dehumidifier, the ratio of liquid to solid will be equal to the ratio of humidity drops. Therefore the liquid capacity will be lower than the solid value by about 30 %.

5.2 Adiabatic Operation (Equilibrium assumed)

This analysis takes into account the exothermic nature of adsorption/absorption of a vapor and also provides for the changing capacity of the desiccant with temperature. The assumptions of plug flow and equilibrium still exist, however. The reductions in performance can then be seen which are caused only by the adiabatic nature of the process.

5.2.1 Silica Gel

A characteristic plot (figure 5.5) has been prepared using the fortran program HODO (see Appendix C). The coordination of the characteristic plot and the z-t characteristics to produce adiabatic breakthrough curves is discussed in section 2.2.2 and is used here. Along with the characteristic plot is a table of wave speeds (Table 5.1) which correspond to each point on the plot. The units of wave speed are in cm/min. This is used to determine the existence of shock fronts, proportionate pattern waves, or combination waves, and to calculate the time of breakthrough.

The adsorption follows along path A-B-C, and at point B reaches a plateau zone of temperature, humidity, and loading. This is shown in Figure 5.6, which describes the adsorption breakthrough along with the z-t characteristics. This plateau zone remains until the trailing wave (B-C) breaks through. It can be seen that the Γ^+ characteristics for silica gel are asymptotic to the temperature axis, and in the case of a completely dry bed ($c = 0$), there appears no plateau zone for humidity or bed loading.

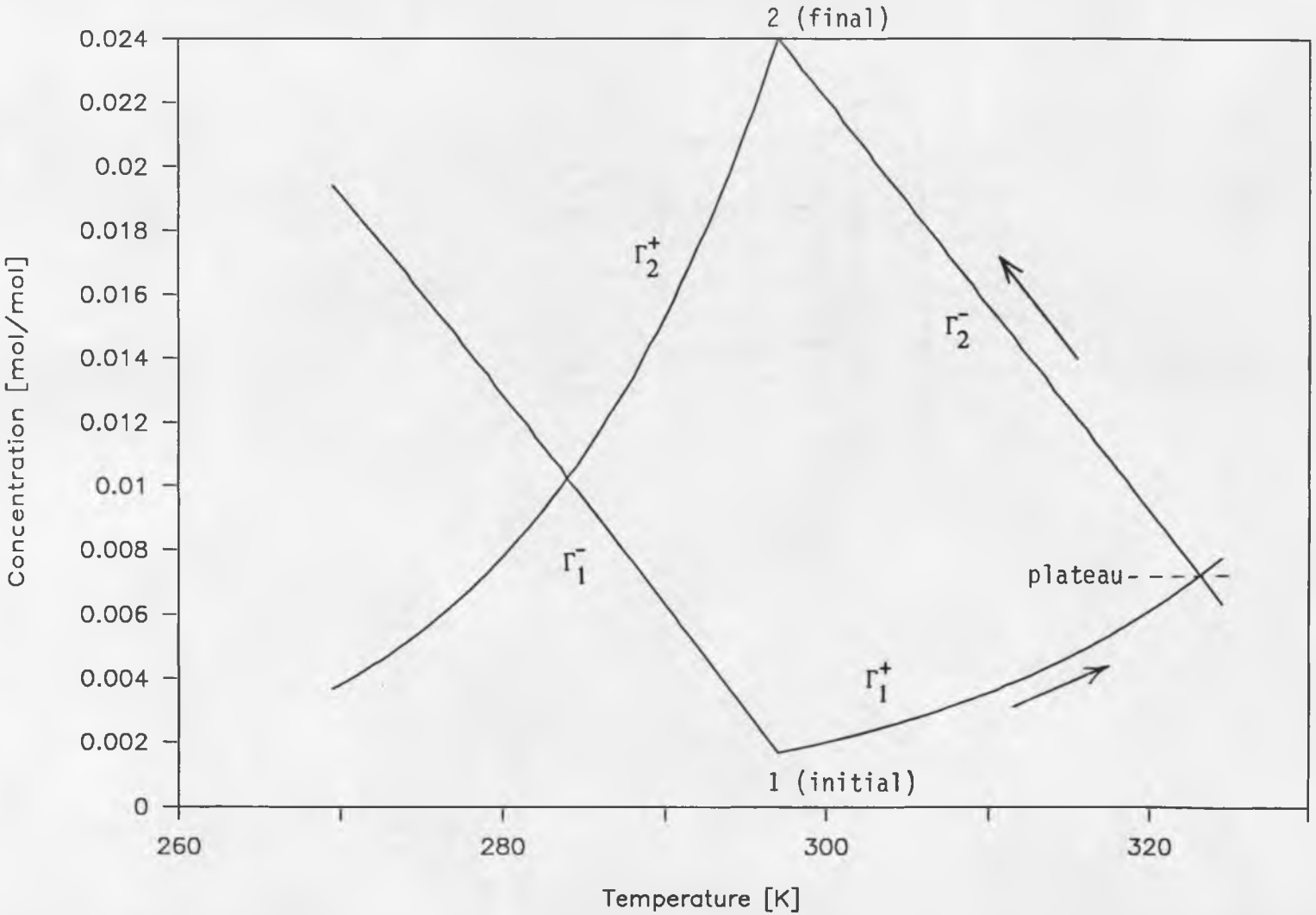

Figure 5.5 - Adiabatic Characteristic Plot for Silica Gel Adsorption. (Breakthrough proceeds from point 1 to point 2 along path indicated by arrows)

Table 5.1

Adsorption Characteristics with Corresponding Wave Velocities

-Silica Gel-

T [K]	Γ_1^+	Γ_2^-	ω_1^+	ω_2^-
297.0	0.0017	0.0240	0.4043	0.0168
297.5	0.0017	0.0237	0.4057	0.0165
298.0	0.0018	0.0234	0.4072	0.0163
298.5	0.0019	0.0230	0.4087	0.0161
299.0	0.0019	0.0227	0.4103	0.0159
299.5	0.0020	0.0224	0.4118	0.0157
300.0	0.0020	0.0221	0.4135	0.0155
300.5	0.0021	0.0218	0.4151	0.0154
301.0	0.0021	0.0214	0.4169	0.0152
301.5	0.0022	0.0211	0.4186	0.0151
302.0	0.0023	0.0208	0.4204	0.0150
302.5	0.0023	0.0205	0.4222	0.0149
303.0	0.0024	0.0201	0.4241	0.0148
303.5	0.0025	0.0198	0.4260	0.0147
304.0	0.0025	0.0195	0.4280	0.0146
304.5	0.0026	0.0192	0.4300	0.0145
305.0	0.0027	0.0189	0.4321	0.0145
305.5	0.0028	0.0185	0.4342	0.0144
306.0	0.0029	0.0182	0.4364	0.0144
306.5	0.0029	0.0179	0.4386	0.0144
307.0	0.0030	0.0176	0.4409	0.0144
307.5	0.0031	0.0172	0.4432	0.0144
308.0	0.0032	0.0169	0.4456	0.0144
308.5	0.0033	0.0166	0.4481	0.0144
309.0	0.0034	0.0163	0.4506	0.0144
309.5	0.0035	0.0159	0.4531	0.0145
310.0	0.0036	0.0156	0.4557	0.0146
310.5	0.0037	0.0153	0.4584	0.0146
311.0	0.0038	0.0150	0.4612	0.0147
311.5	0.0039	0.0147	0.4640	0.0148
312.0	0.0040	0.0143	0.4668	0.0149
312.5	0.0041	0.0140	0.4698	0.0151
313.0	0.0042	0.0137	0.4728	0.0152
313.5	0.0043	0.0134	0.4759	0.0153
314.0	0.0044	0.0130	0.4790	0.0155
314.5	0.0046	0.0127	0.4823	0.0157
315.0	0.0047	0.0124	0.4856	0.0159
315.5	0.0048	0.0121	0.4890	0.0161
316.0	0.0050	0.0118	0.4924	0.0163
316.5	0.0051	0.0114	0.4960	0.0165
317.0	0.0052	0.0111	0.4996	0.0168

317.5	0.0054	0.0108	0.5033	0.0171
318.0	0.0055	0.0105	0.5071	0.0174
318.5	0.0057	0.0102	0.5110	0.0177
319.0	0.0058	0.0098	0.5150	0.0180
319.5	0.0060	0.0095	0.5190	0.0183
320.0	0.0061	0.0092	0.5232	0.0187
320.5	0.0063	0.0089	0.5274	0.0191
321.0	0.0065	0.0086	0.5318	0.0195
321.5	0.0066	0.0083	0.5362	0.0199
322.0	0.0068	0.0079	0.5408	0.0204
322.5	0.0070	0.0076	0.5454	0.0209
323.0	0.0072	0.0073	0.5502	0.0214
323.5	0.0074	0.0070	0.5551	0.0219
324.0	0.0076	0.0067	0.5601	0.0225
324.5	0.0078	0.0064		

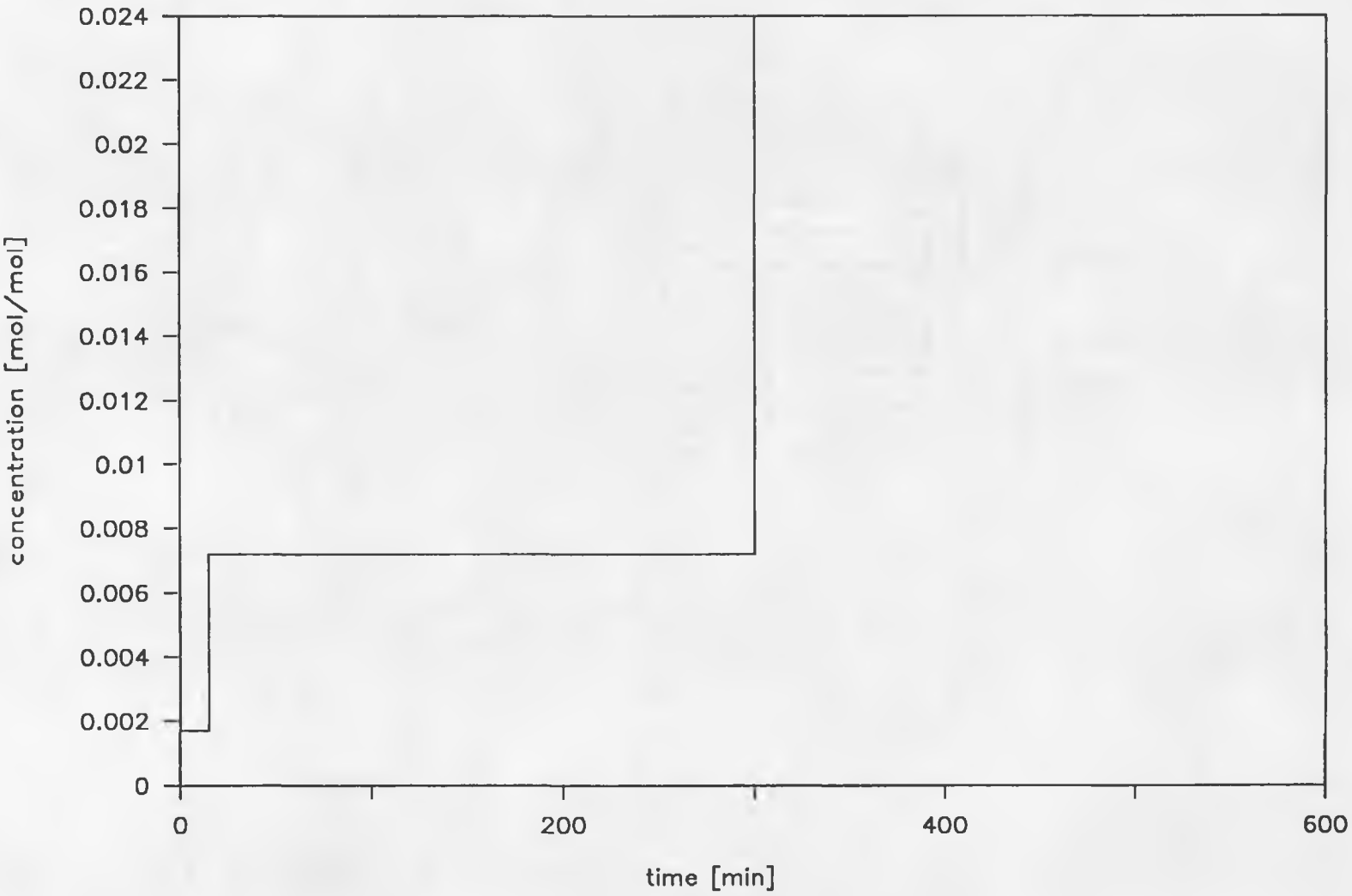

Figure 5.6 - Adiabatic Adsorption Breakthrough for Silica Gel ; Equilibrium Solution (Initial equilibrium humidity of 0.0017 m/m)

The total amount of moisture removed by this system is seen to be equal to the amount removed by the isothermal system. This is because the inlet temperature of the dehumidification stream remains at 297°K, and the bed temperature eventually returns to this value, thus preserving the original capacity of the bed. The bed capacity is reduced by the heat released during adsorption and the overall effect is the abrupt jump to the plateau zone.

The specific cooling capacity is calculated by assuming that the minimum outlet humidity from the dehumidifier is now equal to the value at the plateau zone. Since the jump occurs almost immediately, this is a valid assumption. This would produce a humidity reduction of (0.024 - 0.0072), or 0.0168 moles/mole air as opposed to 0.0223 for the isothermal case. This means that the specific cooling capacity has dropped 25% from the isothermal value. The volumetric flowrate of the adiabatic system must be 1.33 times that of the isothermal system in order to achieve the same amount of cooling under the same conditions.

In the case of the regeneration, the terminal conditions are different and a new characteristic plot (figure 5.7) is needed. Table 5.2 gives the corresponding wave velocities in cm/min. The bed is initially assumed to be saturated with ambient air at 297°K (75°F). The inlet condition to the bed is a heated stream of ambient air (350°K) with the same humidity (0.024 moles/mole). The path then follows along D-E-F, which includes a plateau zone at 0.0488 moles/mole air and 309°K. The jump to the plateau zone is almost immediate, and the trailing wave front is also a shock front which

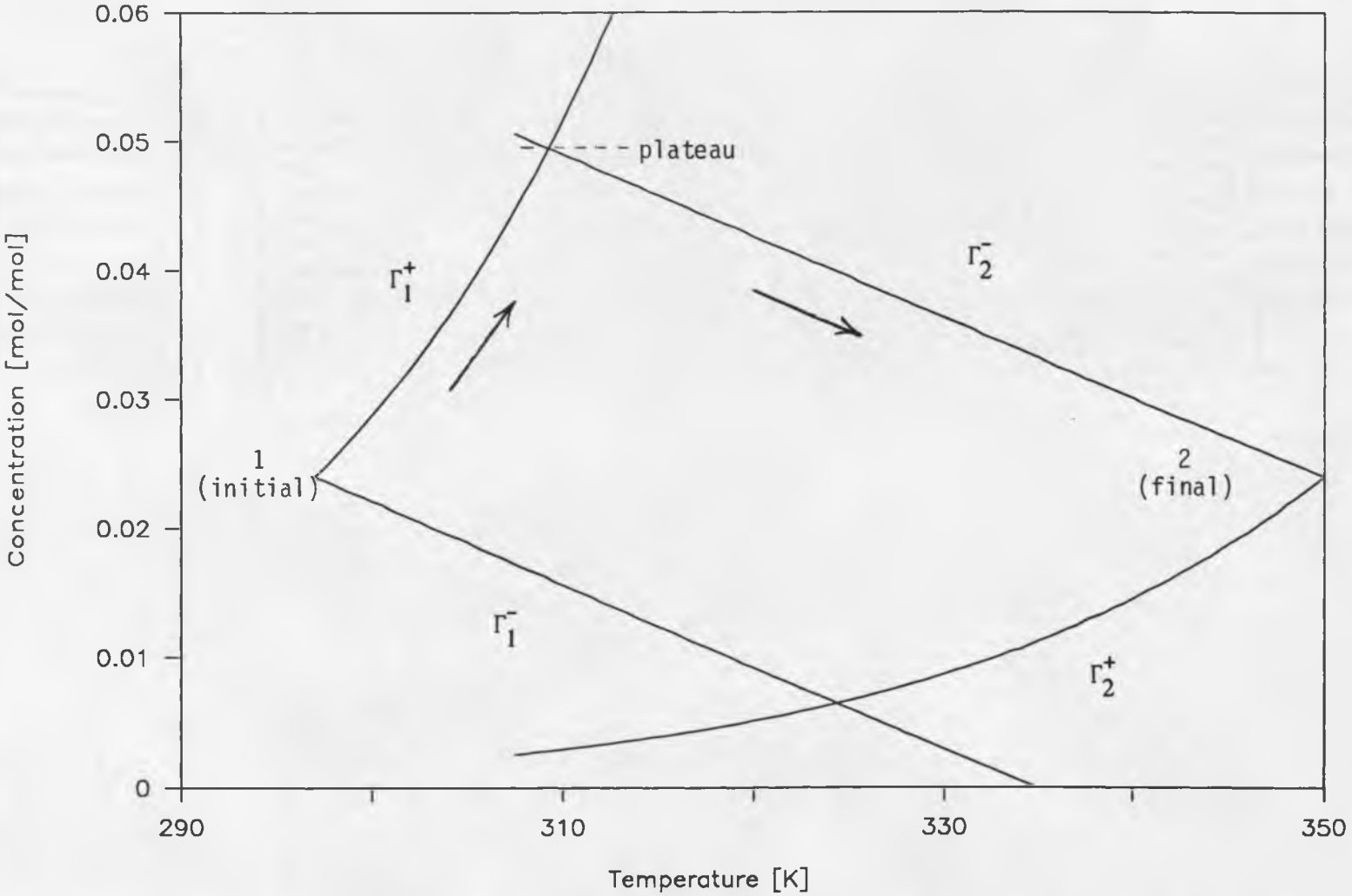

Figure 5.7 - Adiabatic Characteristic Plot for Silica Gel Desorption. (Breakthrough proceeds along path indicated by arrows)

Table 5.2

Desorption Characteristics with Corresponding Wave Velocities

-Silica Gel-

T_2 [K]	Γ_2^-	ω_2^-	T_1 [K]	Γ_1^+	ω_1^+
350.0	0.0240	0.0423	339.0	0.2390	6.4619
349.5	0.0243	0.0415	338.5	0.2330	6.3305
349.0	0.0246	0.0406	338.0	0.2280	6.2015
348.5	0.0249	0.0398	337.5	0.2220	6.0749
348.0	0.0252	0.0390	337.0	0.2170	5.9507
347.5	0.0255	0.0382	336.5	0.2110	5.8289
347.0	0.0258	0.0374	336.0	0.2060	5.7093
346.5	0.0261	0.0367	335.5	0.2010	5.5921
346.0	0.0264	0.0360	335.0	0.1960	5.4770
345.5	0.0267	0.0353	334.5	0.1910	5.3642
345.0	0.0270	0.0346	334.0	0.1870	5.2536
344.5	0.0273	0.0339	333.5	0.1820	5.1450
344.0	0.0276	0.0333	333.0	0.1770	5.0386
343.5	0.0279	0.0327	332.5	0.1730	4.9343
343.0	0.0282	0.0321	332.0	0.1690	4.8320
342.5	0.0285	0.0315	331.5	0.1640	4.7317
342.0	0.0288	0.0309	331.0	0.1600	4.6333
341.5	0.0291	0.0304	330.5	0.1560	4.5369
341.0	0.0294	0.0299	330.0	0.1520	4.4424
340.5	0.0297	0.0293	329.5	0.1480	4.3497
340.0	0.0301	0.0289	329.0	0.1450	4.2589
339.5	0.0304	0.0284	328.5	0.1410	4.1700
339.0	0.0307	0.0279	328.0	0.1370	4.0827
338.5	0.0310	0.0275	327.5	0.1340	3.9973
338.0	0.0313	0.0270	327.0	0.1300	3.9135
337.5	0.0316	0.0266	326.5	0.1270	3.8315
337.0	0.0319	0.0262	326.0	0.1240	3.7510
336.5	0.0322	0.0258	325.5	0.1210	3.6723
336.0	0.0325	0.0254	325.0	0.1170	3.5951
335.5	0.0328	0.0251	324.5	0.1140	3.5195
335.0	0.0332	0.0247	324.0	0.1110	3.4455
334.5	0.0335	0.0244	323.5	0.1090	3.3730
334.0	0.0338	0.0241	323.0	0.1060	3.3020
333.5	0.0341	0.0238	322.5	0.1030	3.2324
333.0	0.0344	0.0235	322.0	0.1000	3.1643
332.5	0.0347	0.0232	321.5	0.0975	3.0976
332.0	0.0350	0.0229	321.0	0.0950	3.0323
331.5	0.0354	0.0226	320.5	0.0924	2.9684
331.0	0.0357	0.0224	320.0	0.0900	2.9058
330.5	0.0360	0.0222	319.5	0.0876	2.8445
330.0	0.0363	0.0219	319.0	0.0852	2.7846

329.5	0.0366	0.0217	318.5	0.0830	2.7259
329.0	0.0369	0.0215	318.0	0.0807	2.6684
328.5	0.0372	0.0213	317.5	0.0785	2.6122
328.0	0.0376	0.0211	317.0	0.0764	2.5572
327.5	0.0379	0.0210	316.5	0.0744	2.5034
327.0	0.0382	0.0208	316.0	0.0723	2.4507
326.5	0.0385	0.0206	315.5	0.0704	2.3992
326.0	0.0388	0.0205	315.0	0.0684	2.3488
325.5	0.0391	0.0204	314.5	0.0666	2.2995
325.0	0.0395	0.0202	314.0	0.0647	2.2513
324.5	0.0398	0.0201	313.5	0.0630	2.2041
324.0	0.0401	0.0200	313.0	0.0612	2.1580
323.5	0.0404	0.0199	312.5	0.0595	2.1129
323.0	0.0407	0.0198	312.0	0.0579	2.0688
322.5	0.0411	0.0198	311.5	0.0563	2.0256
322.0	0.0414	0.0197	311.0	0.0547	1.9834
321.5	0.0417	0.0196	310.5	0.0532	1.9422
321.0	0.0420	0.0196	310.0	0.0517	1.9019
320.5	0.0423	0.0196	309.5	0.0502	1.8625
320.0	0.0426	0.0195	309.0	0.0488	1.8240
319.5	0.0430	0.0195	308.5	0.0474	1.7864
319.0	0.0433	0.0195	308.0	0.0461	1.7496
318.5	0.0436	0.0195	307.5	0.0448	1.7136
318.0	0.0439	0.0195	307.0	0.0435	1.6785
317.5	0.0442	0.0195	306.5	0.0423	1.6442
317.0	0.0445	0.0196	306.0	0.0410	1.6107
316.5	0.0449	0.0196	305.5	0.0399	1.5779
316.0	0.0452	0.0197	305.0	0.0387	1.5459
315.5	0.0455	0.0197	304.5	0.0376	1.5147
315.0	0.0458	0.0198	304.0	0.0365	1.4842
314.5	0.0461	0.0199	303.5	0.0355	1.4544
314.0	0.0465	0.0200	303.0	0.0344	1.4253
313.5	0.0468	0.0201	302.5	0.0334	1.3969
313.0	0.0471	0.0202	302.0	0.0324	1.3691
312.5	0.0474	0.0203	301.5	0.0315	1.3420
312.0	0.0477	0.0204	301.0	0.0306	1.3156
311.5	0.0480	0.0206	300.5	0.0297	1.2898
311.0	0.0484	0.0207	300.0	0.0288	1.2646
310.5	0.0487	0.0209	299.5	0.0279	1.2400
310.0	0.0490	0.0210	299.0	0.0271	1.2160
309.5	0.0493	0.0212	298.5	0.0263	1.1926
309.0	0.0496	0.0214	298.0	0.0255	1.1697
308.5	0.0499	0.0216	297.5	0.0247	1.1474
308.0	0.0503	0.0218	297.0	0.0240	1.1257

drops the outlet humidity back down to the ambient value and increases the temperature from the plateau value back to the regeneration temperature. Figure 5.8 shows the breakthrough along with the z-t characteristics which determine the break time (about 210 minutes). The COP is determined by the increase of humidity (rollup) and is equal to about 0.66. This is less than one tenth of the value at isothermal conditions.

It is interesting to note that although the solid desiccant isotherm predicts proportionate pattern breakthrough for regeneration at isothermal conditions, the adiabatic results show a shock front instead. This is due to the phenomenon of "rollup", which occurs at elevated temperatures. As the regeneration temperature is increased, the wave front is compressed more and more, causing a faster wavefront and a higher outlet humidity. If the bed had been regenerated with a dry airstream at ambient temperature, the breakthrough would have been proportionate pattern.

5.2.2 Ethylene Glycol

Figure 5.9 is a characteristic plot for ethylene glycol generated by program HODO. Table 5.3 gives corresponding wave velocities for these characteristics. Similar to the solid system, the liquid desiccant produces a plateau zone at 310.5°K and 0.0161 moles/mole humidity. Inspection of the wave velocities indicates that the initial bed concentration velocity is less than the plateau velocity. The inlet concentration velocity is also less than the plateau

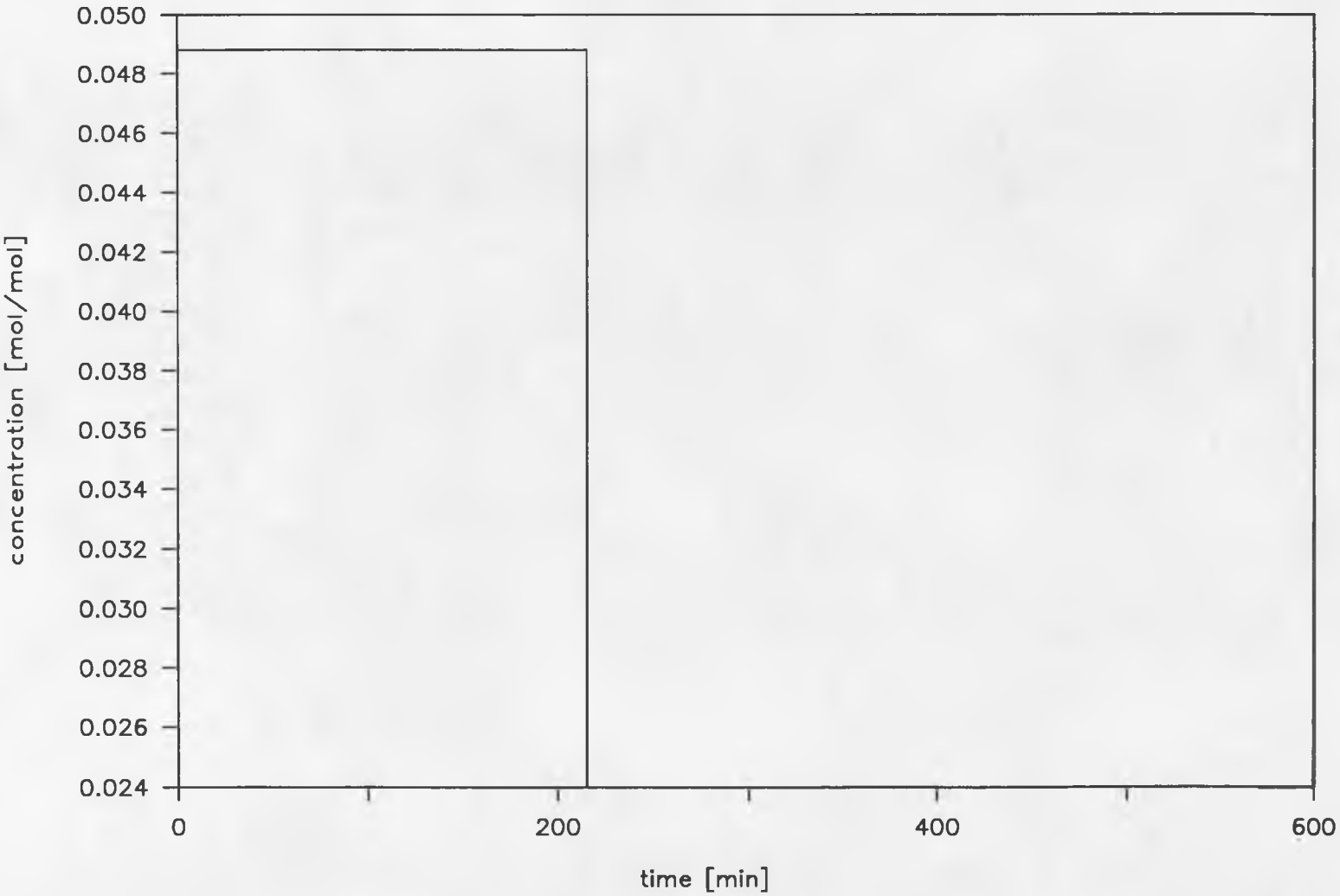

Figure 5.8 - Adiabatic Desorption Breakthrough for Silica Gel ; Equilibrium Solution (Initially saturated bed, i.e. c_o = 0.024 m/m)

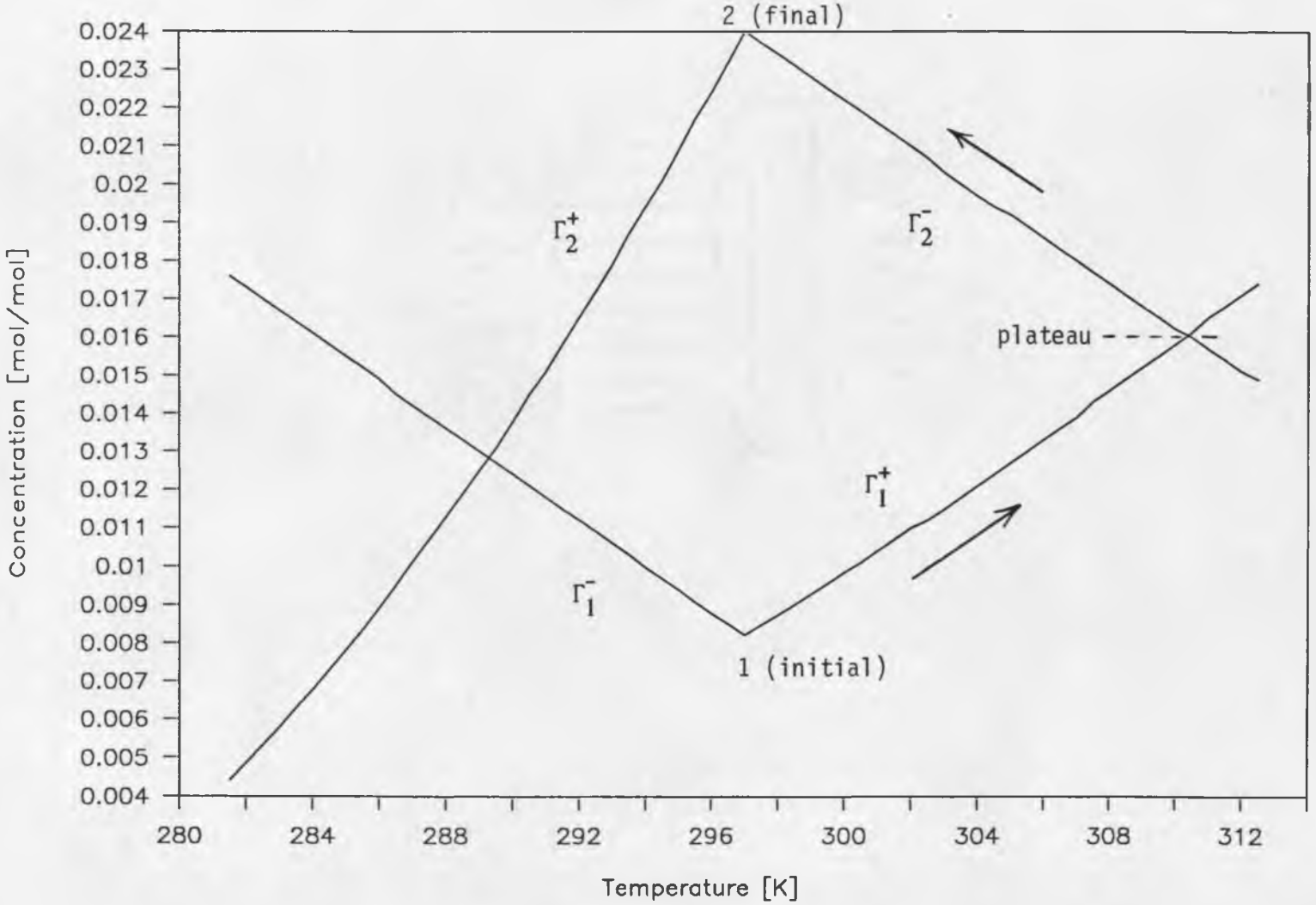

Figure 5.9 - Adiabatic Characteristic Plot for Ethylene Glycol Dehumidification. (Breakthrough proceeds along path indicated by arrow)

Table 5.3

Adsorption Characteristics with Corresponding Wave Velocities

-Ethylene Glycol-

T [K]	Γ_1^+	Γ_2^-	ω_1^+	ω_2^-
297.0	0.0082	0.0240	1.6417	0.0022
297.5	0.0085	0.0237	1.6492	0.0027
298.0	0.0087	0.0234	1.6566	0.0033
298.5	0.0090	0.0231	1.6639	0.0040
299.0	0.0093	0.0228	1.6710	0.0049
299.5	0.0096	0.0225	1.6780	0.0059
300.0	0.0098	0.0222	1.6849	0.0070
300.5	0.0101	0.0219	1.6917	0.0083
301.0	0.0104	0.0216	1.6984	0.0098
301.5	0.0107	0.0213	1.7050	0.0114
302.0	0.0110	0.0210	1.7114	0.0132
302.5	0.0112	0.0207	1.7178	0.0152
303.0	0.0115	0.0203	1.7240	0.0175
303.5	0.0118	0.0200	1.7301	0.0199
304.0	0.0121	0.0197	1.7361	0.0226
304.5	0.0124	0.0194	1.7421	0.0256
305.0	0.0127	0.0192	1.7479	0.0288
305.5	0.0130	0.0189	1.7536	0.0322
306.0	0.0133	0.0186	1.7592	0.0360
306.5	0.0136	0.0183	1.7647	0.0400
307.0	0.0139	0.0180	1.7701	0.0443
307.5	0.0143	0.0177	1.7754	0.0490
308.0	0.0146	0.0174	1.7806	0.0539
308.5	0.0149	0.0171	1.7857	0.0591
309.0	0.0152	0.0168	1.7908	0.0647
309.5	0.0155	0.0165	1.7957	0.0705
310.0	0.0158	0.0162	1.8005	0.0767
310.5	0.0161	0.0160	1.8053	0.0832
311.0	0.0165	0.0157	1.8099	0.0901
311.5	0.0168	0.0154	1.8145	0.0973
312.0	0.0171	0.0151	1.8190	0.1048
312.5	0.0174	0.0149		

velocity. This indicates that the initial jump to the plateau zone is a shock wave and the subsequent saturation of the bed with the inlet air stream follows along a proportionate pattern wave. The jump to the plateau zone is almost immediate, being in the neighborhood of 2-3 minutes, and this plateau zone lingers until the second breakthrough occurs at 60 minutes. The complete saturation of the bed occurs at 2270 minutes. Figure 5.10 shows the breakthrough curve along with the z-t characteristics.

The desorption follows along the Γ^+ characteristic to a plateau region of 309 °K and 0.045 moles/mole. Figure 5.11 is the characteristic plot for the regeneration which corresponds to Table 5.4. The first wave to the plateau region is a shock and the trailing wave after the plateau zone is also a shock front. The overall breakthrough curve for the regeneration is shown in figure 5.12.

The specific cooling capacity and COP of the liquid system under adiabatic conditions are less than those of same system under isothermal conditions. The ratio of the two capacities is the same as the ratio of the humidity depressions of the dehumidification streams. The specific cooling capacity for the adiabatic system is therefore equal to about 1/2 that of the isothermal system. The COP of the system is determined again by the regeneration "roll-up". In this case, the adiabatic COP is nearly equal to that of the solid system, being approximately 0.6.

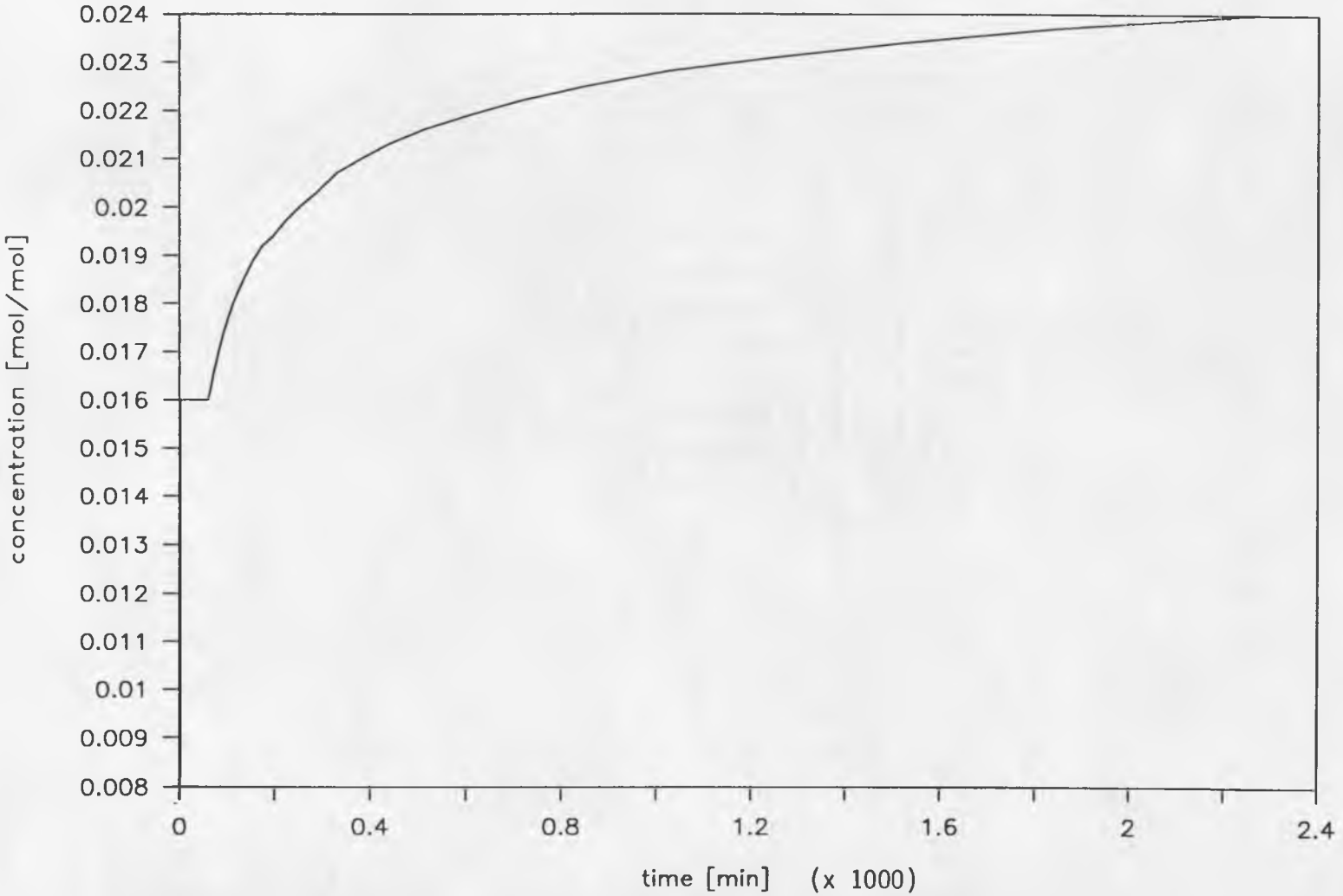

Figure 5.10 - Adiabatic Dehumidification Breakthrough for Ethylene Glycol ; Equilibrium Solution (Initial equilibrium humidity of 0.0082 m/m)

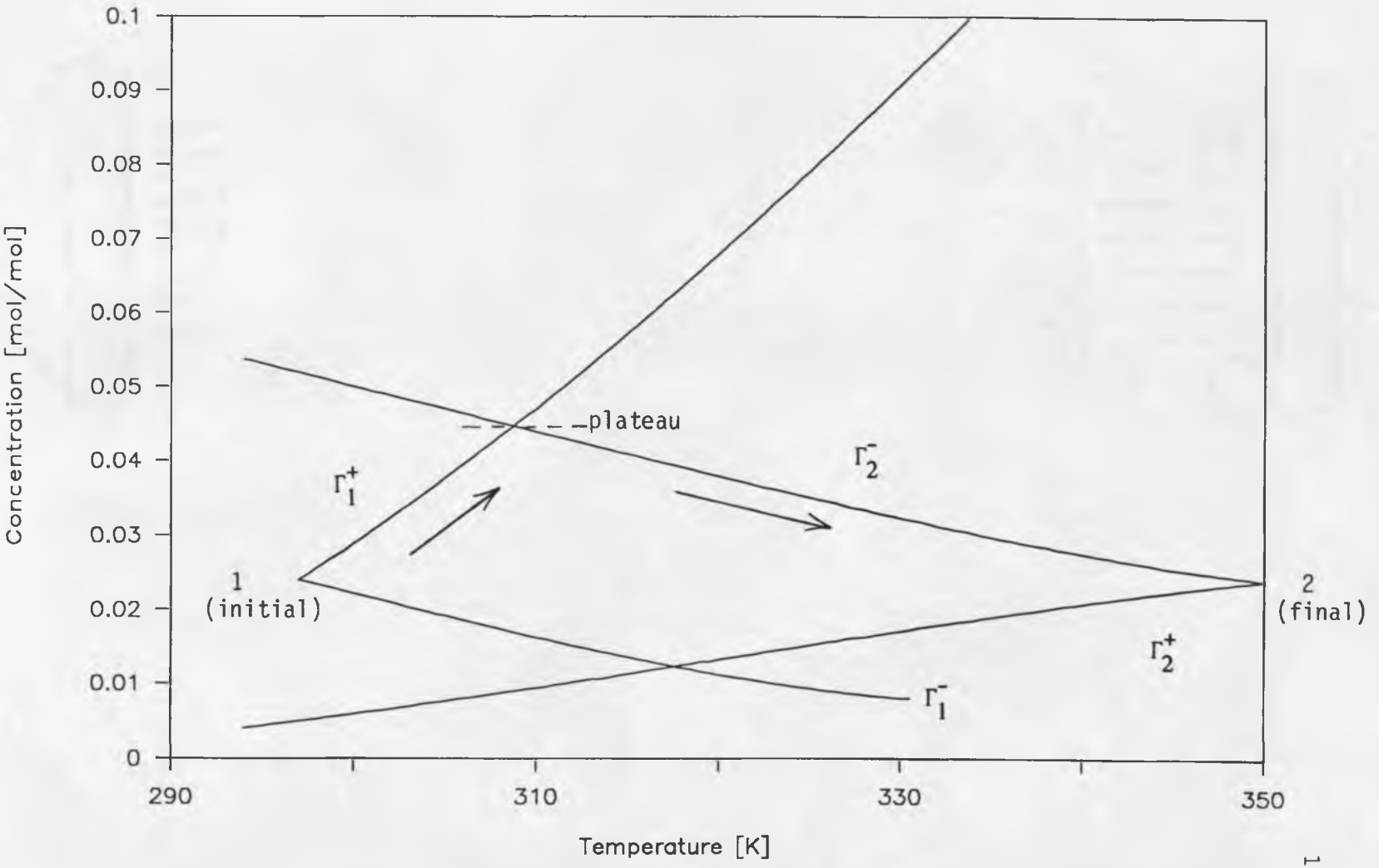

Figure 5.11 - Adiabatic Characteristic Plot for Ethyene Glycol Regeneration. (Breakthrough proceeds along path indicated by arrows)

Table 5.4

Desorption Characteristics with Corresponding Wave Velocities

-Ethylene Glycol-

T_2 [K]	Γ_2^-	ω_2^-	T_1 [K]	Γ_1^+	ω_1^+
350.0	0.0240	0.1373	297.0	0.0240	0.8652
349.5	0.0241	0.1333	297.5	0.0248	0.8719
349.0	0.0243	0.1294	298.0	0.0256	0.8787
348.5	0.0244	0.1257	298.5	0.0264	0.8853
348.0	0.0246	0.1221	299.0	0.0272	0.8918
347.5	0.0248	0.1185	299.5	0.0280	0.8983
347.0	0.0249	0.1151	300.0	0.0289	0.9046
346.5	0.0251	0.1117	300.5	0.0297	0.9109
346.0	0.0253	0.1084	301.0	0.0306	0.9171
345.5	0.0254	0.1052	301.5	0.0314	0.9232
345.0	0.0256	0.1020	302.0	0.0323	0.9293
344.5	0.0258	0.0989	302.5	0.0332	0.9352
344.0	0.0260	0.0959	303.0	0.0340	0.9412
343.5	0.0262	0.0929	303.5	0.0349	0.9470
343.0	0.0264	0.0900	304.0	0.0358	0.9528
342.5	0.0266	0.0872	304.5	0.0367	0.9584
342.0	0.0268	0.0844	305.0	0.0376	0.9641
341.5	0.0270	0.0817	305.5	0.0386	0.9697
341.0	0.0272	0.0790	306.0	0.0395	0.9751
340.5	0.0274	0.0764	306.5	0.0404	0.9806
340.0	0.0276	0.0738	307.0	0.0414	0.9859
339.5	0.0279	0.0713	307.5	0.0423	0.9912
339.0	0.0281	0.0688	308.0	0.0433	0.9965
338.5	0.0283	0.0664	308.5	0.0442	1.0017
338.0	0.0286	0.0640	309.0	0.0452	1.0068
337.5	0.0288	0.0617	309.5	0.0462	1.0118
337.0	0.0290	0.0595	310.0	0.0471	1.0169
336.5	0.0293	0.0572	310.5	0.0481	1.0218
336.0	0.0295	0.0551	311.0	0.0491	1.0267
335.5	0.0298	0.0529	311.5	0.0501	1.0315
335.0	0.0300	0.0508	312.0	0.0511	1.0363
334.5	0.0303	0.0488	312.5	0.0521	1.0410
334.0	0.0305	0.0468	313.0	0.0532	1.0457
333.5	0.0308	0.0449	313.5	0.0542	1.0503
333.0	0.0310	0.0430	314.0	0.0552	1.0549
332.5	0.0313	0.0411	314.5	0.0562	1.0594
332.0	0.0316	0.0393	315.0	0.0573	1.0638
331.5	0.0318	0.0376	315.5	0.0583	1.0682
331.0	0.0321	0.0359	316.0	0.0594	1.0726
330.5	0.0324	0.0342	316.5	0.0604	1.0768

330.0	0.0326	0.0326
329.5	0.0329	0.0310
329.0	0.0332	0.0295
328.5	0.0335	0.0280
328.0	0.0337	0.0266
327.5	0.0340	0.0252
327.0	0.0343	0.0239
326.5	0.0346	0.0226
326.0	0.0349	0.0213
325.5	0.0352	0.0201
325.0	0.0355	0.0190
324.5	0.0358	0.0178
324.0	0.0360	0.0168
323.5	0.0363	0.0157
323.0	0.0366	0.0147
322.5	0.0369	0.0138
322.0	0.0372	0.0129
321.5	0.0375	0.0120
321.0	0.0378	0.0112
320.5	0.0381	0.0104
320.0	0.0384	0.0096
319.5	0.0387	0.0089
319.0	0.0390	0.0083
318.5	0.0394	0.0076
318.0	0.0397	0.0070
317.5	0.0400	0.0064
317.0	0.0403	0.0059
316.5	0.0406	0.0054
316.0	0.0409	0.0049
315.5	0.0412	0.0045
315.0	0.0415	0.0041
314.5	0.0418	0.0037
314.0	0.0421	0.0033
313.5	0.0424	0.0030
313.0	0.0428	0.0027
312.5	0.0431	0.0024
312.0	0.0434	0.0021
311.5	0.0437	0.0019
311.0	0.0440	0.0017
310.5	0.0443	0.0015
310.0	0.0446	0.0013
309.5	0.0450	0.0011
309.0	0.0453	0.0010
308.5	0.0456	0.0009
308.0	0.0459	0.0007
307.5	0.0462	0.0006
307.0	0.0465	0.0005
306.5	0.0469	0.0005

317.0	0.0615	1.0811
317.5	0.0626	1.0854
318.0	0.0636	1.0895
318.5	0.0647	1.0936
319.0	0.0658	1.0977
319.5	0.0669	1.1017
320.0	0.0680	1.1057
320.5	0.0691	1.1096
321.0	0.0702	1.1135
321.5	0.0713	1.1173
322.0	0.0724	1.1211
322.5	0.0735	1.1249
323.0	0.0747	1.1286
323.5	0.0758	1.1323
324.0	0.0769	1.1359
324.5	0.0781	1.1395
325.0	0.0792	1.1430
325.5	0.0804	1.1465
326.0	0.0815	1.1499
326.5	0.0827	1.1533
327.0	0.0838	1.1567
327.5	0.0850	1.1600
328.0	0.0862	1.1634
328.5	0.0873	1.1666
329.0	0.0885	1.1698
329.5	0.0897	1.1730
330.0	0.0909	

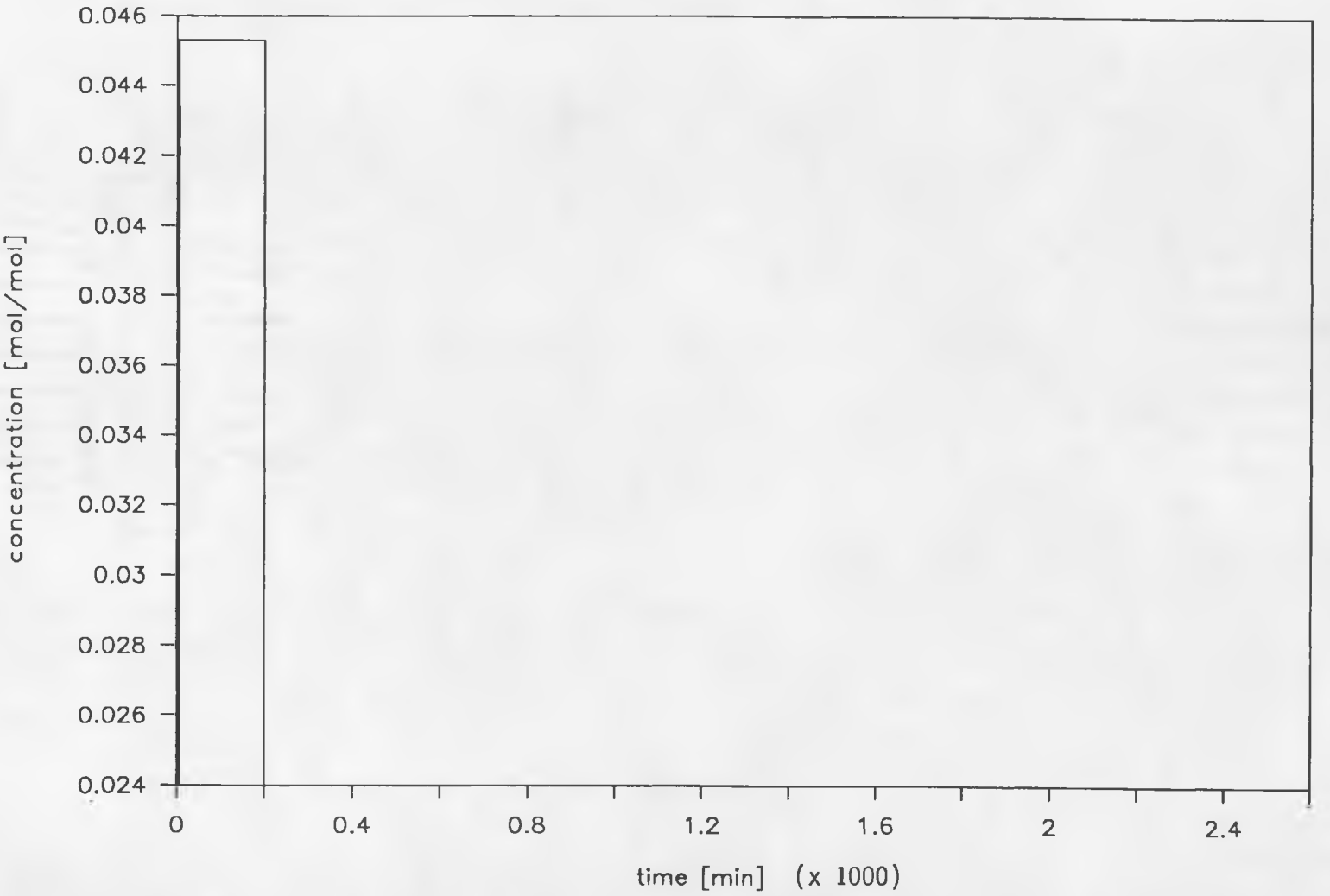

Figure 5.12 - Adiabatic Regeneration Breakthrough for Ethylene Glycol ; Equilibrium Solution
(Initially saturated liquid, i.e. c_o = 0.024 m/m)

5.3 Thomas Solution (Isothermal w/mass transfer resistance)

This section deals with the effect that mass transfer resistance has on the breakthrough behavior of the system. As discussed in section 2.2.3, this analysis assumes isothermal, plug flow behavior with a linear isotherm.

Figure 5.13 shows a theoretical adsorption curve for silica gel at 297°K. Compared to the isothermal analysis, the effect of the mass transfer resistance can be seen. The lower the resistance (i.e. higher value of mass transfer coefficient $K_f a$), the steeper the breakthrough curve becomes until at infinite mass transfer rate the profile becomes a step function, as in the isothermal equilibrium case. The total amount of water adsorbed remains the same for all values of mass transfer coefficient.

In order to calculate desorption breakthrough curves using this method, the boundary conditions are simply reversed, resulting in a mirror image of the adsorption case. However, since this method assumes linear equilibrium characteristics, the regeneration temperature does not change the shape of the curve at all, as opposed to the isothermal method which predicts a sharp increase in the wave speed. The reason for this is that the only parameter which takes the equilibrium effects into account is the distribution coefficient, K_D.

Since in actuality the slope of the equilibrium curve changes with temperature and concentration, a method to approximate this effect on the breakthrough curve would be to approximate the slope of the isotherm at the conditions of the adsorption/desorption. At the

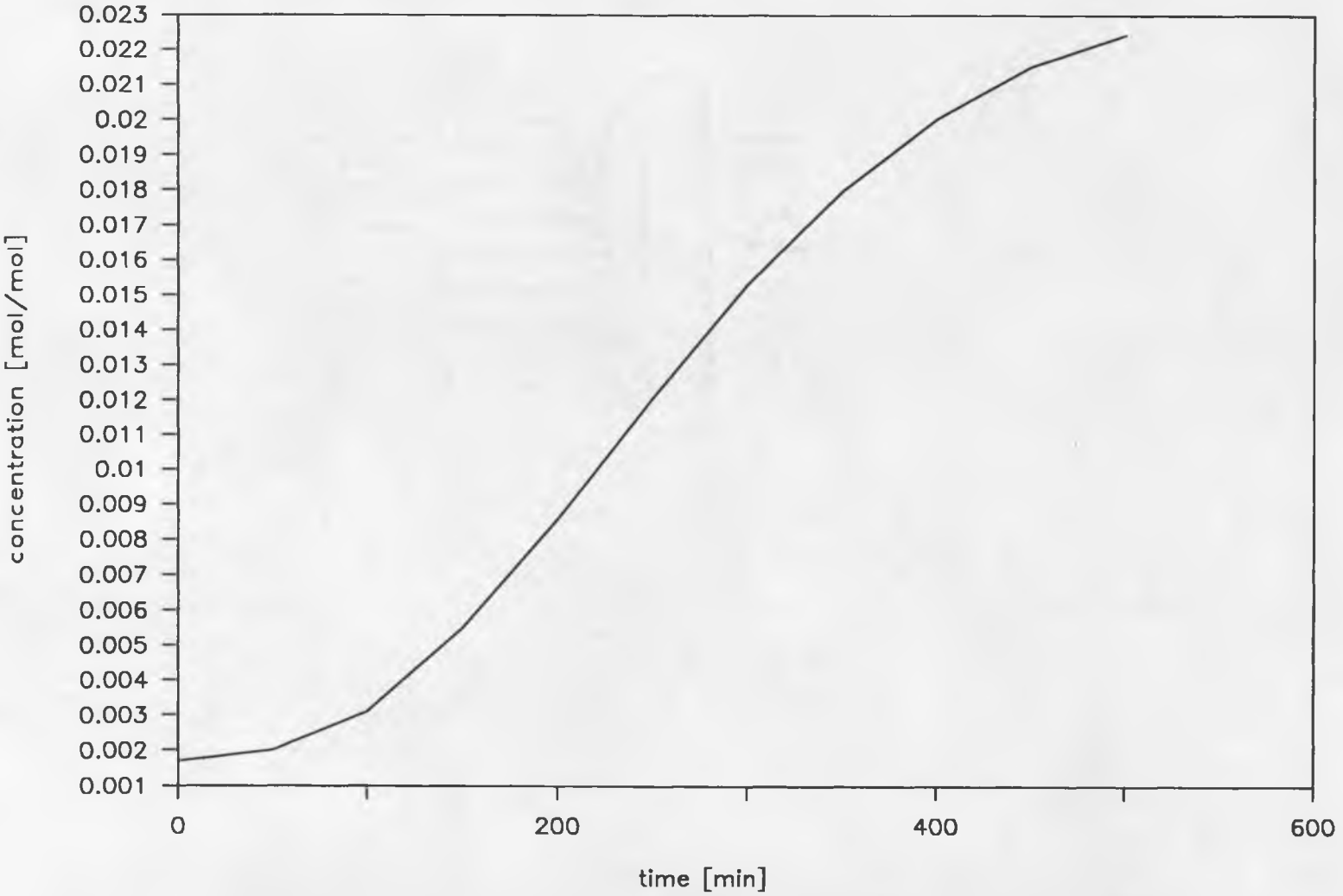

Figure 5.13 - Isothermal Adsorption Breakthrough for Silica Gel ; Thomas Solution
(Initial equilibrium humidity of 0.0017 m/m)

regeneration temperature of 350°K and the equilibrium humidity of 0.34 moles/mole, the actual slope of the silica gel isotherm is very close to zero, which would greatly increase the time parameter constant. This would put the desorption curve in a more similar relationship to the isothermal equilibrium model. The same is true for the liquid desiccant, since the average slope greatly decreases with temperature.

5 4 Numerical Analysis (mass and heat transfer resistance)

This section uses the finite difference scheme developed in section 2.2.4 to calculate breakthrough curves for a theoretical adiabatic system with finite heat and mass transfer resistance. The analysis still assumes the flow to be plug flow.

5.4.1 Silica Gel

Figures 5.14 and 5.15 show the adsorption breakthrough curves calculated with dry bed conditions and regeneration conditions, respectively. It can be seen that the dry bed shows no plateau region while the bed with 0.00263 moles/gram initial loading shows a jump to a plateau region of approximately 0.0072 moles/mole humidity. This is in close agreement with the plateau region calculated by the adiabatic equilibrium method. The gradual breakthrough to the inlet humidity is caused both by the dispersive nature of the trailing wave and by the mass transfer resistance which broadens it even more.

Figure 5.16 shows the numerical results for the desorption case. This also very closely agrees with the adiabatic equilibrium value of the plateau humidity, 0.0488 moles/mole. The trailing wave is more disperse than the initial wave due to the dispersive nature predicted by the equilibrium method as well as the added mass transfer effects. All of the numerical results serve to validify the adiabatic equilibrium analysis and to give an idea as to the effect that the mass transfer resistance has on the performance.

Also, figure 5.17 shows a temperature breakthrough for dehumidification, which corresponds to figure 5.15. This agrees well

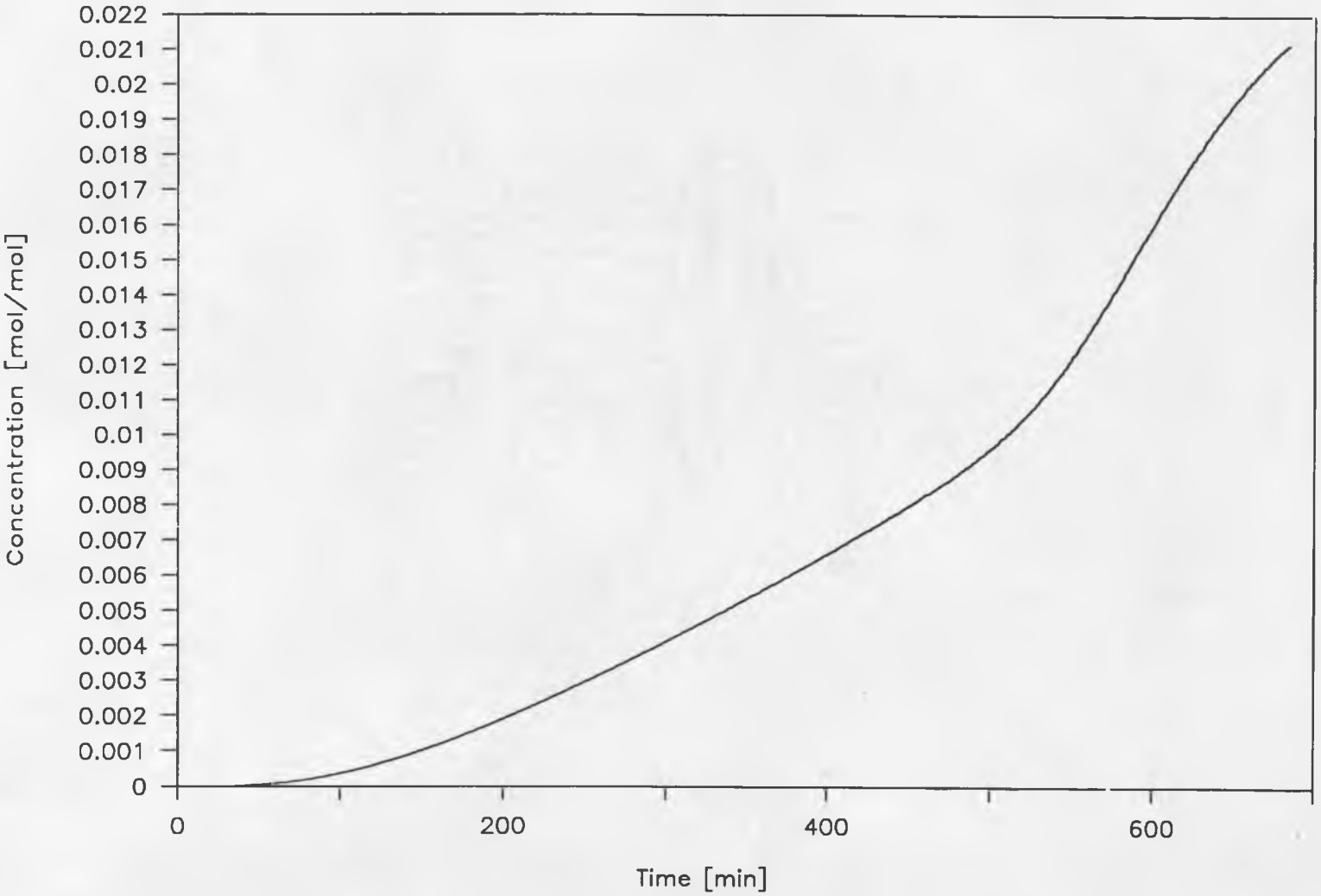

Figure 5.14 - Adiabatic Adsorption Breakthrough for Silica Gel ; Numerical Solution (Initially dry bed, i.e. $c_o = 0$)

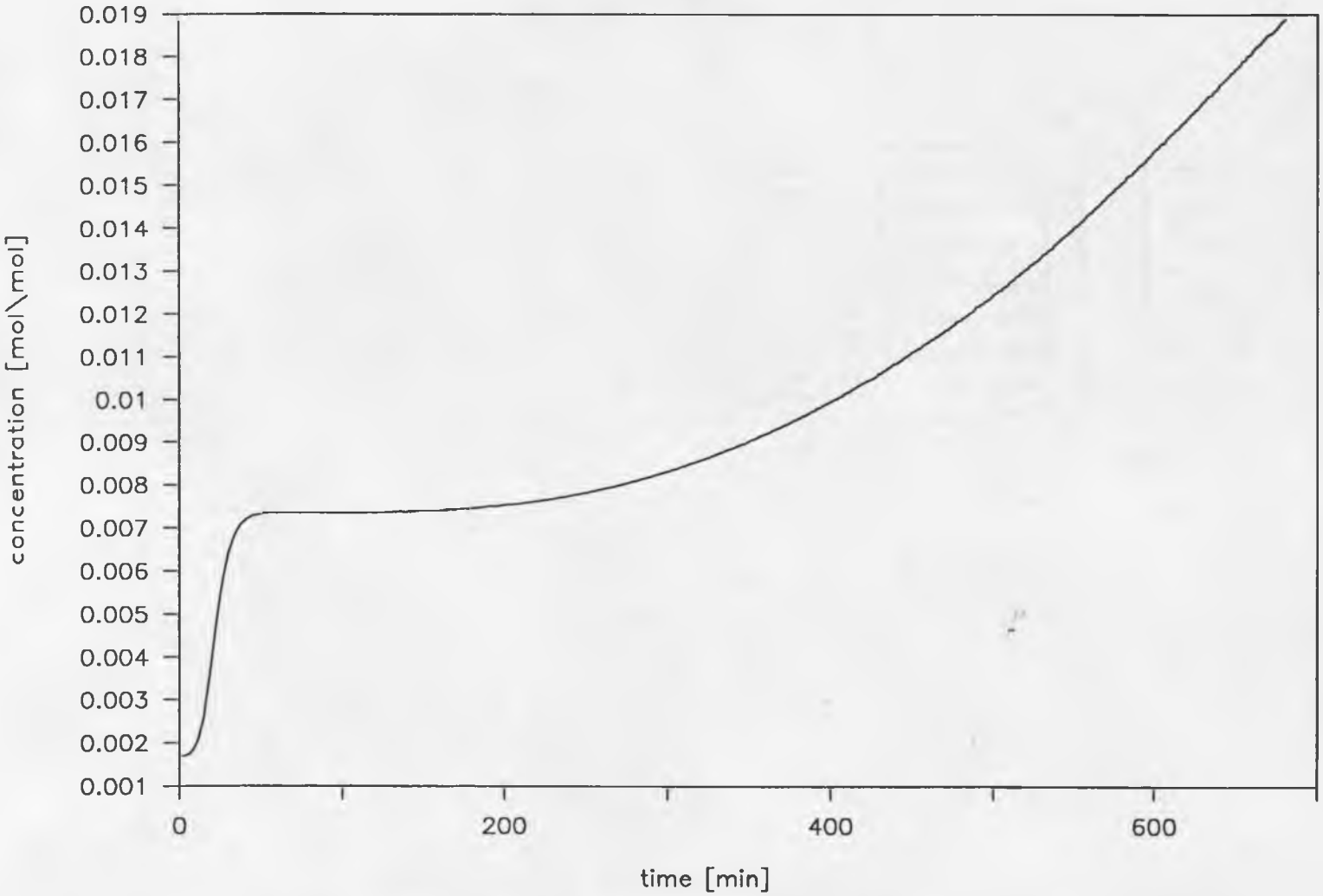

Figure 5.15- Adiabatic Adsorption Breakthrough for Silica Gel ; Numerical Solution (Initial equilibrium humidity of 0.0017 m/m)

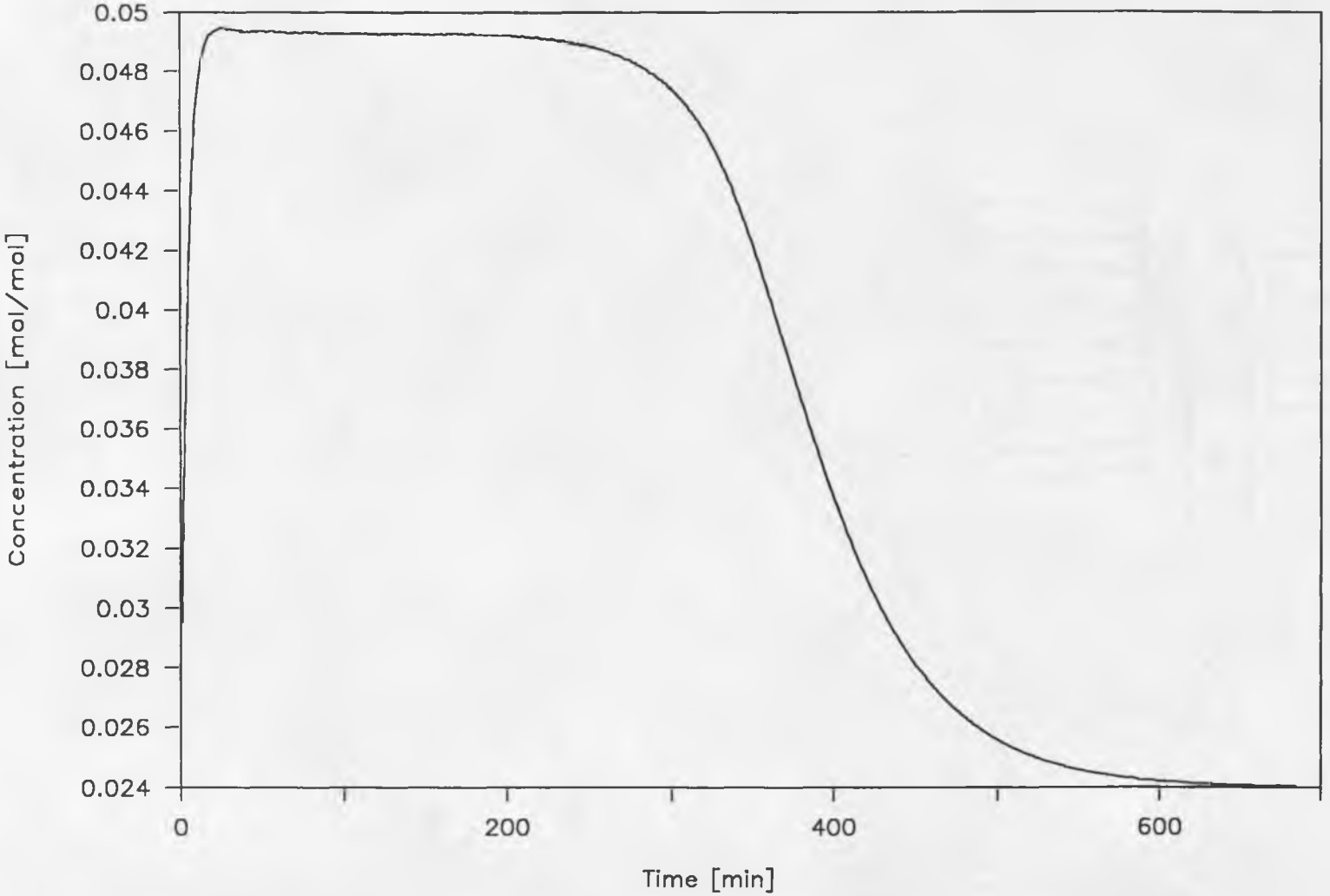

Figure 5.16- Adiabatic Desorption Breakthrough for Silica Gel ; Numerical Solution (Initially saturated bed, i.e. co = 0.024 m/m)

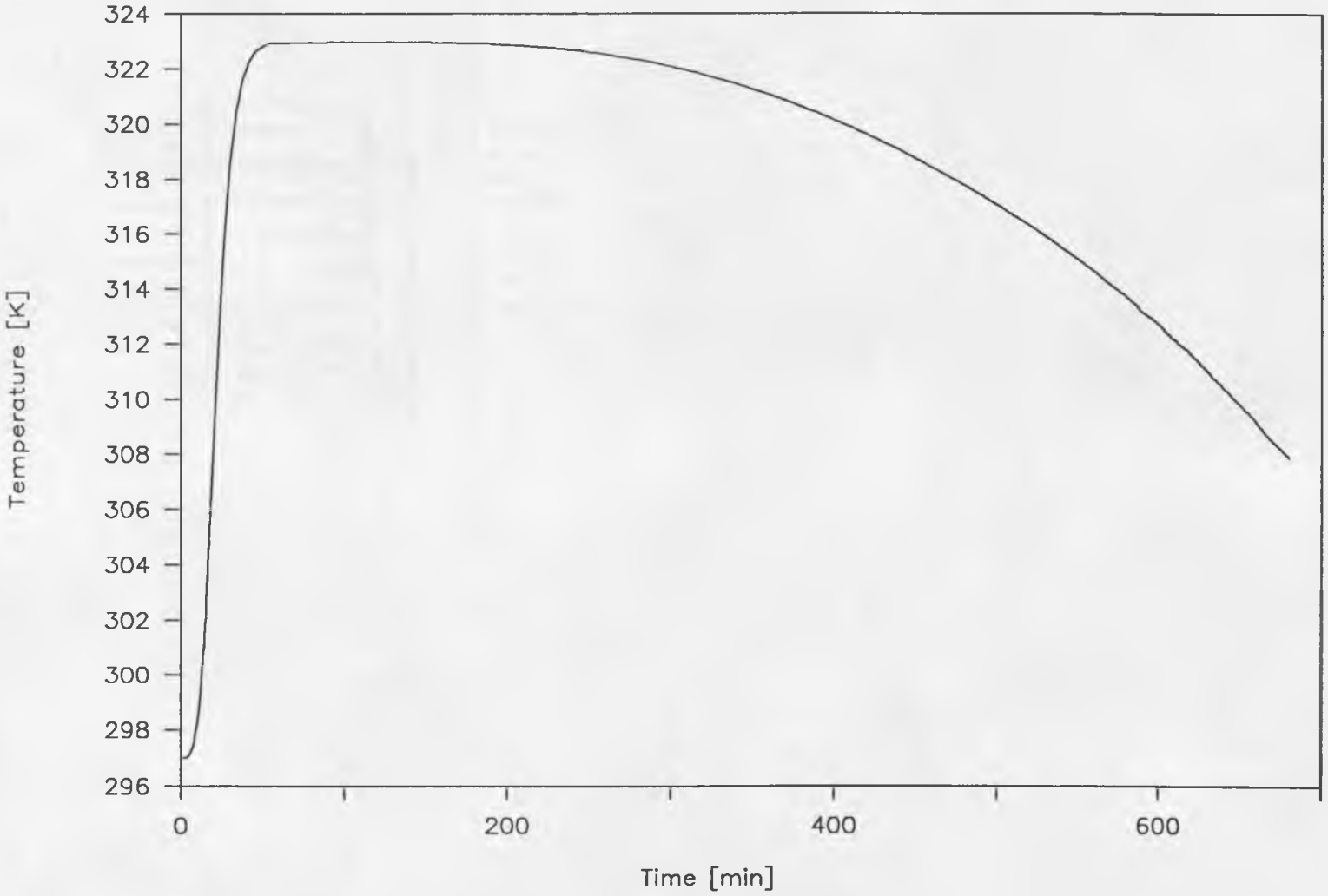

Figure 5.17- Numerically Calculated Temperature Breakthrough for Silica Gel - Dehumidification.

with the plateau temperature predicted by the equilibrium model and is seen to validify the assumption of coherence of wave fronts, since the temperature wave follows proportionately to the concentration wave.

5.4.2 Ethylene Glycol

The same results are seen for the ethylene glycol simulation. Figure 5.18 shows the development of the dehumidification concentration breakthrough curve. Once again, the behavior is similar to the equilbrium adiabatic analysis, and the added effect of mass transfer resistance is seen. The plateau zone is too small to show up on the numerical model as the mass transfer effect diminishes it greatly.

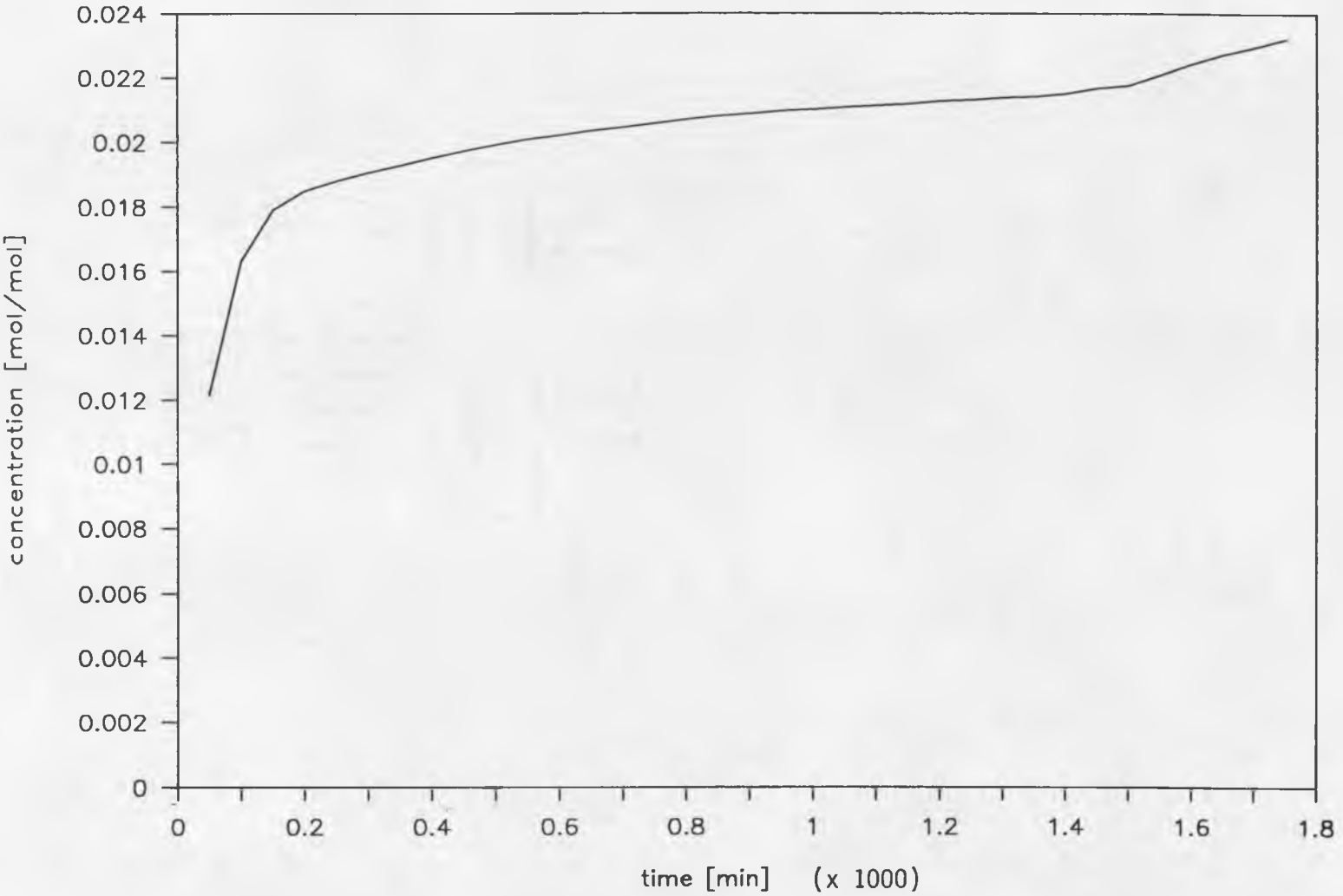

Figure 5.18- Dehumidification Breakthrough for Ethylene Glycol, Numerical Solution (Initial equilibrium stream concentration = 0.0082 moles/mole)

5.5 Experimental Results

Figures 5.19, 5.20, and 5.21 show the experimental breakthrough curves for silica gel alone, ethylene glycol alone, and the liquid-solid bi-desiccant. The concentration output is given as a normalized concentration with C_o representing the minimum value of humidity registered by the humidity sensor. C_f represents the inlet fluid concentration, or 0.024 moles H_2O/moles air at 297°K. The x-axis is simply time, given in minutes.

The experimental breakthrough curves for silica gel were performed for 2 inches ($\approx$ 5 cm) and 4 inches. As expected, the slope of the curves remains relatively constant with respect to bed height due to the isotherm shape. The total capacity for moisture is seen to nearly double for the 4 inch run compared to the 2 inch run, which is to be expected. However, the break time for the 4 inch run was much greater than twice that of the 2 inch run. This indicates that the concentration profile inside the column is fairly wide so that the total distance travelled by the leading edge is more than doubled.

Comparing the experimental results with calculated results, as seen in Figure 5.22, a few points can be deduced. First of all, there is a difference in the total capacity of the desiccant for the experimental case and that calculated with the theoretical models. This is explained by the fact that the maximum theoretical loading at 297°K is 0.0145 moles/gram desiccant as opposed to a more accurate value of 0.022 moles/gram obtained from the literature, so that the theoretical capacity will decrease accordingly. Secondly, the

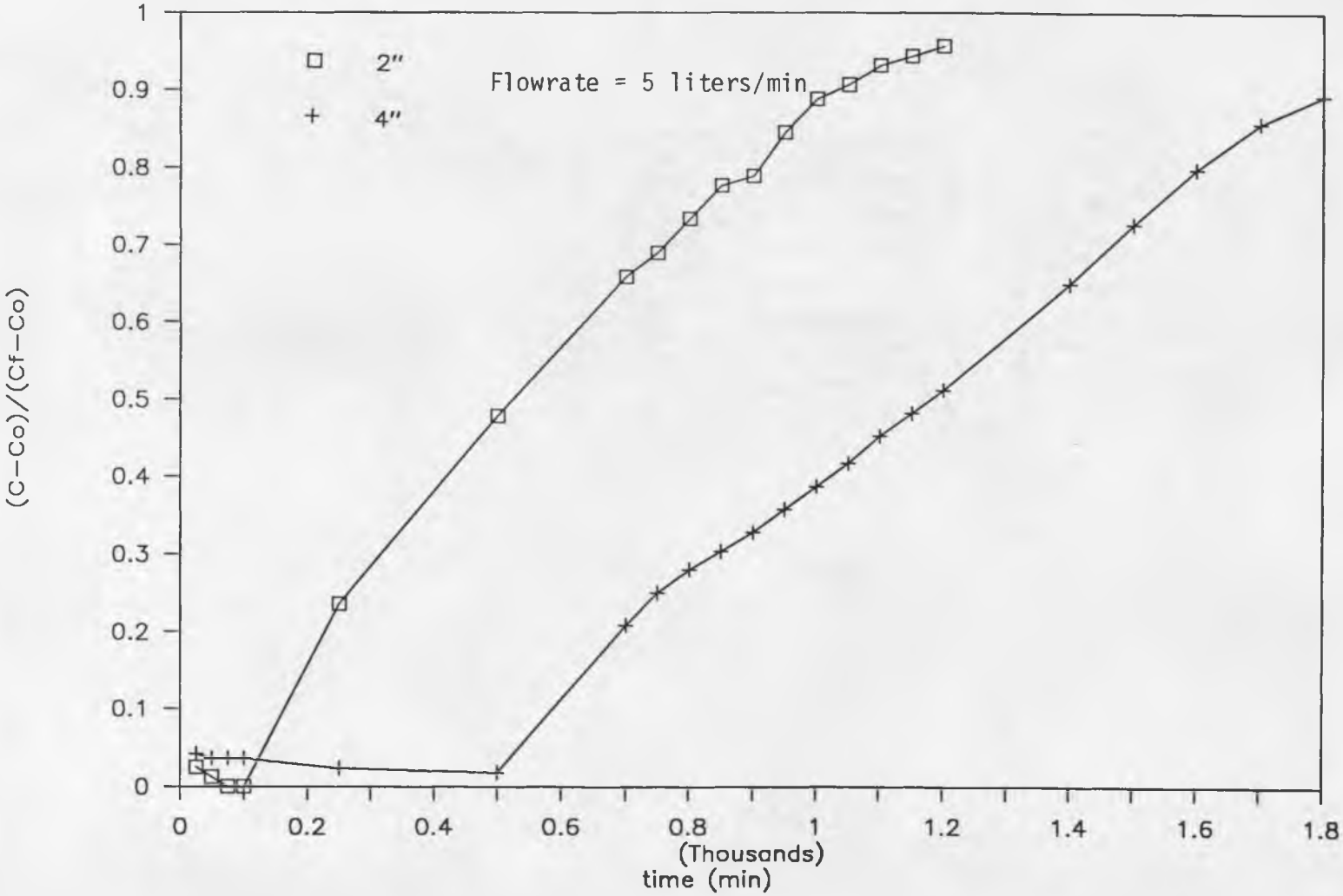

Figure 5.19 - Experimental Dehumidification Breakthrough Curves for Silica Gel (Solid initially free of moisture, i.e. $c_o = 0$)

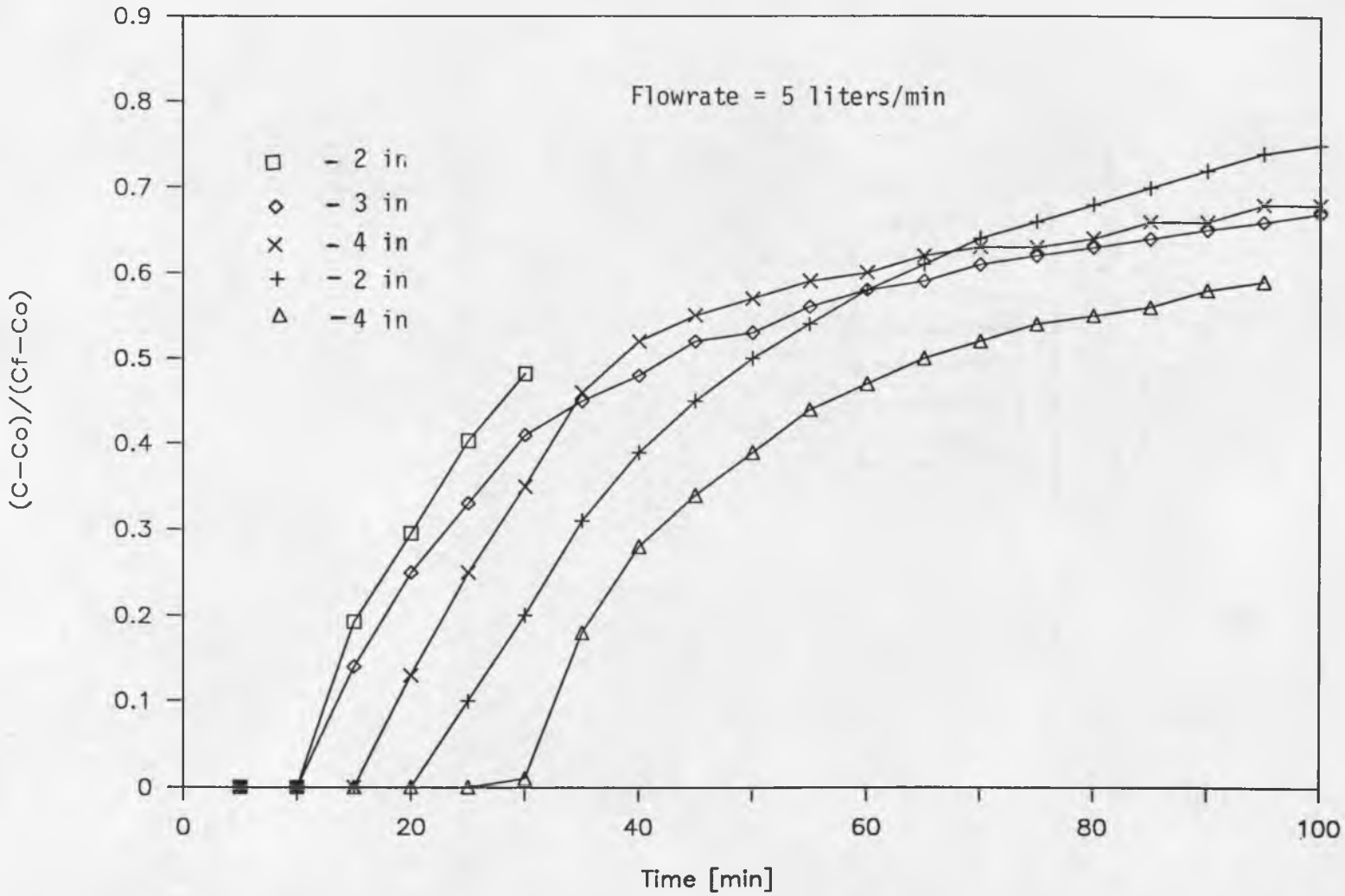

Figure 5.20 - Experimental Dehumidification Breakthrough Curves for Ethylene Glycol (Liquid initially free of moisture, i.e. $c_o = 0$)

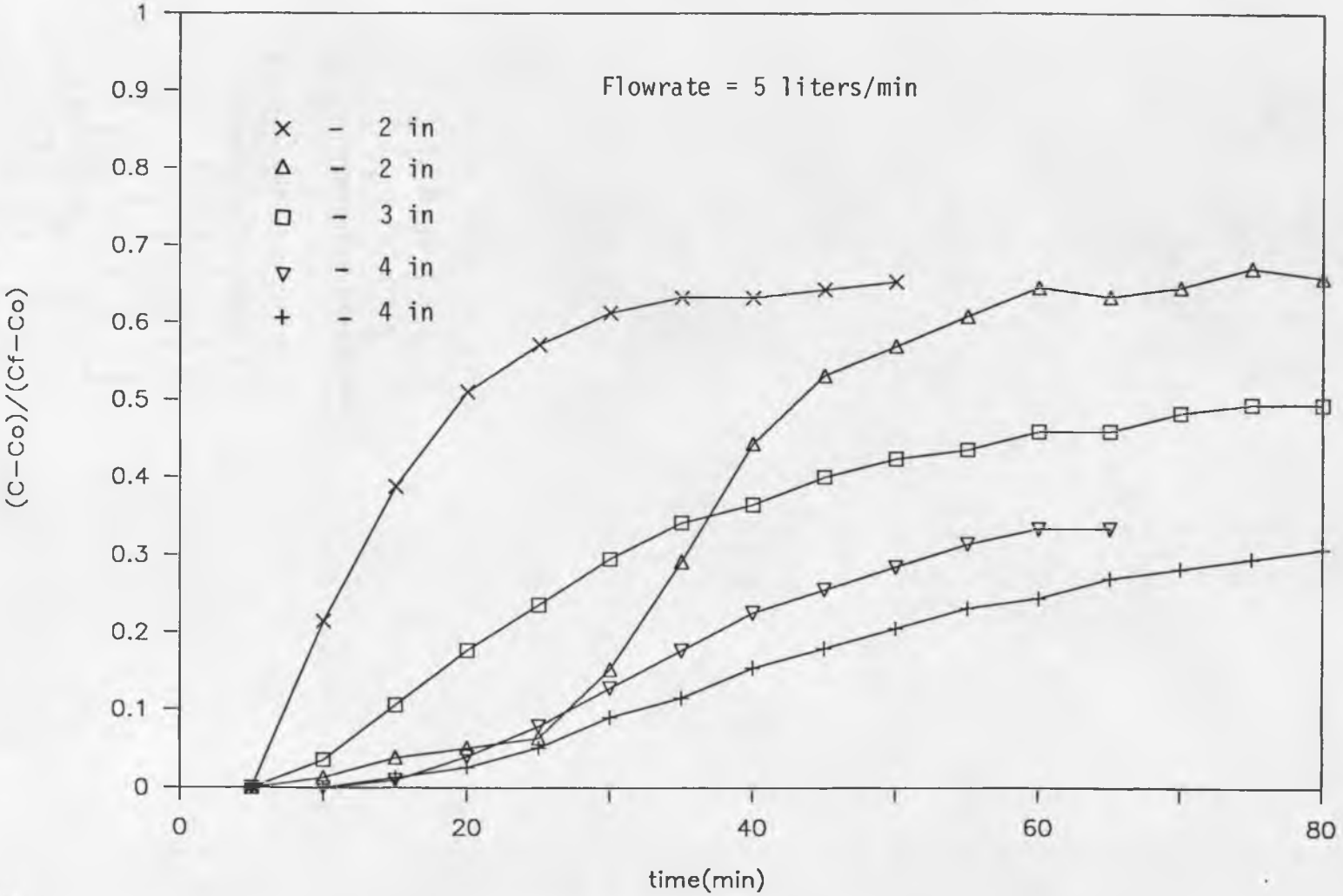

Figure 5.21 - Experimental Dehumidification Breakthrough Curves for Bi-Desiccant (Bi-desiccant initially free of moisture, i.e. $c_o = 0$)

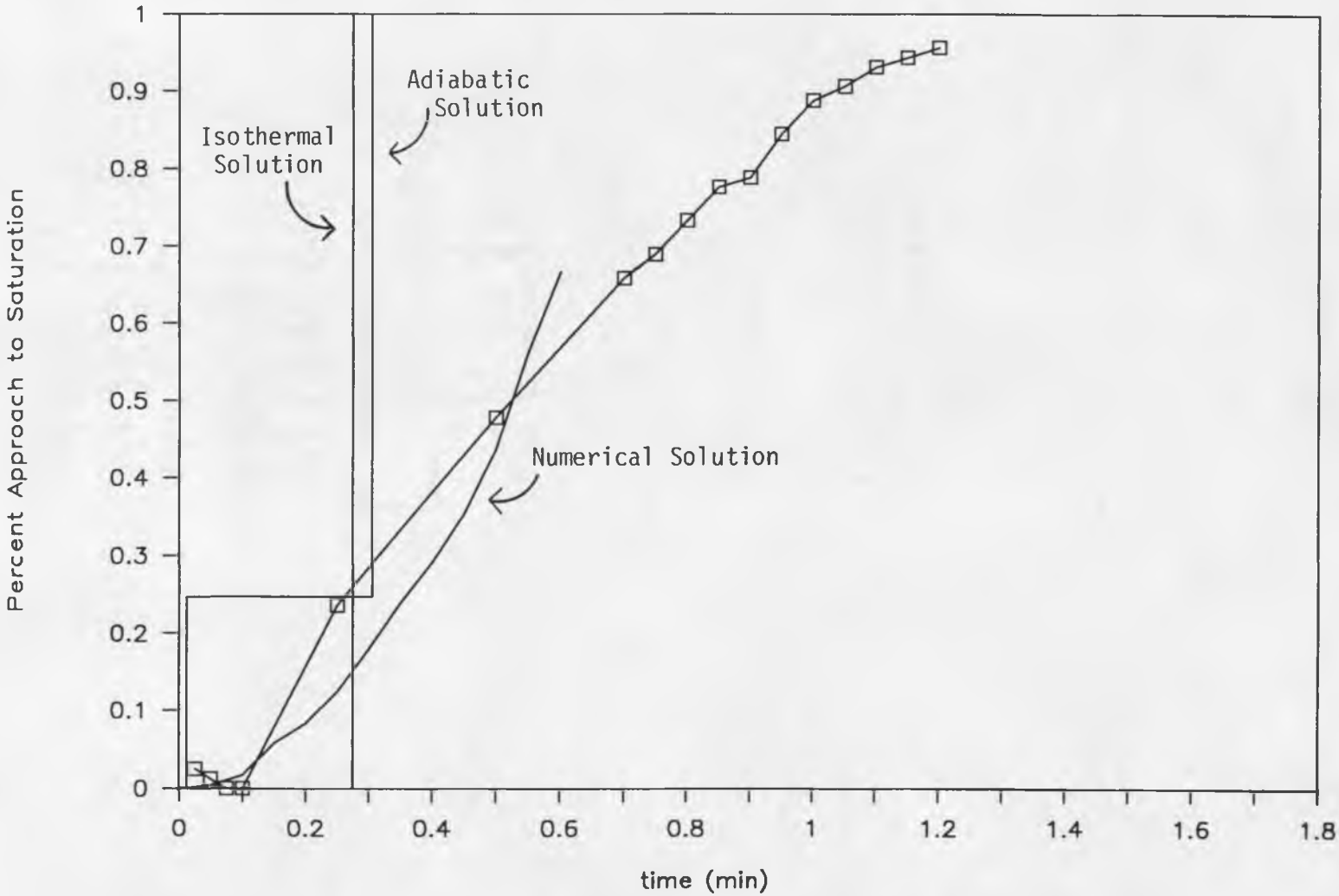

Figure 5.22 - Comparison of Silica Gel Breakthrough to Calculated Results.
(Approach to saturation = $c-c_o/c_f-c_o$)

numerical solution shows approximately the same slope of breakthrough as for the experimental run, which verifies that the mass transfer coefficient of 0.0069 grams/cm^3-sec used in the model closely approximates the real value. Also, there is no plateau zone present in the experimental run, since the silica gel used is essentially pure. The numerical solution was run at zero initial concentration, therefore, and compares fairly well. The total capacity is therefore higher that those for the isothermal and adiabatic equilibrium cases, which show the breakthroughs which would exist at 0.0017 moles/gram initial loading.

The breakthrough curves for the ethylene glycol system were performed at 2,3, and 4 inches. The isothermal analysis predicts that at longer bed lengths, the breakthrough curves should become more and more diffuse. However, the small increases in bed height for this experimentation do not effect a noticable change. Also, there appears to be a fast approach to a plateau after about 40 minutes with little or no further saturation of the bed. This can be explained by the fact that there is a certain degree of channelling within the bed around glycol coated particles. The higher the degree of channelling, the quicker the approach to this plateau and the slower the saturation rate. The total amount of moisture absorbed will be constant, however.

Figure 5.23 compares a 4 inch glycol breakthrough curve on a longer time scale to theoretical results. It can be seen that the

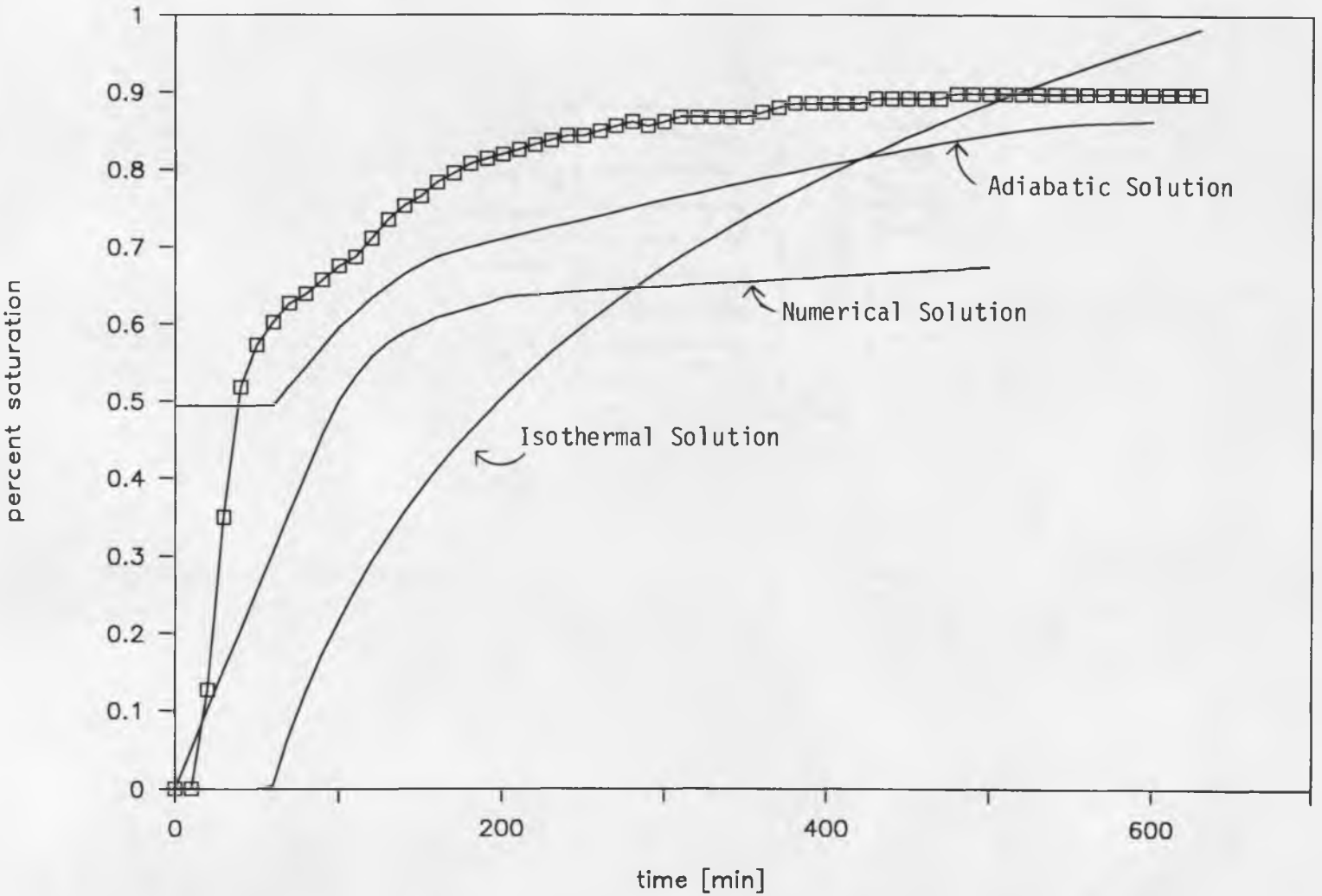

Figure 5.23 - Comparison of Ethylene Glycol Breakthrough to Calculated Results.
(Approach to saturation = $c-c_o/c_f-c_o$)

experimental curve resembles the adiabatic solution more than the isothermal one. The total breakthrough time surpasses that of the isothermal case, which is around 630 minutes. The apparant levelling off at around 70% saturation in Figure 5.20 is shown to be simply a very slow rate of absorption, probably due in part to the adiabatic process and to the channelling effect.

The breakthrough curves of the bi-desiccant system resemble those of the pure glycol with the exception that they are generally flatter and show an increase in the total area under the curve. Figure 5.24 illustrates this for a 4 inch column.

A change in the overall mass transfer coefficient would change the shape of the curve without affecting the area under the curve, or total capacity of the bed. This increase in capacity is due therefore either to a change in equilibrium characteristics or to a change in the bulk density of the desiccant.

The holdup of glycol in the bi-desiccant case is more than that in the liquid case (65 ml vs. 25 ml) so there is definitely an increase due to the change in liquid bulk density. The isothermal equilibrium model predicts a decrease in slope of the characteristics as well and therefore a more disperse front.

However, the Thomas model predicts an increase in capacity with no change in the slope of the breakthrough curve due to the increase in bulk density. The difference between this and the isothermal model lies in the definition of the isotherm. The isothermal model would predict Thomas behavior if the isotherm were linear or favorable. The

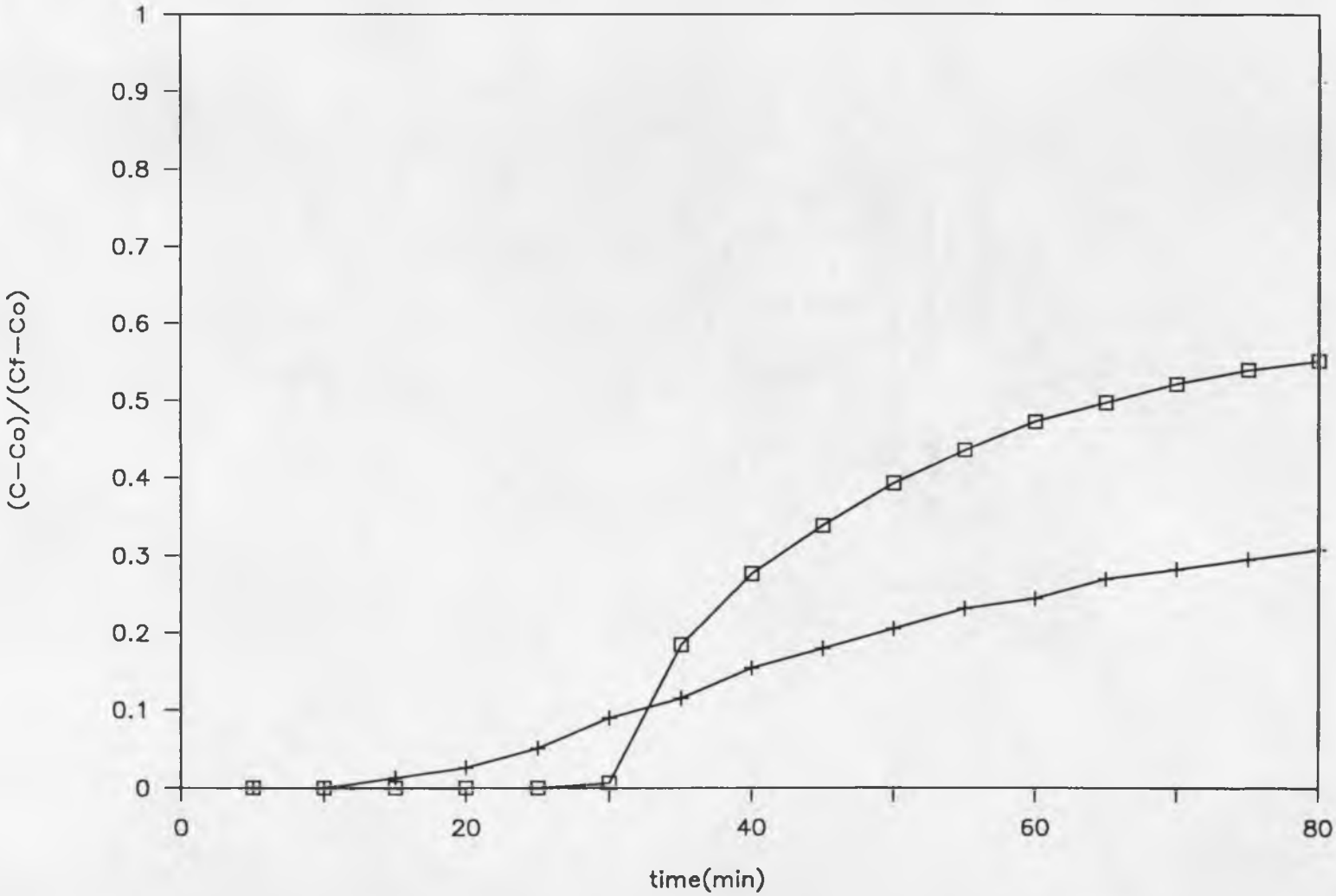

Figure 5.24 - Comparison of Bi-Desiccant (+) and Liquid Desiccant (□) Breakthrough curves (Both runs done on 4 inch columns at 5 liters/min flowrate)

Thomas model would predict a change in capacity with a different distribution coefficient. Since there is a change in the slope of the experimental breakthrough curves, it is not known to what extent this is caused by the change in the isotherm (i.e. from liquid-gas equilibrium to liquid-solid-gas equilibrium).

If there were a change in the capacity due to the change in the equilibrium isotherm, then this would also have a corresponding change to the temperature breakthrough as well according to the adiabatic equilibrium model. This predicts that the plateau temperature is dependent only on the initial temperature and loading of the bed and on the humidification stream conditions. However, the plateau temperature will remain the same in the case of simply a change in the desiccant bulk density. In the case of a change in the distribution coefficient (i.e. a change in the shape of the isotherm) the adiabatic characteristics are altered according to eqn. 2-14, since both the temperature and concentration derivatives of the isotherm are altered, and the plateau temperature will change. This indicates that inspection of the temperature breakthrough for plateau temperatures will yield more information about the interaction of the liquid and solid.

The factor which determines the specific cooling capacity of the system is the degree of humidity depression in the dehumidification stream. In the bi-desiccant case, this depends on the phase equilibrium between the solid and liquid. Figure 5.25 shows

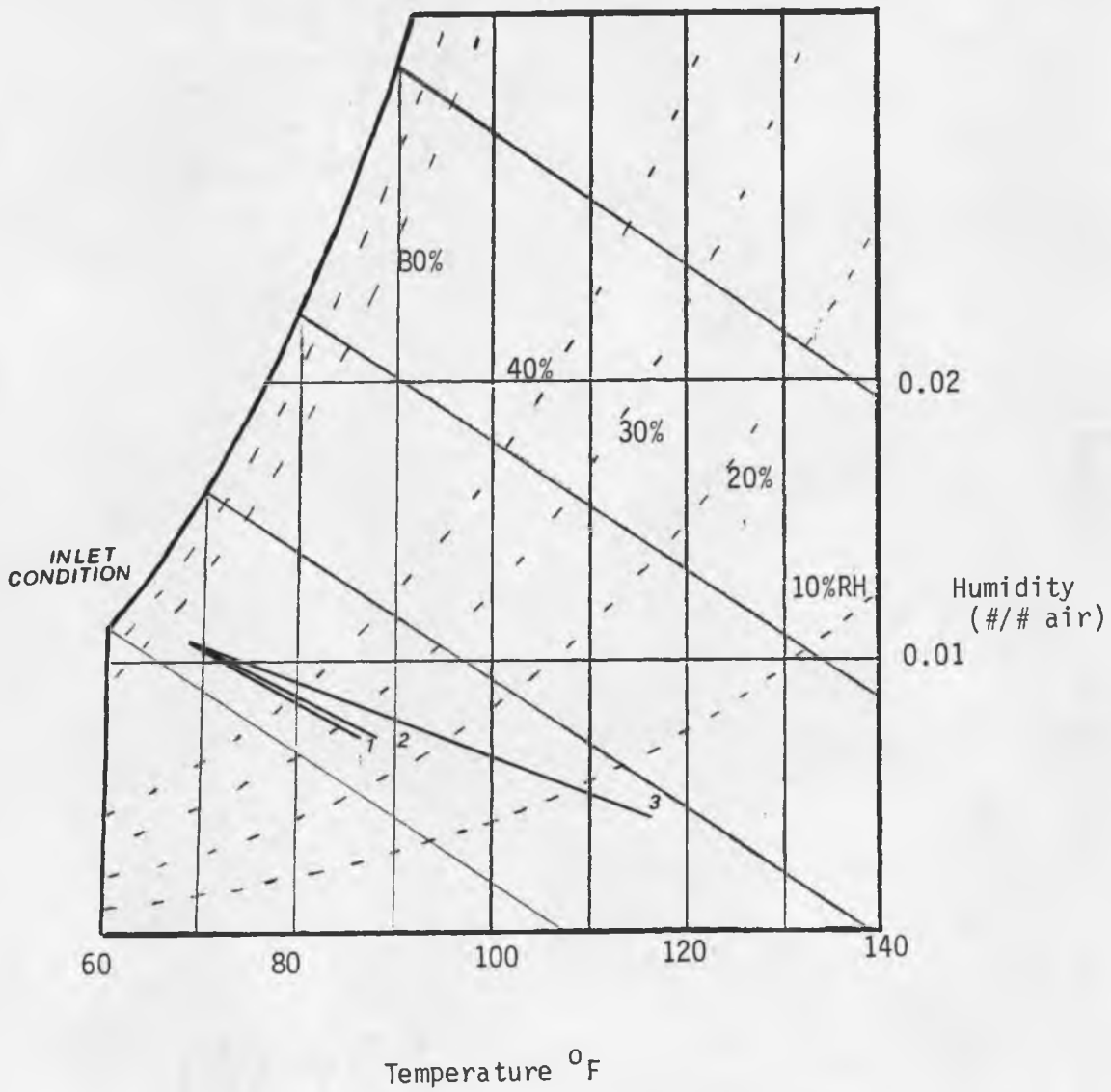

Figure 5.25 - Experimental Breakthroughs Shown on the Psychrometric Diagram (1 = Ethylene Glycol, 2 = Bi-Desiccant, 3 = Silica Gel)

experimental breakthrough curves for silica gel and ethylene glycol systems depicted on a psychrometric chart. As expected, these curves follow generally along the corresonding adiabatic saturation lines on the chart. It can be seen that the ethylene glycol system falls short of the silica gel system in its plateau temperature, peaking at near approximately 90 °F as opposed to the silica gel temperature of nearly 120 °F. This is due to the higher purity of the solid desiccant than the liquid desiccant. Also, the adiabatic characteristic plot of ethylene glycol compared to that of silica gel shows that low concentrations of water in the glycol lead to higher plateau concentrations than for the same amount in silica gel (steeper Γ^{+} characteristics in the dehumidification plot). This is a result of the temperature dependence of the glycol isotherms. This means that the humidity reduction (and therefore the temperature increase) of the dehumidification stream is more sensitive to the initial concentration in the liquid.

The maximum temperature of the bi-desiccant system is seen to be slightly greater than that of the liquid system alone (86 °F versus 84 °F in one case). Since the change in bulk density of the desiccant has no effect on the plateau temperature, and the mass transfer coefficient only affects the slope of the curve, these effects can be ruled out. This suggests that there is a slight shift in the solid-liquid equilibrium causing a lower outlet humidity (i.e. higher outlet temperature) than that achieved with the liquid system alone. The temperature difference is not so great as to indicate considerable

interaction between the two desiccants. Also, a change in the mass transfer coefficient may have broadened the profiles enough so that the profile width surpasses the length of the column. This would cause incomplete breakthrough development and a lowering of the maximum outlet temperature. The temperature was not decreased, however.

Since the silica gel temperature is so much higher that the glycol's, there is no evidence of substantial interaction between the desiccants. This suggests that the ethylene glycol has an overwhelming effect on the solid desiccant, which may be due to the fact that the liquid is easily adsorbed onto the solid as well as the water vapor. The degree of selectivity for silica gel for adsorption follows the pattern:

water > alcohols > alkanes

Therefore, the glycol may not be as preferred as the water, but it takes a percentage of the available sites for adsorption and is also higher in concentration on the surface.

CHAPTER 6: CONCLUSIONS AND RECOMMENDATIONS

The application of desiccant materials for the design of air conditioning systems has resulted in limited success and the material properties have proven to be the determining factor for their performance. Liquid systems typically suffer from the lack of favorable isotherms while maintaining an advantage in flexibility. Solid systems suffer the restriction of operating under adiabatic conditions but exhibit more favorable phase equilibrium.

This study has attempted to illustrate a successful application of a bi-desiccant approach to utilizing the best aspects of both desiccants. The solid and liquid systems are split such that the liquid is used in the regeneration portion and the solid is used in the dehumidification. In this way, the limitations of single desiccant systems may be removed.

It has been determined that the critical aspect of a bi-desiccant system is the liquid/solid/adsorbate equilibrium. The COP, which determines the amount of energy required to achieve a certain amount of dehumidification, is determined by the amount of water cycled by the system under given initial bed and stream conditions. The regeneration conditions control the cycling capacity when the humidity increase across the regeneration bed is greater than the humidity decrease across the dehumidifier. In the bi-desiccant system under investigation, the liquid desiccant becomes the sole medium for

removing moisture from the system and therefore determines the COP. The specific cooling capacity (i.e. tons of cooling/CFM) is determined by the humidity reduction in the dehumidification stream. The greater the humidity reduction, the higher is the rate of dehumidification and the greater is the specific cooling capacity. The liquid/solid combination therefore determines the system specific cooling capacity by controlling the outlet humidity of the air stream. A bi-desiccant system which causes a lowering of equilibrium humidity from the dehumidifier improves the overall performance of the system in comparison to a liquid system.

The results of this research, which combines Silica Gel solid desiccant with Ethylene Glycol liquid desiccant, show a very slight increase in dehumidification compared with that of the Ethylene Glycol system alone. The minimum humidities achieved by each system are :

	Maximum Bed Temperature(°F)	Humidity (#/# air)
Silica Gel	120	0.004
Eth. Gly.	84	0.007
Bi-Dess.	85	0.007

This indicates an overwhelming influence by the liquid on the performance of the bi-desiccant. The solid interaction is masked almost completely. This may be due to the glycol reducing the available sites for adsorption on the silica gel surface. The

capacity of the system is increased over that of the liquid system alone, but that is due mostly to the increased amount of glycol present. The capacity of the desiccant material does not determine the system performance, however.

This research has suggested that the choice of desiccants which are by themselves some of the best desiccants for application in single component systems may not be the best choice for a bi-desiccant system. The choice of silica gel as the solid and ethylene glycol as the liquid resulted from the consideration that they are considered the best in their class of desiccant. However, results of this investigation suggest that the interaction and phase equilibrium between the two may not be optimum for a bi-desiccant application.

It is recommended that a search be done for a liquid/solid pair which exhibits favorable behavior for this application. The liquid should exhibit strong temperature dependence to allow for favorable regeneration characteristics, and the solid should show increasing preference for water vapor with increasing temperature when in contact with the liquid. In this way, the solid will maintain good dehumidification characteristics by keeping the liquid concentration low during adiabatic operation, and the liquid effectively regenerates the bi-desiccant at lower temperatures. Also, the mass transfer resistance should be low in order to avoid the need for large bed heights.

APPENDIX 1 : DATA

SILICA GEL CONCENTRATION BREAKTHROUGH CURVES

Operating Conditions:

Air Flowrate = 5000 ml/min
Inlet Humidity = 75 - 85% RH
Inlet Air Stream Temperature = 70 °F
Z_o = Actual sensor reading
Z' = Percent approach to saturation

time(min)	4" column		2" column	
	Z_o	Z'	Z_o	Z'
25	34	0.04	33	0.02
50	33	0.04	31	0.01
75	33	0.04	29	0.00
100	33	0.04	29	0.00
250	31	0.02	67	0.24
500	30	0.02	106	0.48
700	62	0.21	135	0.66
750	69	0.25	140	0.69
800	74	0.28	147	0.74
850	78	0.30	154	0.78
900	82	0.33	156	0.79
950	87	0.36	165	0.84
1000	92	0.39	172	0.89
1050	97	0.42	175	0.91
1100	103	0.45	179	0.93
1150	108	0.48	181	0.94
1200	113	0.51	183	0.96
1400	136	0.65		
1500	149	0.73		
1600	161	0.80		
1700	171	0.86		
1800	177	0.89		

ETHYLENE GLYCOL BREAKTHROUGH DATA

Operating Conditions:

Air Flowrate = 5 liters/min
Inlet Temperature = 70 °F
Inlet Humidity = 75 - 85 %RH

time (min)	Sensor Reading				
	2"	2"	3"	4"	4"
5	34	51	30	32	28
10	34	51	30	32	28
15	66	51	53	32	28
20	83	51	72	32	50
25	101	65	85	32	70
30	114	80	97	33	87
35		95	104	62	104
40		107	110	77	115
45		116	115	87	120
50		123	118	96	124
55		129	122	103	127
60		134	125	109	129
65		139	127	113	131
70		143	130	117	133
75		146	132	120	134
80		149	134	122	135
85		152	135	124	138
90		154	137	126	139
95		157	139	128	141
100		159	141		142
105		161	143		143
110		162	145		145
115		164	147		149
120		165	149		151
125		167			152
130		168			154
135		169			155
140		170			156
145		171			157
150		172			159
155		173			160
160		173			161
165		174			162
170		175			163
175		175			163
180		176			164
185		177			165
190		177			165

195	177	166
200	178	166
205	178	167
210	179	167
215	179	168
220	180	168
225	180	169
230	180	169
235	181	170
240	181	170
245	181	171
250		171
255		171
260		172
265		172
270		172
275		172
280		172
285		172
290		172
295		173
300		173

PERCENT APPROACH TO SATURATION FOR ABOVE RUNS

time (min)	2"	2"	3"	4"	4"
5	0.00	0.00	0.00	0.00	0.00
10	0.00	0.00	0.00	0.00	0.00
15	0.19	0.00	0.14	0.00	0.00
20	0.30	0.00	0.25	0.00	0.13
25	0.40	0.10	0.33	0.00	0.25
30	0.48	0.20	0.41	0.01	0.35
35		0.31	0.45	0.18	0.46
40		0.39	0.48	0.28	0.52
45		0.45	0.52	0.34	0.55
50		0.50	0.53	0.39	0.57
55		0.54	0.56	0.44	0.59
60		0.58	0.58	0.47	0.60
65		0.61	0.59	0.50	0.62
70		0.64	0.61	0.52	0.63
75		0.66	0.62	0.54	0.63
80		0.68	0.63	0.55	0.64
85		0.70	0.64	0.56	0.66
90		0.72	0.65	0.58	0.66
95		0.74	0.66	0.59	0.68
100		0.75	0.67		0.68
105		0.76	0.68		0.69

110	0.77	0.70	0.70
115	0.78	0.71	0.72
120	0.79	0.72	0.74
125	0.81		0.74
130	0.81		0.75
135	0.82		0.76
140	0.83		0.77
145	0.83		0.77
150	0.84		0.78
155	0.85		0.79
160	0.85		0.80
165	0.85		0.80
170	0.86		0.81
175	0.86		0.81
180	0.87		0.81
185	0.88		0.82
190	0.88		0.82
195	0.88		0.83
200	0.88		0.83
205	0.88		0.83
210	0.89		0.83
215	0.89		0.84
220	0.90		0.84
225	0.90		0.84
230	0.90		0.84
235	0.90		0.85
240	0.90		0.85
245	0.90		0.86
250			0.86
255			0.86
260			0.86
265			0.86
270			0.86
275			0.86
280			0.86
285			0.86
290			0.86
295			0.87
300			0.87

EXPERIMENTAL BI-DESICCANT BREAKTHROUGH RESULTS

Operating Conditions :

Air Flowrate = 5 liters/min
Inlet Temperature = 70 °F
Inlet Humidity = 75 - 85 % RH

SENSOR OUTPUT

time (min)	2" column		3" column		4" column	
	(a)	(b)	(a)	(b)	(a)	(b)
5	119	111	103	113	122	89
10	120	132	103	116	122	96
15	122	149	104	122	123	104
20	123	161	107	128	124	112
25	124	167	111	133	126	119
30	131	171	116	138	129	124
35	142	173	121	142	131	128
40	154	173	126	144	134	129
45	161	174	129	147	136	130
50	164	175	132	149	138	131
55	167		135	150	140	131
60	170		137	152	141	131
65	169		137	152	143	131
70	170			154	144	131
75	172			155	145	131
80	171			155	146	132
85	172			157	146	132
90	173			157	148	132
95	174			159	148	132
100	174			159	149	132
105	173			160	150	133
110	175			161	149	133
115	176			159	151	133
120				161		134
125						134
130						135
135						136
140						136
145						137
150						137
155						138
160						138
165						138

170	139
175	139

Percent approach to saturation for above runs

	2"		3"		4"	
time (min)	(a)	(b)	(a)	(b)	(a)	(b)
5	0.00	0.00	0.00	0.00	0.00	0.00
10	0.01	0.24	0.00	0.03	0.00	0.06
15	0.04	0.43	0.01	0.10	0.01	0.14
20	0.05	0.56	0.04	0.17	0.03	0.21
25	0.06	0.63	0.08	0.23	0.05	0.27
30	0.15	0.67	0.13	0.29	0.09	0.32
35	0.28	0.70	0.19	0.33	0.12	0.35
40	0.43	0.70	0.24	0.36	0.15	0.36
45	0.52	0.71	0.27	0.39	0.18	0.37
50	0.56	0.72	0.30	0.41	0.21	0.38
55	0.59		0.33	0.43	0.23	0.38
60	0.63		0.35	0.45	0.24	0.38
65	0.62		0.35	0.45	0.27	0.38
70	0.63			0.47	0.28	0.38
75	0.65			0.48	0.29	0.38
80	0.64			0.48	0.31	0.39
85	0.65			0.51	0.31	0.39
90	0.67			0.51	0.33	0.39
95	0.68			0.53	0.33	0.39
100	0.68			0.53	0.35	0.39
105	0.67			0.54	0.36	0.40
110	0.69			0.55	0.35	0.40
115	0.70			0.53	0.37	0.40
120				0.55		0.41
125						0.41
130						0.41
135						0.42
140						0.42
145						0.43
150						0.43
155						0.44
160						0.44
165						0.44
170						0.45
175						0.45

Temperature Breakthrough Data

*all temperatures are given in °F

**This data was obtained with a mercury thermometer inserted into the column at a depth of 2 inches

Time(min)	Silica Gel	Ethylene Glycol	Bi-Desiccant
0	71.0	73.3	75.7
1	71.0	74.0	75.7
2	71.0	75.3	75.7
3	71.1	76.8	75.7
4	71.3	78.3	75.8
5	72.1	79.7	76.1
6	73.9	80.8	76.6
7	77.0	81.6	77.1
8	82.2	82.2	77.7
9	87.5	82.7	78.3
10	93.0	83.0	79.0
11	97.9	83.3	79.6
12	101.8	83.5	80.2
13	105.2	83.6	80.7
14	108.0	83.7	81.2
15	111.7	83.8	81.7
16	113.2	83.9	82.0
17	114.4	83.9	82.4
18	115.2	84.0	82.7
19	115.8	84.0	83.0
20	116.4	84.0	83.3
21	116.8	83.9	83.5
22	117.1	83.8	83.7
23	117.4	83.8	83.9
24	117.5	83.8	84.1
25	117.8	83.7	84.2
26			84.3
27			84.5
28			84.6
29			84.7
30			84.8
31			84.8
32			84.8
33			84.9
34			84.9
35			85.0

APPENDIX 2: FORTRAN PROGRAM ADSORB

Program Adsorb

Finite Difference adiabatic adsorption analysis

This program uses a finite difference routine to calculate the breakthrough curve for the dehumidification of air using a packed bed of desiccant material.

The following is a list of constants used in this program:

AREA = Cross sectional area of bed
CI = Initial concentration of air stream in equilibrium with the bed
CPS = Heat capacity of the solid/liquid
DIVS = Number of divisions within the column
DS = Density of the solid/liquid
DT = Time increment for finite difference calculations
HA = Overall heat transfer coefficient
HADS = Heat of adsorption/absorption of the desiccant
HUM = Initial inlet humidity of the air stream
KF1 = Time at which bed profile is logged
KF2 = Spacial increments of bed profile
KF3 = Number of iterations in DO LOOP
KF4 = Time at which the breakthrough is logged
KPA = Overall mass transfer coefficient
PRESS = Pressure of system
QI = Initial loading of the column
RLEN = Length of the bed
TEMP = Temperature of incoming air
TEMPB = Initial temperature of the bed
VFLOW = Flowrate of the air stream

The following is a list of variables used in this program:

C(100) = Concentration of air stream at a certain position in the bed
Q(100) = Loading of the bed at a certain position
QE(100) = Equilibrium loading at the same position
TG(100) = Gas temperature at a certain position
TS(100) = Desiccant temperature at the same position

```
INTEGER DIVS
REAL C(100),Q(100),QE(100),TG(100),TS(100)
REAL KPA,KO,HA,MBEDIN,MBEDOUT,M1FRSTR,M2FRSTR
OPEN(UNIT=11,FILE='DATA.DAT',STATUS='OLD')
OPEN(UNIT=10,FILE='PROF.DAT',STATUS='UNKNOWN')
OPEN(UNIT=12,FILE='BRK.DAT',STATUS='OLD')
READ(11,'(2 G10.2)') TEMP,TEMPB
```

```
      READ(11,*) HUM
      READ(11,*) PRESS
      READ(11,*) QI,CI
      READ(11,*) DS,CPS
      READ(11,*) RLEN
      READ(11,*) DIVS
      READ(11,*) DT
      READ(11,*) VFLOW
      READ(11,*) DZ
      READ(11,*) KF1,KF2,KF3,KF4
      READ(11,*) AREA
```

The bed conditions are initialized as follows:

```
2     DO 10 J=1,DIVS
            C(J)=ACMAX
            Q(J)=QMAX0
            TS(J)=TEMPB
            TG(J)=TEMP
10    CONTINUE
```

The parameters for the finite difference equations are then determined,

```
      CALL DENS(TEMP,PRESS,DG)
      VEL=VFLOW/AREA
      CALL HCAPG(TEMP,CPG)
      KPA=0.00036      (The heat and mass transfer coefficients are
      HA=0.0001      determined by methods discussed in the literature)
      A=DS*(1.-ETA)/(DG*ETA)
      B=CPS*A/CPG
      D=HADS*A/CPG
      E=KPA/DS
      F=HA/(DS*CPS)
      G=HADS/CPS

1     CALL ISOTHERM(TEMP,HUM,QEQ)

      WRITE(10,45) 'INITIAL LOADING OF COLUMN =',QMAX0
      WRITE(10,45) 'AMBIENT TEMPERATURE =', TEMP
      WRITE(10,45) 'BED TEMPERATURE =', TS(1)
      WRITE(10,45) 'REGENERATION TEMPERATURE =', TEMPREG
      WRITE(10,45) 'HUMIDITY OF AIRSTREAM [molH2O/molGAS] =', HUM
45    FORMAT(1X,A,G10.5)
```

summations for the time average values of concentration and temperature at breakthrough

```
      SUM0=0
      TUM0=0
      QUM0=0

      WRITE(12,102)
      DO 30 K=1,KF3

      summations for the spacial average values of concentration
      and temperature.

      SUM01=0.0
      TUM01=0.0
      QUM01=0.0


      TG0X=TEMPA
      C0X=HUM
      IF(MOD(K,KF1).EQ.0) THEN
           WRITE(10,50) K*DT/60.0
           WRITE(10,49)
      END IF
```

The following loop calculates the bed temperature and concentration profiles for succeeding time intervals. The finite difference scheme uses a first order forward difference for the time derivatives and a first order backward difference for the spacial derivatives.

```
DO 20 L=1,DIVS
      OLD2=TS(L)
      OLD1=Q(L)
      Q(L)=E*DT*(QEQ-Q(L))+Q(L)
      IF(Q(L).LT.0) Q(L)=0.0
      TS(L)=F*DT*(TG(L)-TS(L))+TS(L)+G*(OLD1-Q(L))
      C0=C0X
      C0X=C(L)
      C(L)=C(L)+VEL*DT/DZ*(C0-C(L))+A*(OLD1-Q(L))
      IF(C(L).LT.0) C(L)=0.0
      TG0=TG0X
      TG0X=TG(L)
      TG(L)=TG(L)+B*(OLD2-TS(L))+VEL*DT/DZ*(TG0-TG(L))
*           +D*(OLD1-Q(L))
      IF(Q(L).LT.1E-10) Q(L)=0.0
      IF(QEQ.LT.1E-10) QEQ=0.0
      IF(C(L).LT.1E-10) C(L)=0.0
      IF(MOD(K,KF1).EQ.0.AND.MOD(L,KF2).EQ.0) THEN
           WRITE(10,100) DZ*L,Q(L),TS(L),C(L),TG(L),QEQ
      END IF
```

The following block is inserted to log the values of C, Q, TG, and TS in the output file for the breakthrough curve. The value of

KF4 determines the time increment for the data logging procedure. The values are also summed over the breakthrough period in order to determine an average value for mass balance calculations.

```
IF((MOD(K,KF4).EQ.0).AND.(ABS(DZ*L-RLEN).LT.0.001)) THEN
     SUM0=SUM0+C(L)
     TUM0=TUM0+TG(L)
     QUM0=QUM0+Q(L)
     CMAX=C(L)
     QMAX=Q(L)
     WRITE(12,101) K*DT/60.0,C(L),Q(L),TG(L),TS(L)
END IF
```

```
SUM01=SUM01+C(L)
TUM01=TUM01+TS(L)
QUM01=QUM01+Q(1)
```

The conditions at position (i,t) are now used to determine the equilibrium loading at position (i+1,t). This provides the mathematical driving force to calculate q(i+1,t+1).

```
CALL ISOTHERM(TG(L),COX,QEQ)
```

```
20   CONTINUE
```

The average values of concentration and temperature over the entire bed are computed.

```
AVECS=SUM01/DIVS
AVETS=TUM01/DIVS
AVEQS=QUM01/DIVS
```

The equilibrium loading calculation is now begun over again at the inlet of the bed and the whole procedure is repeated for the next time increment, if the breakthrough is still incomplete.

```
CALL ISOTHERM(TEMP,HUM,QEQ)
```

The breakthrough curve is determined to be complete when the loading at the outlet of the column reaches 90% of the value in equilibrium with the incoming air. QMAX is the value of the bed loading at the outlet of the bed.

```
          IF(QMAX.GT.(0.90*QEQ)) THEN
               AVEC=SUM0/K*KF1
               AVET=TUM0/K*KF1
               AVEQ=QUM0/K*KF1
               MBEDIN=(AVEQS-QI)*DS*AREA*RLEN
               M1FRSTR=(HUM-AVEC)*DG*VEL*AREA*K*DT
               WRITE(10,23) AVEQ,AVEC,AVET
               GO TO 99
          END IF
 30   CONTINUE


  21 FORMAT(1X,F8.3,5X,E10.4,5X,E10.4,5X,F8.2,5X,F8.2)
  23 FORMAT(1X,'average bed loading=',G10.5,/,1X,'average outlet
              concentration =',E10.2,/,1X,'average outlet
              temperature =',F8.2)
  49 FORMAT(3X,'X[CM]',8X,'Q[mol/gs]',5X,'TS[K]',8X,
               'C[mol%]',2X,'TG[K]',8X,'QEQ[mol/gs]')
  50 FORMAT(/30X,'time =',F10.1,3X,'minutes')
 100 FORMAT(1X,F5.2,5X,E10.4,5X,F8.2,5X,E10.4,5X,F8.2,5X,E10.4)
 101 FORMAT(1X,F7.2,2X,E10.4,2X,E10.4,2X,F8.2,2X,F8.2)
 102 FORMAT(1X,'time(min)',5X,'Cout',5X,'Qout',5X,'TEMPgas',5X,
             'TEMPsol')
  99 STOP
     END

     SUBROUTINE ISOTHERM(T,CON,QEQ)
     REAL T,CON,QEQ,K,K0
     R=1.987
     TREF=273.16
     K=370.68*EXP(10343/R*(1/T-1/TREF))
     QEQ=K*0.022*CON/(1.+K*CON)
     RETURN
     END

     SUBROUTINE DENS(TEMP,PRESS,DG)
     R=10.73
     T=1.8*TEMP
     DG=PRESS*14.7/(R*T*62.37)
     RETURN
     END

     SUBROUTINE HCAPG(TEMP,CPG)
     CPG=(28.09+0.001965*TEMP+0.4799E-05*TEMP**2)/4.184
     RETURN
     END
```

APPENDIX 3: FORTRAN PROGRAM FOR HODOGRAPH PLOTS

PROGRAM HODO

This program calculates the hodographic characteristics corresponding to a given isotherm equation and initial and final conditions of the process air stream. Only four characteristics will be calculated by this program. These are the two which originate from each of the initial and final conditions given.

```
PROGRAM HODO
REAL HADS,VC(10),VT(10)
COMMON CPS,CPF,HADS,DB,ETA
OPEN(UNIT=1,FILE='HOD.DAT',STATUS='UNKNOWN')
OPEN(UNIT=2,FILE='VELOC.DAT',STATUS='UNKNOWN')
PRINT*,'WHAT ARE THE INLET AND OUTLET CONCENTRATIONS AND
* TEMPERATURES, RESPECTIVELY ?'
READ*,C0,T0,CF,TF
PRINT*,'WHAT ARE CPS,CPF,DF,HADS,DT,ETA AND DB?'
READ*,CPS,CPF,DF,HADS,DT,ETA,DB
PRINT*,'WHAT IS THE SUPERFICIAL VELOCITY ?'
READ*,VEL
WRITE(1,50)
WRITE(2,103)
```

The initial and final conditions are first inputted.

```
T1=T0
T2=T0
T3=TF
T4=TF
C1=C0
C2=C0
C3=CF
C4=CF
PRINT 100, T1,C1,T2,C2,T3,C3,T4,C4
WRITE(1,100) T1,C1,T2,C2,T3,C3,T4,C4
```

The isotherm is now evaluated for its temperature and concentration derivatives.

```
CALL DQDT(T1,C1,QT1)
CALL DQDC(T1,C1,QC1)
```

The quadratic equation is then used to evaluate dc/dT at the initial conditions.

```
A1=QT1
B1=QC1-CPS/(DF*CPF)+HADS/(DF*CPF)*QT1
D1=HADS/(DF*CPF)*QC1
DCDT11=2*A1/(-B1+SQRT(B1**2-4*A1*D1))
DCDT12=2*A1/(-B1-SQRT(B1**2-4*A1*D1))
```

Start the initial and final conditions on their characteristics.

```
          ..initial condition


   CALL WAVE(VEL,QC1,QT1,DCDT11,DCDT12,WC11,WC12,WT11,WT12)
```

This block designates each derivative dc/dT to its correct characteristic. If the derivative is positive, the characteristic is positive.

```
   IF(DCDT11.GT.0.0) THEN
        T1=T1-DT
        T2=T2+DT
        C1=C1-DCDT11*DT
        C2=C2+DCDT12*DT
        VC(1)=WC11
        VT(1)=WT11
        VC(2)=WC12
        VT(2)=WT12
        DCDT1=DCDT11
        DCDT2=DCDT12
   ELSE
        T1=T1-DT
        T2=T2+DT
        C1=C1-DCDT12*DT
        C2=C2+DCDT11*DT
        VC(1)=WC12
        VT(1)=WT12
        VC(2)=WC11
        VT(2)=WT11
        DCDT1=DCDT12
        DCDT2=DCDT11
        END IF

        ...final condition


   CALL DQDT(T3,C3,QT3)
   CALL DQDC(T3,C3,QC3)
   A3=QT3
   B3=QC3-CPS/(DF*CPF)+HADS/(DF*CPF)*QT3
   D3=HADS/(DF*CPF)*QC3
   DCDT31=2*A3/(-B3+SQRT(B3**2-4*A3*D3))
   DCDT32=2*A3/(-B3-SQRT(B3**2-4*A3*D3))

   CALL WAVE(VEL,QC3,QT3,DCDT31,DCDT32,WC31,WC32,WT31,WT32)

   IF(DCDT31.LT.0.0) THEN
        T3=T3-DT
        T4=T4+DT
```

```
        C3=C3-DCDT31*DT
        C4=C4+DCDT32*DT
         VC(3)=WC31
        VT(3)=WT31
        VC(4)=WC32
        VT(4)=WT32
        DCDT3=DCDT31
        DCDT4=DCDT32
    ELSE
        T3=T3-DT
        T4=T4+DT
        C3=C3-DCDT32*DT
        C4=C4+DCDT31*DT
        VC(3)=WC32
        VT(3)=WT32
        VC(4)=WC31
        VT(4)=WT31
        DCDT3=DCDT32
        DCDT4=DCDT31
    END IF
    PRINT 100, T1,C1,T2,C2,T3,C3,T4,C4
```

The initial and final points have been started. Four curves will now spread out until they intersect, determining the path which the desorption and adsorption will follow.

```
    DO 10 J=1,1000
        WRITE(1,100) T1,C1,T2,C2,T3,C3,T4,C4
        WRITE(2,101) DCDT1,VC(1),DCDT2,VC(2),DCDT3,VC(3),DCDT4,VC(4)
        CALL DQDT(T1,C1,QT1)
        CALL DQDC(T1,C1,QC1)
        A1=QT1
        B1=QC1-CPS/(DF*CPF)+HADS/(DF*CPF)*QT1
        D1=HADS/(DF*CPF)*QC1
        DCDT11=2*A1/(-B1+SQRT(B1**2-4*A1*D1))
        DCDT12=2*A1/(-B1-SQRT(B1**2-4*A1*D1))

         CALL WAVE(VEL,QC1,QT1,DCDT11,DCDT12,WC11,WC12,WT11,WT12)

        IF(DCDT11.GT.0.0) THEN
            T1=T1-DT
            C1=C1-DCDT11*DT
            VC(1)=WC11
            VT(1)=WT11
            DCDT1=DCDT11
        ELSE
            T1=T1-DT
            C1=C1-DCDT12*DT
            VC(1)=WC12
            VT(1)=WT12
            DCDT1=DCDT12
```

```
END IF


CALL DQDT(T2,C2,QT2)
CALL DQDC(T2,C2,QC2)
A2=QT2
B2=QC2-CPS/(DF*CPF)+HADS/(DF*CPF)*QT2
D2=HADS/(DF*CPF)*QC2
DCDT21=2*A2/(-B2+SQRT(B2**2-4*A2*D2))
DCDT22=2*A2/(-B2-SQRT(B2**2-4*A2*D2))

CALL WAVE(VEL,QC2,QT2,DCDT21,DCDT22,WC21,WC22,WT21,WT22)

IF(DCDT21.LT.0.0) THEN
     T2=T2+DT
     C2=C2+DCDT21*DT
     VC(2)=WC21
     VT(2)=WT21
     DCDT2=DCDT21
ELSE
     T2=T2+DT
     C2=C2+DCDT22*DT
     VC(2)=WC22
     VT(2)=WT22
     DCDT2=DCDT22
END IF


CALL DQDT(T3,C3,QT3)
CALL DQDC(T3,C3,QC3)
A3=QT3
B3=QC3-CPS/(DF*CPF)+HADS/(DF*CPF)*QT3
D3=HADS/(DF*CPF)*QC3
DCDT31=2*A3/(-B3+SQRT(B3**2-4*A3*D3))
DCDT32=2*A3/(-B3-SQRT(B3**2-4*A3*D3))

CALL WAVE(VEL,QC3,QT3,DCDT31,DCDT32,WC31,WC32,WT31,WT32)

IF(DCDT31.LT.0.0) THEN
     T3=T3-DT
     C3=C3-DCDT31*DT
     VC(3)=WC31
     VT(3)=WT31
     DCDT3=DCDT31
ELSE
     T3=T3-DT
     C3=C3-DCDT32*DT
     VC(3)=WC32
     VT(3)=WT32
     DCDT3=DCDT32
END IF
```

```
          CALL DQDT(T4,C4,QT4)
          CALL DQDC(T4,C4,QC4)
          A4=QT4
          B4=QC4-CPS/(DF*CPF)+HADS/(DF*CPF)*QT4
          D4=HADS/(DF*CPF)*QC4
          DCDT41=2*A4/(-B4+SQRT(B4**2-4*A4*D4))
          DCDT42=2*A4/(-B4-SQRT(B4**2-4*A4*D4))

          CALL WAVE(VEL,QC4,QT4,DCDT41,DCDT42,WC41,WC42,WT41,WT42)

          IF(DCDT41.LT.0.0) THEN
               T4=T4+DT
               C4=C4+DCDT42*DT
               VC(4)=WC42
               VT(4)=WT42
               DCDT4=DCDT42
          ELSE
               T4=T4+DT
               C4=C4+DCDT41*DT
               VC(4)=WC41
               VT(4)=WT41
               DCDT4=DCDT41
          END IF
          PRINT 100, T1,C1,T2,C2,T3,C3,T4,C4
 10   CONTINUE
 50   FORMAT(4X,'T1',8X,'C1',6X,'T2',8X,'C2',7X,'T3',
     * 8X,'C3',8X,'T4',6X,'C4')
 100  FORMAT(2X,4(F5.1,2X,E10.3,2X))
 101  FORMAT(8(1X,F8.5))
 103  FORMAT(3X,'DCDT1',5X,'VC1',5X,'DCDT2',5X,'VC2',5X,'DCDT3',5X,
     1'VC3',6X,'DCDT4',4X,'VC4')
 99   STOP
      END
```

This subroutine is arbitrary, since it determines the temperature gradient of the equilibrium isotherm. For this program, this is the only section which must be changed for each desiccant chosen. The isotherm seen here is for ethylene glycol.

```
      SUBROUTINE DQDT(T,C,QT)
      REAL K
      T=T-273.16
      C=C/24.4
      K=EXP(13.376)
      A=0.001363*EXP(0.00874*T)
      B=K*T**(-1.6257)
      DADT=1.1913E-05*EXP(0.00874*T)
      DBDT=-K*1.6257*T**(-2.6257)
      QT=A*EXP(B*C)*C*DBDT+EXP(B*C)*DADT
      C=C*24.4
```

```
      T=T+273.16
      RETURN
      END
```

This subroutine is also arbitrary, depending on the equation chosen to represent the isotherm. The only requirement is that the isotherm be represented in terms of the appropriate temperature and concentration. The following is for the isotherm of ethylene glycol.

```
      SUBROUTINE DQDC (T,C,QC)
      REAL K
      T=T-273.16
      C=C/24.4
      K=EXP(13.376)
      A=0.001363*EXP(0.00874*T)
      B=K*T**(-1.6257)
      QC=A*EXP(B*C)*B
      QC=QC/24.4
      T=T+273.16
      C=C*24.4
      RETURN
      END
```

The following subroutine calculates the temperature and concentration wave velocities for both the positive and negative characteristics. The value of 390 is determined based on the units for the bed loading [moles/gram] and the concentration [moles/mole] in order to convert these to dimensionless form.

```
      SUBROUTINE WAVE(VEL,QC1,QT1,DCDT11,DCDT12,WC11,WC12,WT11,WT12)
      DF=1.0
      QCT11=QC1+QT1/DCDT11
      QTT11=QT1+QC1*DCDT11
      QCT12=QC1+QT1/DCDT12
      QTT12=QT1+QC1*DCDT12
      WC11=VEL/(1+DB*390./ETA*QCT11)
      WC12=VEL/(1+DB*390./ETA*QCT12)
      WT11=VEL/(1+DB*390.*CPS/(CPF*DF*ETA)-HADS*DB*390./
     1(ETA*DF*CPF)*QTT11)
      WT12=VEL/(1+DB*390.*CPS/(CPF*DF*ETA)-HADS*DB*390./
     1(ETA*DF*CPF)*QTT12)
      RETURN
      END
```

APPENDIX 4 : HEAT LOSS ANALYSIS

The process of dehumidification in the packed bed of desiccant material is assumed to be adiabatic to allow easier calculation of breakthrough histories. The following analysis will show the approach to adiabatic behavior and provide an idea as to how adiabatic the system actually is.

To simplify the analysis, the governing equation for the heat balance is reduced to a steady state equation so that all of the time derivatives drop out. The partial derivative of T with respect to x then becomes a total derivative and the solution of the resulting ODE is by separation of variables. The assumption of steady-state is adequate if the movement of the concentration/loading profile in the bed is slow enough to neglect the change of temperature with respect to time. This also provides for constant boundary conditions. Also, the temperature of the bed at any point x is assumed to be independent of radial position and equal to the value of the temperature at the surface of the column. This will allow calculation of the maximum possible heat loss from the column.

The governing equation therefore reduces to the following form:

$$\epsilon \rho_f C_{pf} v \frac{dT}{dx} = \frac{-4h_w}{d}(T_\infty - T)$$

Separating the variables and using the following limits of integration:

$$\text{at} \quad x = 0 \; ; \quad T = T_o$$

$$\text{at} \quad x = x \; ; \quad T = T$$

$$\int_{T_o}^{T} (T_\infty - T)\,dT = -4h_w/d\epsilon\rho_f C_{pf} \upsilon \int_0^x dx$$

This yields the following equation after integration:

$$\ln\left(\frac{T_\infty - T}{T_\infty - T_o}\right) = \frac{-4h_w x}{d\epsilon\rho\upsilon C_p}$$

This leads to the equation of temperature as a function of x:

$$T = T_\infty - (T_\infty - T_o)e^{-\beta x} \qquad (\text{where} \quad \beta = 4h_w/d\epsilon\rho\upsilon C_p)$$

The following list of material properties and process variables are chosen for the conditions used in the experiment. The desiccant bed will have a different steady state temperature profile than the outlet line from the column to the temperature sensor, and therefore will require a different value for β. For the silica gel bed, the following variables are used:

h_w = 0.1485 BTU/hr-ft^2-°F
($h_w \approx 0.27\Delta T$ [F] from the Chemical Engineer's Handbook p. 474, 3rd Edition, 1950)

d = 0.1875 ft
ϵ = 0.35
ρ_f = 0.073 #/ft^3
υ = 383 ft/hr
C_{pf} = 0.24 BTU/#-°F

The percentage drop in the temperature with bed length is given

by:

$$\% = 1 - \left(\frac{T-T_\infty}{T_o-T_\infty}\right) = 1 - e^{-\beta x}$$

Therefore the maximum amount of temperature drop in 2 inches of bed will be (plugging in the above constants):

$$\% = 1 - e^{-1.35(0.166)} = 0.2 = 20\% \text{ drop in temperature}$$

The amount of temperature drop in 1 foot of 1/4" plastic tubing will use the same equation with the following change of parameters:

h_w = 0.1485 BTU/hr-ft^2-°F
d = 0.021 ft
ϵ = 1.0
ρ_f = 0.073 #/ft^3
υ = 31023 ft/hr
C_{pf} = 0.24 BTU/#-°F

This yields a β value of 0.052 and a percentage drop in temperature of 5 %. Therefore, the maximum total drop in temperature of the air stream due to conduction heat transfer would be:

$$T_{max} - 0.2(T_{max}-T_\infty) - 0.05((T_{max} - 0.2(T_{max}-T_\infty)) - T_\infty)$$

or

$$T_{max} - 0.24(T_{max} - T_\infty)$$

With a maximum temperature of 330 °K and an ambient temperature of 297 °K, this would equal 322 °K, or 119 °F.

APPENDIX 5: CALCULATIONS FOR THEORETICAL RESULTS

1. Isothermal Equilibrium

A. Silica Gel

(a) Dehumidification

The initial bed conditions are assumed to be :

Humidity = 0.00169 moles/mole
Bed loading = 0.00263 moles/gram
Temperature = 297 °K

The inlet stream conditions are assumed to be :

Humidity = 0.024 moles/mole
Temperature = 297 °K

The shock velocity is therefore calculated as:

$$\frac{z}{t} = \frac{\upsilon}{1 + \frac{\rho_b}{\epsilon}\left(\frac{q^*-q_o}{c_o-c^*}\right)}$$

Where

υ = 220 in/min interstitial velocity
q^* = 0.0145 moles/gram (per isotherm)
q_o = 0.00263 moles/gram
c^* = 0.00169 moles/mole
c_o = 0.024 moles/mole
ρ_b = 20430 grams/ft^3
ρ_a = 1.158 moles/ft^3

This yields a value of z/t of 0.0082 in/min which means that breakthrough will occur at 2/0.0082, or 244 minutes.

(b) Regeneration

The initial bed conditions are assumed to be:

Humidity = 0.34 moles/mole (i.e. equilibrium at 350°)
Bed Loading = 0.0145 moles/gram
Temperature = 350 °K

The initial stream conditions are:

Humidity = 0.024 moles/mol
Temperature = 350 °K

The concentration wave velocity at each point in the column is then calculated as:

$$\frac{z}{t} = \frac{v}{1 + (\rho_b/\epsilon)f'(c)}$$

with the derivative of the isotherm defined as:

$$f'(c) = \frac{KQ_m}{(1 + Kc)^2}$$

v = 220 in/min interstitial velocity
ρ_b = 20430 grams/ft^3
ρ_a = 1.158 moles/ft^3
ϵ = 0.35

The derivative of the isotherm for the initial conditions in the bed is then (with K calculated at 350°K as 5.65);

$$f'(c) = 0.0146 \text{ moles/gram}$$

This yields a value of 0.0298 for z/t, or a breakthrough time of 6.7 minutes. The derivative of the isotherm for the inlet stream condition is (with K = 5.65 and c = 0.024);

$$f'(c) = 0.0964 \text{ moles/gram}$$

This yields a value of 0.0453 for z/t and a breakthrough time of 44 minutes. The initial bed wave moves faster than the inlet wave and the breakthrough curve is a dispersive front. The intermediate values are calculated in the same manner as the terminal values, using the intermediate characteristic to back out the derivative of the isotherm

at the time selected, and then using the equation for the derivative to back out the concentration.

B. Ethylene Glycol

(a) Dehumidification

The initial bed conditions are:

Bed Loading = 0.0059 moles/gram (regenerated at 350 °K)
Humidity = 0.0082 moles/mole air
Temperature = 297 °K

The inlet conditions are:

Humidity = 0.024 moles/mole
Temperature = 297 °K

The same equation used for the evaluation of characteristics for silica gel is used here. The derivative of the isotherm is determined as follows:

$$f'(c) = ABexp(Bc)$$

where

$$A = 0.0014exp(0.009T)$$
$$B = 6.44 \times 10^{5}T^{-1.6}$$

The parameters used in the characteristic equation are:

$$\upsilon = 220 \text{ in/min}$$
$$\epsilon = 0.35$$
$$\rho_b = 105 \text{ grams/liter}$$

The derivative of the isotherm for the initial bed conditions is equal to 22 liters/gram. This yields a value of z/t from equation as 0.033. The breakthrough for the bed conditions is then equal to 60 minutes. The derivative of the isotherm for the inlet stream condition is equal to 242 liters/gram. This yields a value of z/t as 0.003. The breakthrough of the inlet stream is then 660 minutes. The overall

breakthrough curve for dehumidification is then a dispersive wave and the intermediate values of concentration are back calculated using the ethylene glycol isotherm and the characteristic equation.

(b) Regeneration

Initial bed conditions:

Bed Loading = 0.065 moles/gram
Humidity = 0.081 moles/mole
Temperature = 350 °K

Inlet stream conditions:

Humidity = 0.024 moles/mole
Temperature = 350 °K

The breakthrough is a shock front as in the dehumidification with silica gel. The following parameters are used for the shock front characteristic equation.

υ = 220 in/min interstitial velocity
q^* = 0.0059 moles/gram (per isotherm)
q_o = 0.065 moles/gram
c^* = 0.081 moles/mole
c_o = 0.024 moles/mole
ρ_b = 105 grams/liter
ϵ = 0.35

This yields a value of z/t for the regeneration cycle of 0.029. The corresponding shock time for the regeneration is then 2/0.029 or 69 minutes.

2. Adiabatic Equilibrium

A. Silica Gel

This analysis uses the same equations for the characteristics as the isothermal analysis. The terminal conditions remain the same as the ones for the isothermal case, but the plateau concentration and temperature is read from the hodographic plot and the concentration and temperature wave speeds are read from the corresponding velocity tables.

(a) Adsorption

The terminal conditions remain the same as in part 1.A(a) with the plateau conditions (read from figure 5.5 and table 5.1) being approximately 323 °K and 0.0072 moles/mole concentration. The first wave is a shock with the initial bed wave velocity being 0.4043 cm/min per table 5.1. The velocity then increases to the plateau zone velocity, which is 0.5502 cm/min. Using equation (2-6) for the shock velocity and assuming the same parameters as were used in the isothermal calculation and substituting the outlet and plateau conditions as terminal conditions ($q^* = 0.00272$, $q_o = 0.00263$, $c^* = 0.00169$, $c_o = 0.0072$), a value of 0.269 in/min is calculated for the shock velocity. This yields a break time of 2/0.269, or 7.4 minutes for the initial wave.

The second wave moves along the Γ^- characteristic as seen on the hodographic plot the initial wave velocity is seen to be 0.0214 cm/min per table 5.1. This decreases until the conditions reach 309 °K and 0.0163 moles/mole

concentration, at which time the velocity is equal to 0.0144 cm/min. This means that the wave is dispersive in this interval, with the leading edge of the wave breaking through at 2(2.54)/0.0214, or 238 minutes. The trailing edge breaks through at the same time that the trailing shock front breaks through which is determined by use of equation (2-6) with the appropriate substitution for the terminal conditions ($q^* = 0.0145$, $q_o = 0.0088$, $c^* = 0.0163$, $co = 0.024$). This yields a shock time of 339 minutes.

Therefore, the entire breakthrough curve consists of a initial shock at 7.5 minutes to the plateau zone, followed by a gradual breakthrough starting at 238 minutes and ending at 339 minutes with a shock to the inlet conditions.

(b) Desorption

The initial wave follows along the Γ^+ characteristic from 297° K and 0.024 moles/mol humidity. The initial wave speed is 1.126 cm/min per table 5.2 and the wave speed at the plateau zone (309 °K, 0.0492 moles/mol) is 1.824 cm/min, so that the wave is a shock with the break time of approximately 2-3 minutes. The trailing wave then travels along the Γ^- characteristic and is seen to have an initial velocity of 0.0214 cm/min and decreases until the velocity reaches 0.0195 cm/min at conditions of 320 °K and 0.0423 moles/mole. There is then a shock front from then on. Terminal conditions used in equation (2-6) are

$q_o = 0.00169$
$q^* = 0.0108$
$c_o = 0.0423$
$c^* = 0.024$

This yields a shock velocity of 0.0088 in/min and therefore a breakthrough time of 228 minutes.

The overall breakthrough curve is therefore an initial jump to an outlet humidity of 0.0492 moles/mole and a temperature of 309 °K followed by a shock front to the regeneration conditions at 238 minutes. The dispersive front is so slight as to be neglected.

B. Ethylene Glycol

(a) Dehumidification

The initial wave follows along a Γ^+ characteristic from 297 °K and 0.0082 moles/mole at a wave speed of 1.64 cm/min and lands in the plateau zone (310.5 °K and 0.016 moles/mole) with a speed of 1.81 cm/min. This indicates a shock front ($q^* = 0.0059$, $q_o = 0.0061$, $c_o = 0.0082$, $c^* = 0\ 016$) with a velocity of 1.26 in/min or a break time of 1.6 minutes. The second wave begins with a velocity of 0.083 cm/min and ends with a velocity of 0.0022 cm/min at the inlet conditions (saturated). This indicates a dispersive wave with a leading edge time of 60 minutes and a final breakthrough of 2272 minutes.

(b) Regeneration

3. Thomas Solution.

A. Silica Gel

Using the correlation of Wakao and Funazkri (1978) and assuming the following parameters for air at 1 atmosphere and 297 °K:

$Sc = 0.6$
$D_{AB} = 0.247\ cm^2/sec$
$Pr = 0.7$
$\mu_{air} = 0.00175\ cP = 1.176 \times 10^{-6}\ lb/ft\text{-}sec$
$\rho_{air} = 0.073\ lb/ft^3$

The Reynolds number is calculated as follows (assuming the same operating conditions as given at the beginning of chapter 5):

$$Re = (0.1065 \times 0.006 \times 0.073)/1.176 \times 10^{-6}$$
$$= 39$$

Therefore, the Sherwood number is :

$$Sh = 2.0 + 1.1(0.6)^{0.33}(39)^{0.6}$$
$$= 10.37$$

and the local gas phase coefficient is calculated as:

$$k_f = Sh D_{AB}/d_p$$
$$= 10.37(0.247)/(0.006 \times 30.48)$$
$$= 14.0\ cm/sec$$

The bed coefficient is calculated with equation (2-29) as follows:

$$1/D_{eff} = 1/D_{AB} + 1/D_{k,\epsilon}$$

where

$$D_{k,\epsilon} = 0.00087\ \ \mu/\sigma\epsilon$$

$\therefore$ $\quad D_{eff} = 0.000867\ cm/sec$

and

$$k_{bed} = 10(0.000867)/(0.006 \times 30.48 \times 0.65)$$

$$= 0.073 \text{ cm/sec}$$

With these two coefficients calculated, the overall mass transfer coefficient can be calculated with the use of equation (2-26):

where

$$a = 6(1-\epsilon)/d_p = 6(0.65)/0.006(30.48) = 21.3 \text{ 1/cm}$$

$$m \approx 0.6 \text{ moles air/gram desiccant}$$

$$K_p a = (1/(0.073x21.3x0.72) + 0.6/(0.35x14.0x21.3x4.04E\text{-}5))^{-1}$$

$$= \underline{0.0069 \text{ grams/cm}^3\text{-sec}}$$

This value is used in the dimensionless bed length and time parameters of the Thomas solution. The two parameters are determined as follows:

$$\tau = 0.0069(60)/0.72(t - 5/195) = 0.575(t-0.073) \approx 0.575t$$

$$\zeta = 5(0.0069x0.6x60)/(0.35x195.0x4.04E\text{-}5) \approx 450$$

The following table is then generated using equation 2-18 (tabulated by Sherwood):

t(min)	τ	ζ	c/c_o
688	400	450	0.013
735	423	450	0.093
782	450	450	0.506
814	469	450	0.829
845	486	450	0.940
876	504	450	0.982

NOMENCLATURE

UPPER CASE VARIABLES

C_i	inlet concentration of dehumidification air stream
$C_o(t)$	time varying outlet concentration of dehumidification stream
COP	coefficient of performance (cooling capacity/work input)
C_{pf}	heat capacity of fluid stream
C_{ps}	heat capacity of desiccant material
D_{AB}	diffusivity of substance A in medium B
D_{eff}	effective diffusivity within a porous particle
D_L	axial dispersion coefficient in cylindrical packed bed
H	specific enthalpy of air stream
H	absolute humidity of air stream (equal to concentration units)
ΔH_{ads}	enthalpy of adsorption (specific to desiccant, exothermic)
J_o	Bessel function of the first kind
K	constant in Langmuir isotherm equation (temperature dependent)
K_D	equilibrium distribution coefficient for a linear isotherm
K_fa	overall mass transfer coefficient for packed beds (fluid concentration driving force)
K_pa	overall mass transfer coefficient for packed beds (solid concentration driving force)
N_w	rate of uptake of water vapor into a desiccant particle
Q_{in}	heat input to a thermodynamic system
Q_{out}	exhaust heat from a vapor compression system
Q	dimensionless variable used in Thomas' solution (q/q^*)
Q_m	maximum capacity of solid desiccant in the Langmuir equation
R	ideal gas constant
T_f	temperature of fluid (air) stream
T_s	temperature of solid (desiccant)
T_w	temperature of column wall
T_o	initial temperature
T_∞	temperature of surrounding air around the column
X	dimensionless variable used in Thomas' solution (c/c_o)

LOWER CASE VARIABLES

c_i	concentration at interface of desiccant and fluid stream
c_o	initial concentration of air stream at inlet
c*	concentration of air stream in equilibrium with desiccant
c(i,t)	concentration of air stream at i^{th} position and time t
d	diameter of column
ha	local heat transfer coefficient between fluid and solid
h_w	local heat transfer coefficient between column wall and surroundings
$k_f a$	local mass transfer coefficient between fluid and particle
$k_p a$	local mass transfer coefficient for transfer within solid (related to the effective diffusivity, D_{eff})
m	average slope of isotherm
q	bed loading in moles water adsorbed/mass desiccant
q_o	initial loading of desiccant bed
q_i	loading at interface of solid and fluid
q*	loading of bed in equilibrium with the inlet air stream
t_b	breakthrough time (time at which outlet humidity exceeds minimum)
z	bed height

GREEK VARIABLES

ϵ	porosity of desiccant bed
Γ^+,Γ^-	c,T characteristics for adiabatic equilibrium analysis
λ_f	thermal conductivity of fluid (air stream)
μ_f	viscosity of fluid stream
ρ_f	density of fluid stream
ρ^b	buld density of desiccant bed
τ	dimensionless time parameter in Thomas' solution
υ	velocity of fluid stream
ω_c	concentration wave velocity
ω_T	temperature wave velocity
ζ	dimensionless bed length parameter in Thomas' solution

PREDEFINED DIMENSIONLESS NUMBERS

Nu	Nusselt number (hd/λ)
Pr	Prandtl number ($C_p\mu_f/k_f$)
Re	Reynolds number (vd/ν)
Sh	Sherwood number ($k_f d_p/D_{AB}$)
Sc	Schmidt number ($\mu_f/\rho_f D_{AB}$)

REFERENCES

Arnold, Frances H., "Dehumidification in Passively Cooled Buildings." Solar Energy Research Institute. Golden, Colorado 1979

ASHRAE, Handbook of Fundamentals American Society for Heating, Refrigeration, and Air Conditioning Engineers. Atlanta, 1981

Canjar, L.N., Physical Adsorption Processes and Principles. CEP Symposium Series 74, Volume 63. AICHE 1967

Collier, R.K., "Analysis and Simulation of Open Cycle Absorption Refrigeration Systems." Solar Energy. Volume 23, (pp 357-366) 1979

Collier, R.K., Desiccant Materials. Desiccant Cooling and Dehumidification Opportunities for Buildings Workshop, Chattanooga, Tn. 1986

Curme, G.O., Glycols. Reinhold Publishing Corp. New York, NY 1952

Felder, Elementary Principles of Chemical Processes. Wiley, New York, NY 1980

Hines, A.L., Mass Transfer: Fundamentals and Applications. Prentice-Hall, Inc. New York. 1985

Holmberg, R.B., "Combined Heat and Mass Transfer in Regenerators with Hygroscopic Materials". Journal of Heat Transfer. Volume 101 (pp205-210) 1979

Hougan, O.A., Chemical Process Principles - Part 3: Kinetics and Catalysis. John Wiley and Sons, Inc. New York 1957

Jurinak, J.J., "Effects of Matrix Properties on the Performance of a Counterflow Rotarty Dehumidifier." ASME Transactions. Volume 106 (pp 638-645) 1984

Kettleborough, "Solar Assisted Comfort Conditioning." Mechanical Engineering. Dec., 1983

Osborn, Donald E. and Hanson, Simon P., "Bi-Desiccant, Staged, Solar Cooling System", Report to Arizona Solar Energy Commision, ASES Contract No. 800 -87, June 1987.

Peng, "The Performance of Various Types of Regenerators for Liquid Desiccants." Journal of Solar Energy Engineering. Volume 106 (pp 133-141) May, 1984

Rosen, J.B., "Kinetics of a Fixed Bed System for Solid Diffusion into Spherical Particles." Journal of Chemical Physics. Volume 20 (No. 3) 1952

Ruthven, Principles of Adsorption and Adsorption Processes. Wiley, New York, 1984

Shelpuk, "Overview of Desiccant Cooling Systems and their Storage Requirements." SERI/TP-34-202

Sherwood, Mass Transfer.

Smith, Introduction to Chemical Ingineering Fundamentals. 3rd Edition. McGraw-Hill